

TECHNICAL REVIEW

2002 NO. 14



MITSUBISHI MOTORS CORPORATION
TOKYO, JAPAN



- **Cover Photograph**

The cover photograph shows the results of computer-aided-engineering analysis of an offset-deformable-barrier crash test conducted on the Mitsubishi eK-WAGON, which was launched in the autumn of 2001.

The eK-WAGON employs the Mitsubishi-developed Realized Impact Safety Evolution (RISE) body structure, which combines energy-absorbing front and rear sections and a rigid occupant cell. As a result, it offers levels of occupant protection corresponding to the highest available scores in Japan's new car assessment program.

Published by Editorial Committee for the Technical Review
c/o Environmental & Technical Affairs Department
MITSUBISHI MOTORS CORPORATION,
33-8, Shiba 5-chome, Minato-ku, Tokyo 108-8410, Japan
Phone: +81-3-5232-7643
Fax: +81-3-5232-7770



Previous page (top)

Mitsubishi PAJEROs dominated the 2002 Paris-Dakar Rally with a historic sweep of first, second, third, and fourth places. From the starting line in Arras (about 170 km north of Paris), this year's Dakar rally covered a total distance of 9,432 km including 4,030 km of special stages. First across the finishing line was Japanese driver Hiroshi Masuoka, who completed the special stages in 46 hours, 11 minutes, and 30 seconds. Second place was taken by last year's winner, Jutta Kleinschmidt of Germany. And third place was taken by Kenjiro Shinozuka of Japan. This year's Dakar's victory is the seventh for Mitsubishi Motors since the company began competing in 1983. The photograph shows the celebration at the finish.

Previous page (bottom)

Hiroshi Masuoka's Mitsubishi PAJERO powers through desert terrain toward the finishing line of the 2002 Paris-Dakar Rally.

Contents

Foreword

Customer Oriented Innovation as a Goal of Engineering	4
---	---

Technical Perspective

Towards Enhanced Safety – Technology Innovation and Future Efforts –	6
--	---

Technical Papers

Development of Virtual Powertrain Model	16
Development of Multivariate Analysis Scheme for Simultaneous Optimization of Heavy-Duty Diesel Engines	24
Development of New Index Capable of Optimally Representing Automobile Aerodynamic Noise	31
Design of Air Conditioning System Using CFD Combined with Refrigeration Cycle Simulator	38

New Technologies

Development of 4M42T Engine for Powering Light-Duty Trucks for European Market	47
Use of Recycled Plastic as Truck and Bus Component Material	51
Molding of Cylinder Head Materials by the Lost-Wax Casting Process Using a Gypsum Mold	56

Technical Topics

Development of New PAJERO Rally Car for Paris-Dakar Rally	60
Development of Rally Car for World Rally Championship	63
Mitsubishi's ASV-2 Passenger Car Obtained Japan's Land, Infrastructure and Transport Ministerial Approval – Testing on Public Roads Prior to Commercialization –	66
Development of Concept Cars for the 2001 Tokyo Motor Show – Embodying the Message of the Reborn Mitsubishi Motors –	69

New Products

eK-WAGON	72
AIRTREK	74
Small-Sized Non-Step Bus "AERO-MIDI ME"	76



Customer Oriented Innovation as a Goal of Engineering

Ulrich W. Walker
Senior Vice President

At MMC, we are reforming our corporate culture at full speed, to revive the company under our Turnaround Plan.

People say MMC has been an engineering-driven company, and as a matter of fact, MMC has invented many remarkable innovative technologies thanks to its superior engineering and introduced them to the marketplace.

Although we have very competitive engineering capabilities especially in the power train as well as drive train, why is MMC currently forced to restructure to survive?

The answer is in customer's hand. New technology must bring merits to our customers, such as more convenience or better performance. At the same time, it should result in greater economic efficiency and reduced environmental impact.

Needless to say, customers select their cars based on complex buying criteria such as brand, price, design, dimension, performance, economy, environmental-friendliness, etc. A car which has only superior technology cannot be a best seller.

Of course, engineering capability will be still the one of most important factors for future survival, but we must abandon those technologies which customers do not regard as worth their price as well as those technologies which do not reinforce the MMC brand. Instead, we should depend upon outsourcing from companies with specialty in technologies.

We also must be able to predict those future technologies which customers will think are worth paying for, as well as future market trends, including competitors' strategies.

Therefore, it will be much more important to improve our market research activities as well as crossover activities between engineering and marketing.

Also, we have to clearly define our brand value as well as brand commitment to customers, and transform these principles into engineering guidelines as concretely as possible. Otherwise, we can not offer distinctive products with distinctive technology.

MMC's ultimate goal must be to offer exciting products to customers worldwide based on the appeal of the MMC brand. Therefore, we must develop vehicle technologies which excite and please customers. To create appealing technologies, engineers must have passion.

The growing integration of Seeds "Engineering" and Needs "Market" is feasible only after the realization of the above actions.

However, we should not forget the importance of production engineering as well as a production system that provides models with the highest-level of quality and reliability at the most competitive cost.

The Quality Gate system, which has been newly installed in MMC, assures the quality of our products and minimizes the gap between product concept and the actual product.

However, this system can be effective only based upon the consistent discipline of all its members.

In carrying out all these activities, we shall fully utilize the benefits of the alliance with DaimlerChrysler and harmonize it within MMC's engineering culture, to make MMC a unique Japanese automobile manufacturer with global competence.

Then, our Turnaround will be truly accomplished and we can prepare ourselves for the post-Turnaround future.

Towards Enhanced Safety

– Technology Innovation and Future Efforts –

Yoshihiro GOI* Yuusuke KONDO** Isamu NISHIMURA**
Tetsushi MIMURO** Keiichi YAMAMOTO** Yasushi CHIKATANI**

Abstract

In 1769, Cugnot's steam-powered vehicle crashed into a wall during a test. This accident which occurred in France can be regarded as the first automobile accident. Almost a century later, Great Britain introduced the first legislation established to regulate automobile traffic, under the Red Flag act* of 1865.

In Japan, a variety of safety-oriented measures have worked effectively to keep the number of fatalities resulting from traffic accidents below 10,000 a year over the last decades. However, the number of the injured persons has followed an upward curve in proportion to the increase in the number of vehicles owned. Reflecting such an environment, vehicle users are becoming increasingly hardened to safety aspects, thus requiring a higher level in safety technologies and regulative standards to assure increased safety.

This article is an overview of developments surrounding car safety issues and describes the corresponding safety technologies.

* Legislation requiring every steam-powered vehicle on public roads to run at a speed lower than 4 mph in rural areas and 2 mph in cities and to be preceded by a man carrying a red flag. It is said that the act stifled the development of the British motor car industry for as long as 30 years.

Key words: Safety, Accident, Crashworthiness, Pedestrian, Occupant Protection

1. Introduction

The advent of the automobile was also the advent of the traffic accident. The number of traffic accidents continues to grow in proportion to the number of automobile units in operation. In industrialized countries, stringent safety regulations, improved road environments, and emergency services have contributed to a downward trend in traffic fatalities recently years (Table 1). Worldwide, however, the annual number of traffic fatalities remains close to 500,000 (source: 1996 estimates from the International Road Traffic and Accident Database) and is expected to grow as motorization continues throughout developing countries. In Japan, the annual number of traffic fatalities has leveled off and slightly decreased but there has been no significant change in the number of injuries per unit in operation. Consequently, injury numbers continue to grow in line with increases in the number of units in operation (Fig. 1).

Japan's central government has responded by outlining its Seventh Fundamental Traffic Safety Program, that includes targets for cutting traffic fatalities to an annual figure 600 less than that recorded in 2000 by 2005, lower than the 1979 figure (8,466), the lowest over past 30 years. Japan's Ministry of Land, Infrastructure, and Transport is promoting vehicle-related measures

Table 1 Numbers of traffic fatalities in major countries in 1998

Note: Fatality figures apply to deaths occurring within 30 days of accidents.

	No. of fatalities (persons) (): Change from 1990	Vehicle units in operation (x 1,000)	No. of fatalities per 10,000 units in operation
Japan	10,805 (-26 %)	77,056	1.40
United States	41,471 (-7 %)	207,588	2.00
European Union (15 countries)	42,400 (-25 %)	206,018	2.06
France	8,918 (-20 %)	29,487	3.02
Germany	7,792 (-29 %)	49,586	1.57
Italy	6,326 (-12 %)	37,836	1.67
United Kingdom	3,581 (-34 %)	28,140	1.27
South Korea	10,416 (-27 %)	12,966	8.03

Source: International Road Traffic and Accident Database

with the stated goal of cutting traffic fatalities to an annual figure 1,500 lower than that recorded in 2000 by 2010.

To achieve these fatality reduction targets by vehicle-safety measures, it is essential not only to make further advances in technologies that protect vehicle occupants in collisions but also to develop pedestrian protection and compatibility technologies that protect oth-

* Environmental & Technical Affairs Dept.

** Advanced Engin. Concept Dept., Advanced Electrical/Electronics Dept., and Safety Test Dept., Car Research & Dev. Office

*** Vehicle Research Dept. and Function Testing Dept., Truck & Bus Research & Dev. Office

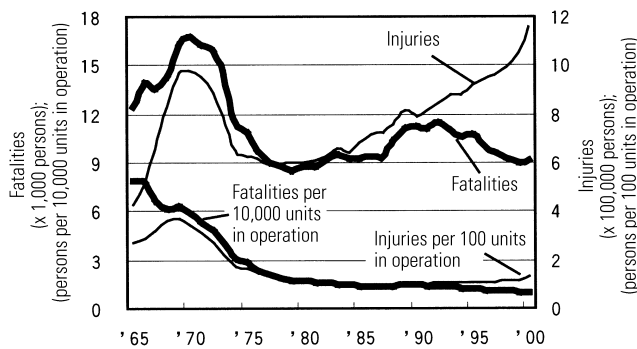


Fig. 1 Traffic accident trends in Japan

er people involved in accidents. (Compatibility technologies allow smaller, lighter vehicles to co-exist safely with larger, heavier ones in the same traffic environment.) Nevertheless, harm to humans cannot be prevented by passive safety measures alone. It is also essential to make wider use of advanced-safety-vehicle (ASV) technologies and other active-safety technologies that counteract driver error and help prevent accidents from happening in the first place. In addition, collision prediction technologies are attracting attention as a future means of preventing accidents and injuries. Active and passive safety technologies will likely become more integrated as further advances are made.

2. Safety-related trends in various countries

2.1 Passive safety trends

Numerous crash-test methods have been devised for the purpose of improving the safety of automobiles in collisions. These test methods entail evaluations of damage incurred by dummies, of body deformation, of fuel leakage, and of other relevant variables, and the evaluations become more stringent with each passing year. The published, non-legal test conditions used by third-party institutions and the legal test conditions that are used in various countries at the time of writing are shown in Table 2.

The results of information-disclosure tests are made available to the public and serve as indices for people purchasing automobiles. Increasingly close attention will likely be paid to these data as the motoring public becomes more safety-conscious.

Tests that simulate side impacts suffered by sport utility vehicles (SUVs) will be conducted by the Insurance Institute for Highway Safety (IIHS) in the United States from 2002. Also, offset collisions will be included in rear-end crash tests conducted in the United States from 2005.

Legislation on occupant head protection was recently enacted in the United States. As a result, the use of advanced airbags, whose deployment can be optimized for various collision conditions, will be mandatory in new automobiles from 2003.

With respect to pedestrian protection, tests are conducted under published, non-legal conditions in the European Union. Activities including those intended to establish legal standards are also taking place in Japan.

Compliant vehicles have already appeared in limited numbers in Japan and are likely to rapidly become more common.

In addition, efforts to harmonize the legal requirements of various countries are being made under the terms of the International Harmonization Research Activities agreement. Regulations on side impacts and crash-test dummies are among those being considered.

2.2 Active safety trends

In the area of crash avoidance, efforts to improve visibility-enhancement measures, display systems, and other technologies that help drivers perception and decision-making with respect to hazards are being made while control assistance technologies like antilock braking systems (ABSs), brake assist systems, and stability control systems (including Mitsubishi Motors's Active Stability Control System continue to spread). Advanced safety systems employing information technology are also being developed and adopted. Major trends are shown in Table 3.

As information exchange becomes an increasingly prevalent aspect of daily life, accidents caused by mobile telephones used in vehicles and navigation systems are becoming a matter of concern. In Japan, therefore, it has been made illegal to use a mobile telephone (except for hands-free models) while driving and to watch a navigation screen continuously while driving. Safety standards for related display systems are being formulated in various countries.

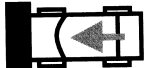

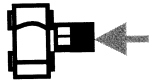
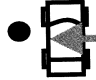



In the United States, rollover accidents caused by tire-tread separation have occurred in large numbers and have become a serious social issue. As a result, the federal government has announced plans to establish dynamic testing methods for tires and to make tire-pressure alarms mandatory.

In Japan, development of ASV and Advanced Cruise-Assist Highway System (AHS) technologies is progressing. A major publicized demonstration was conducted in 2000 and the third phase of the ASV project, intending to promote the adoption of relevant technologies began in 2001. In the United States, the National Transportation Safety Board (NTSB) is playing an advisory role in promoting the adoption of adaptive cruise control (ACC) devices and other advanced safety technologies related to intelligent transportation systems (ITSs). Similar efforts are being made around the world.

The technologies with the greatest potential for reducing accidents are those designed for collision prediction and avoidance. DaimlerChrysler has exhibited the technological concept for a collision prediction system that uses high-precision sensors to determine the likelihood of a collision and, when necessary, takes evasive braking action and simultaneously activates the vehicle's seatbelt pretensioners and optimizes the deployment timing and pressure of vehicle airbags.

Table 2 Major trends in passive safety technologies in major markets

● : Published, non-legal test condition ○ : Legal test condition

Item			Japan	United States	European Union
Frontal impact	Full-width rigid barrier		● 55 km/h ○ 50 km/h	● 35 mph ○ 30 mph	–
	Offset deformable barrier		● 64 km/h ○ (work on legislation in progress)	● 40 mph (IIHS) ○ 25 mph (planned)	● 64 km/h ○ 56 km/h
Side impact	Deformable barrier		● 55 km/h ○ 50 km/h	● 38.5 mph (oblique impact) ● 38.5 mph (under consideration for SUVs) ○ 33.5 mph (oblique impact)	● 50 km/h ○ 50 km/h
	Side pole		–	○ 18 mph (substitute legislation)	● 29 km/h (optional)
Rear impact	Full-width rigid barrier		○ 50 km/h	○ 30 mph	–
	Offset deformable barrier		–	○ 50 mph (planned)	–
Pedestrian protection			● (implementation from 2003 under consideration) ○ (work on legislation in progress)	–	● 40 km/h ○ (self-regulation planned)
Other			● Child seats	○ Interior head-protection structures ○ Advanced airbags (planned)	● Seatbelt reminders ● Child seats

(As of October 2001)

Table 3 Major trends in crash-avoidance technology in major markets

Category	Item	Japan	United States	European Union
Cognition and decision-making support	Strengthening of passenger-car field-of-vision standards	• Regulations on forward and side blind spots (from 2003)		• Creation of standards for vehicle fields of vision in progress
	Safety measures related to mobile telephones and onboard display devices	• Use of mobile telephone while driving prohibited (1999) • Continuous observation of navigation screen while driving prohibited (1999) • Creation of safety standards for display devices in progress (2002)	• Guidelines on display devices being created by Society of Automotive Engineers	• Guidelines on display devices being created by International Organization for Standardization (ISO)
Control support	Anti-rollover measures	• Research for prevention of rollover of heavy-duty vehicles in progress	• Conduct static evaluation and study dynamic evaluation (from 2001) • Mandatory use of tire-pressure monitor (under consideration)	• Legislation to prevent rollover of heavy-duty vehicles under consideration • Assessment conducted and results published by magazines
	Speed limiters in heavy-duty vehicles	• Mandatory use of 90 km/h limiters (from 2003)		• Regulations on speed limiters in heavy-duty vehicles (1994)
Research and development projects	ITS-related projects; activities to promote adoption of technologies	• Third phase of ASV project (from 2001) • Preliminary introduction of AHS (from 2003)	• Intelligent Vehicle Initiative program ² • Advisory role played by NTSB in ITS adoption (2001)	• Information Society Technologies (IST) program ³ (through 2002)
	External control of vehicle speed (Intelligent Speed Adaptation) ^{*1}			• Operational tests for speed control by means of telecommunications (2001)
	Collision prediction and safety technologies			• Technology exhibited by DaimlerChrysler

*1: ISA (Intelligent Speed Adaptation)

*2: IVI (Intelligent Vehicle Initiative)

*3: IST (Information Society Technologies)

(As of October 2001)

Individual projects are being conducted in the transport and tourism areas of the IST program.

3. Passive safety

3.1 Frontal-impact safety

Frontal collisions can be broadly classified into two types full-lap (in which the entire width of the vehicle

hits a rigid barrier) and offset (in which only a part of the vehicle's width hits another vehicle). Although the distinction between these two collision types can be ambiguous in an actual accident, the classification of collisions into full-lap collisions (in which vehicle occu-



Fig. 2 New-generation frontal-impact dummy (THOR Alpha ATD⁽¹⁾)

pants suffer high levels of deceleration) and offset collisions (which tend to cause significant cabin deformation) is a fundamental aspect of the thinking behind passive safety measures.

Occupants' lower legs can easily be injured by rearward movement of the dashboard, brake pedal, and other parts in an offset collision. An optimally rigid cabin is thus essential to minimize such injuries. In a full-lap collision, however, higher cabin rigidity causes higher levels of body deceleration, which is harmful to occupants. The best possible combination of measures to satisfy the conflicting occupant-safety requirements of offset and full-lap collisions must be incorporated into every vehicle's body.

Effective restraint systems are also essential. Basic seatbelts cannot be used to restrain occupants gently enough during rapid deceleration, so vehicles are increasingly being equipped with airbags and with seatbelts that have pretensioners and load limiters. Research into other, more effective occupant-restraint devices is continuing. These devices include double-pretensioner seatbelts and airbelts. They also include advanced airbags, which deploy with full pressure in the event of a high-speed collision but automatically reduce their deployment pressure in the event of a low-speed collision and in accordance with the users' physical sizes and seating positions.

Another area of recent concern is compatibility between larger, heavier vehicles and smaller, lighter ones. Increased rigidity in a larger vehicle detracts from compatibility by increasing the extent of damage that the vehicle can inflict upon a smaller one. Compatibility is known to be greatly influenced by bumper positions, bumper structures, and frame heights, but appropriate testing methods and evaluation standards have yet to be found at the time of writing. Qualitative studies that encompass measures such as large-area bumper beams (these help to prevent impacting vehicles' front frames from pushing into impacted vehicles) and increased consistency in the front- and rear-frame heights of different vehicles are under way.



Fig. 3 Computer-aided-engineering simulation of SUV barrier hitting two-door passenger car at 38 mph

In the area of impact dummies, an international development program is being conducted with the goal of producing a next-generation dummy to replace the Hybrid III adult dummy that is currently a global standard (Fig. 2). Efforts are focused on more closely replicating the human body in terms of the shape and rigidity of its ribs, the movement of its spine, the responsiveness of its neck, and the structure of its lower limbs. New dummies representing children of various ages and sizes are also being developed.

3.2 Side-impact safety

The need for side-impact measures is constantly increasing; research efforts are being conducted vigorously with the goal of reducing deaths and injuries in side impacts at ever-higher speeds and with increasingly severe impact configurations. In Japan and the United States, published, non-legal tests are conducted with speeds 10 % higher than the legally required ones. Further, the IIHS in the United States has proposed a new test method involving a side impact from a sled that replicates an SUV, which is a relatively tall type of vehicle (Fig. 3). With this test method, the sled directly hits the occupants' heads, making curtain airbags, which provide head protection and are fitted in a growing number of vehicles, an effective means of protecting the occupants (Fig. 4). Since the sled makes contact at a position significantly higher than the side sills of a passenger car, cabin deformation tends to be relatively severe and the provision of a survival space is concomitantly critical.

In the area of International Harmonization Research Activities, tests combining SUV side impacts and relatively small female dummies, tests in which side impacts take place with poles, and methods for determining the safety of occupants seated on the side opposite to the impacted side are being discussed.

A major obstacle in efforts to ensure side-impact safety is the legally required use of different dummies in different countries. Given that human bodies are the same everywhere irrespective of differences in traffic conditions, Japanese, American, and European automotive manufacturers' associations and other organizations are working to overcome this obstacle by devel-



Fig. 4 Curtain airbag during 30 km/h side impact with pole (photo taken immediately after deployment)



Fig. 5 New side-impact dummy (WorldSID)⁽²⁾

oping a world-standard side-impact dummy known as WorldSID (Fig. 5).

Curtain airbags (mentioned earlier) can conceivably be given, in addition to their functionality for protection of occupants in side impacts, functionality for protection of occupants in rollover accidents and functionality to prevent occupants from being thrown out of vehicles. Rollover accidents are not common in Japan, but they represent more than 20 % of fatal automobile accidents in the United States. Curtain airbags with rollover-accident functionality are thus likely to be adopted in production vehicles.

3.3 Rear-end collision safety

Research efforts related to rear-end collision safety can currently be broadly divided into those aimed at preventing whiplash in low-speed rear-end collision and those aimed at preventing vehicle fires in high-speed rear-end collision.

Various seat mechanisms designed to minimize whiplash have been devised by manufacturers, and the number of vehicles employing such mechanisms is increasing. The physiological mechanism of whiplash has not been completely clarified, but there is scope for



Fig. 6 Computer-aided-engineering simulation of offset rear impact by deformable barrier at 50 mph

further improvement in anti-whiplash measures as progress is made in medical research.

With regard to high-speed rear-end collision, proposals for significantly tougher legislation were recently announced in the United States. Under the proposed legislation, a deformable barrier would replace the currently used rigid barrier and would be propelled at 80 km/h toward the rear of the vehicle body at a position offset from the center. The proposed new barrier shape more closely reflects real-world conditions, and the proposed impact speed is extremely high. The severe new test method is apparently appropriate for the traffic conditions in the United States (Fig. 6). Accident conditions of such severity are not currently being considered for inclusion in regulations in Japan and Europe. Given that vehicle fires resulting from fuel leakage can give rise to serious accidents, however, concern about high-speed rear impacts is likely to grow internationally.

3.4 Pedestrian protection

Legislation on pedestrian protection is due to be adopted in Japan in the near future. Automakers' self-regulation on pedestrian protection is expected to come into effect in Europe. To protect pedestrians by means of vehicle-design measures, it is necessary to ensure that external parts that might make contact with pedestrians are as yielding as possible and to create sufficient clearance between external parts and hard internal members. However, vehicle shapes and layouts are subject to major limitations. It is particularly difficult to simultaneously satisfy styling requirements and pedestrian protection requirements with a sporty body that has a low hood. Smaller engines, smaller suspension components, pedestrian protecting airbags, and other measures will be necessary to enable pedestrian protection with the full range of body styles. Related technological problems must be addressed and overcome.

3.5 Passive safety of heavy-duty vehicles

The occurrences of bus accidents on highways have prompted comprehensive studies of the safety of trucks and buses. Crash-test guidelines have been established from the standpoint of driver and passenger protection, and methods for evaluation of occupant-injury levels



Fig. 7 Processing of rearview camera image for Side-rear Monitor (detection of overtaking vehicle by tracing of reference points (optical flow detection))

resulting from frontal impacts with full-lap flat barriers have, as with passenger cars, been adopted.

Research and development efforts aimed at further improving occupant safety in collisions are focused on the following issues:

- Mitigation of damage in rear-end collision peculiar to trends accidents
- Mitigation of chest and abdominal injuries caused by steering wheels
- Mitigation of leg injuries caused by instrument panels and nearby parts
- Improvement of the ease with which occupants can be rescued

Given that accidents involving trucks can be extremely serious, measures to mitigate the damage to by other vehicles in such accidents are also vital. The risk of fatalities is particularly high when a passenger car suffers a frontal collision with a truck since the front of the passenger car slides under the front of the truck. Mandatory use of front under-run protectors, which are mounted under the front frames of trucks, is being considered as a means of preventing such incidents.

3.6 Collision prediction

Efforts to further improve the performance of seatbelts, airbags, and pedestrian protection devices may necessitate the adoption of collision prediction systems that employ sensing technologies (described later in this paper).

If a vehicle could be able to predict the risk of an accident just before a collision, it could maximize safety by taking such action as tightening the seatbelts and deploying pedestrian protecting airbags. Research in this field has only just begun but is expected to yield great benefits.

4. Active safety

4.1 Cognition and decision-making support

(1) Measures against blind spots

In recent years, much attention has been focused on accidents in which small children are hit and killed by slow-moving vehicles while hidden from drivers by blind spots. According to research conducted by Japan's Institute for Traffic Accident Research and Data

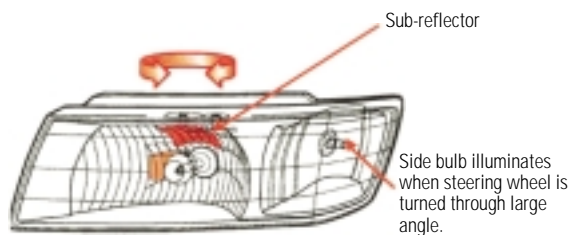
Analysis⁽³⁾, most cases involve children of two years of age and younger and the vehicle in many cases is, tragically, driven by a parent or other close relative. As one way to prevent such accidents, members of the Japan Automotive Manufacturers Association (JAMA) have voluntarily fitted side undermirrors (auxiliary mirrors) on tall, light-duty, cab-behind-engine vehicles since 1991. Also, falling prices of compact cameras have helped to make blind-spot monitor systems increasingly common. A Side-rear Monitor (the first of its kind) that detects overtaking vehicles in the adjacent lane during high-speed driving and provides the driver with appropriate warning in the event of any imprudent lane-change maneuver was realized by Mitsubishi Motors in February 2000 as a function of a Driver Support System (Fig. 7).

(2) Improvement of nighttime visibility

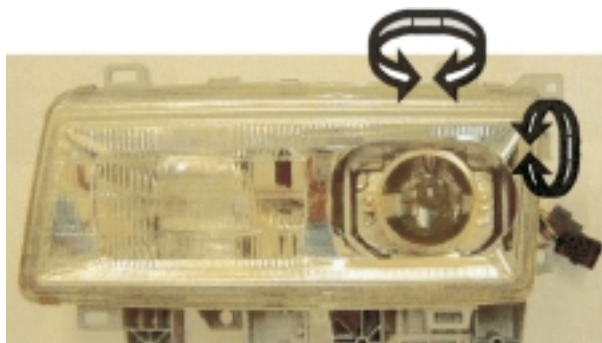
Visual information accounts for the majority of information received by a driver, so improvements in nighttime visibility are particularly desirable. Discharge headlamps are advantageous in this regard, so Mitsubishi Motors began using them on its heavy-duty trucks in 1996 following a full model change. The superior brightness and visibility realized by discharge headlamps has been welcomed by users. At the time of writing, therefore, Mitsubishi Motors uses discharge headlamps on 95 % of its heavy-duty trucks, on 80 % of its medium-duty trucks, and on 98 % of its heavy-duty buses. Mitsubishi Motors also uses discharge headlamps on passenger cars; at the time of writing, it uses them on at least 90 % of CHARIOT GRANDIS models and on certain models of the PAJERO, RVR, and LANCER EVOLUTION.

Cornering lamps, which illuminate the areas forward and sideways of the vehicle during leftward and rightward turns, have been put to practical use. As a further advance, technologies that optimize the distribution of light from headlamps in accordance with road conditions are being developed. Headlamps equipped with such technologies illuminate the road over a long forward distance during high-speed driving but direct their beams in the direction of steering when the vehicle negotiates a curve. In addition, they minimize dazzle for drivers of oncoming vehicles. Various designs for variable-light-distribution headlamps have been devised. Examples are shown in Fig. 8. The JAMA lighting-device group⁽⁴⁾ is studying relevant technological and legal issues with a view to enabling practical adoption. Steps (including discussions about the establishment of relevant regulations) are also being taken in Europe.

Further-advanced systems that provide the driver with information on the presence of pedestrians at night are being developed. If effective systems of this type are widely adopted, they can be expected to significantly reduce nighttime vehicle-to-pedestrian collisions, which account for about 70 % of total vehicle-to-pedestrian collisions. A system that shows unmodified images from an infrared camera on a head-up display (HUD) has been commercialized, but a driver cannot easily identify pedestrians in infrared images of urban



Movable sub-reflector and multiple bulbs for Mitsubishi passenger car ASV



Movable bulb unit for Mitsubishi truck ASV

Fig. 8 Variable-light-distribution mechanisms

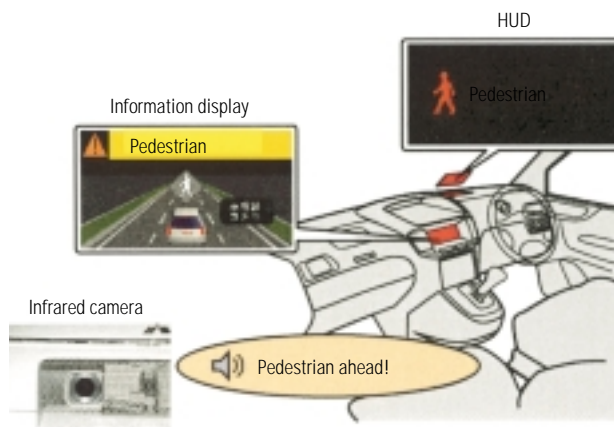
roads and other complex driving environments. To overcome this problem, pedestrian detection technologies and an appropriate human interface to the driver must be studied. Conceivably usable methods for detection of pedestrians include trigonometric distance measurement using stereoscopic vision and identification of human outlines by means of template matching. With regard to the human interface, adoption of HUDs that can be used with minimum movement in the driver's line of sight and indication of the presence of pedestrians by means of icons, are being considered (Fig. 9).

For practical adoption of technologies in this area, the development of pedestrian detection technologies must be complemented by reductions in the cost of infrared cameras and by the development of technologies that accommodate the different needs of different markets.

(3) Driver distraction

As more devices for telematics services (services that use communications technologies to provide information needed by drivers) are adopted in vehicles, drivers receive a concomitantly increased flow of information. As a result, driver distraction has become a matter of concern for Japanese, American, and European experts.

The main short-term focus of discussion is the deterioration in concentration that drivers suffer when using navigation systems and mobile telephones. Since drivers have widely differing levels of cognitive ability, a single, universally applicable solution will likely be difficult to find. In Japan and Europe (the first markets to see widespread use of telematics devices), using a mobile telephone while driving has been made illegal and guidelines on the use of telematics devices (these

**Fig. 9 Nighttime pedestrian monitoring system of Mitsubishi ASV**

include guidelines laid down by automotive manufacturers' associations and those defined in an EU Statement of Principles) have been formulated; the focus of interest has shifted to an effort to establish a means of quantifying a driver's cognitive burden. In the United States, the world's second-largest market for mobile telephones, too, there is growing public concern about the problem of driver distraction; numerous bills to outlaw the use of mobile telephones by drivers are being studied, and work to establish guidelines is progressing. Nevertheless, recent research indicates that use of mobile telephones causes only 0.14 % of all accidents and that hands-free functionality does not improve signal recognition probability or response times; further research is needed for accurate analysis of the causes of driver distraction. Within the ISO, there is vigorous debate – primarily among Japanese and European participants – on ways to quantify driver workload. Numerous indices (these include Single Grance Time, Total Grance Time, and Total Task Time) have been proposed, and work to verify the effectiveness of each index is taking place.

To deal appropriately with rapid technological and commercial advances in the field of telematics, it is essential to improve the onboard technologies of telematics devices while gathering information from all areas concerned. Voice-activated control of devices is one area of technology on which Mitsubishi Motors believes it is particularly important to concentrate.

(4) Improvement of meter visibility

Together with efforts made to address the aforementioned increase in the flow of information received by drivers, efforts are being made to improve meter visibility, which is crucial for the growing number of elderly drivers, whose eyes tend to be poor at making focus adjustments. Some of these efforts are reflected in Mitsubishi ASVs, which promote the company's "universal design" concept. In the first phase of the ASV project, Mitsubishi Motors proposed instrumentation consisting of a center meter (this shows the vehicle speed and other information and is located on the cabin's center line, where it is easy to see) and a navigation



Fig. 10 Navigation system mounted in eK-WAGON



Fig. 11 Rollover test

screen that is located directly in front of the driver. In the second phase of the ASV project, Mitsubishi Motors proposed using a liquid crystal display, whose design can be changed as desired, and a high-resolution HUD.

In the eK-WAGON, which was launched in the autumn of 2001, Mitsubishi Motors adopted a layout in which analog meters and various functions are located centrally and a navigation screen can be placed directly in front of the driver (Fig. 10).

4.2 Control support

(1) Vehicle dynamic control systems

For a driver to be able to avoid a hazard and thus avoid having an accident, it must be possible for the vehicle to be controlled exactly in accordance with the driver's wishes. A dynamic control system that prevents the tires' grip limits from being exceeded is an effective means of enabling a driver of average skill to remain in control of the vehicle in the event of an emergency. Antilock braking systems, traction control systems, active stability control (ASC) systems, and other dynamic control systems developed in accordance with this principle are used in a growing number of production vehicles. An ASC system monitors the vehicle's cornering movements and controls the braking force of each wheel individually – and the engine output when necessary – to prevent spin and driftout. ASC systems are given different names by different manufacturers (for example, DaimlerChrysler calls its system an Electronic Stability Program), but they are similar in terms of configuration and operation. These systems are particularly effective at suppressing spin on slippery road surfaces and during high-speed driving.

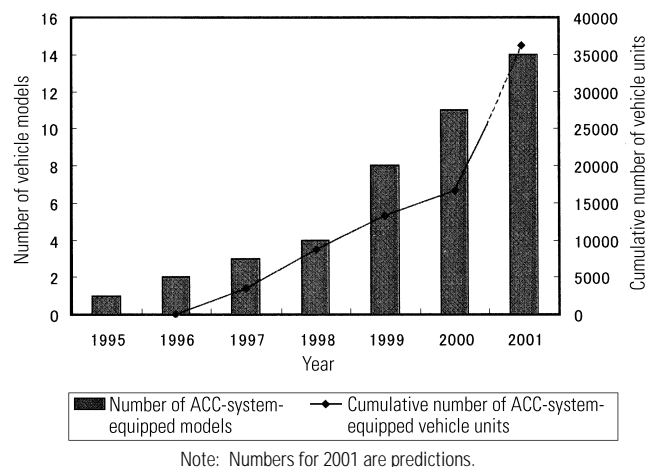


Fig. 12 Number of ACC-system-equipped models and cumulative number of ACC-system-equipped vehicle units (Source: JAMA)

Manufacturers are beginning to extend their application to compact cars. It is conceivable that a future ASC system will effect integrated control over the steering system, braking system, throttle, and suspension system.

With a truck, the load has a significant effect on dynamic characteristics. Accurately ascertaining this effect is central to ensuring dynamic stability. Further, a truck's center of gravity is higher than a passenger car's, making it essential to conduct rollover for verification of the truck's stability limits (Fig. 11). Work to develop ASC systems for trucks and buses is widespread in Europe and the United States. Systems under consideration include those for prevention of jackknifing and those that control shock absorbers in a way that realizes both stability and ride comfort. In Europe, regulations on rollover stability are being developed. The planned first stage of these regulations covers static testing of tank trucks used to transport hazardous substances. The planned second stage covers dynamic testing of commercial vehicles including buses. Efforts to study and improve vehicles' fundamental dynamic performance limits must be made at the same time as efforts to improve their dynamic stability by means of control systems.

(2) ACC systems and collision warning systems (CWSs)

An ACC system supplements conventional cruise control with laser radar or other sensing technology, which it uses to detect preceding vehicles and adjust the headway distance accordingly. In January 1995, Mitsubishi Motors became the first manufacturer to put such a system (named the Preview Distance Control system) to commercial use. Numerous other companies have since entered the market; ACC systems are now used even in compact cars and minivans, and their adoption is likely to become more popular in the near future (Fig. 12). Deceleration for ACC was originally achieved by closure of the throttle and by initiation of automatic-transmission downshifts, but systems that cause deceleration by means of automatic braking have also been developed. Mitsubishi Motors is developing a heavy-duty-vehicle ACC system that controls the ser-



Fig. 13 Mitsubishi's second-phase ASVs: three passenger cars and one truck

vice brakes. Future advances will likely include integration of ACC functions with other brake-related functions (particularly antilock braking and active stability control), rapid adoption of brake-by-wire technologies, and expansion of ACC functionality to include intelligent braking assistance (employing information on the preceding vehicle), automatic impact-mitigating braking, automatic starting, automatic stopping, and other aspects of dynamic control at all vehicle speeds.

Rear-end collision account for many accidents involving heavy-duty trucks in Japan and the United States. Efforts to prevent commercial vehicles from causing rear-end collision are thus being made. In May 2001, the NTSB of the United States announced the results of special research into technologies for prevention of rear-end collision and advised the Department of Transportation (DOT) and National Highway Traffic Safety Administration (NHTSA) to promote the use of ACC systems and CWSs. In July 2001, the NTSB called on the DOT to make CWSs mandatory in all new commercial vehicles. The NHTSA estimates that these safety systems can reduce rear-end collision by 37 – 74 %. Relevant systems in trucks and buses marketed by Mitsubishi Motors include a headway distance warning system, the second-generation Mitsubishi Driver's Attention monitoring System or MDAS II (this combines headway distance warning functions and driver alertness monitoring functions), and an ACC system that employs the auxiliary brakes. Such systems are likely to be adopted more widely in production vehicles if they are proven effective in preventing accidents.

(3) Lane deviation prevention systems

A lane deviation alarm that uses compact cameras to detect white lines on the road and issues a warning whenever the vehicle deviates from its lane owing to reduced driver attention, was realized by Mitsubishi

Motors as a function of the first-generation Mitsubishi Driver Attention monitoring System for trucks. Similar functionality is provided by the Driver Support System used by Mitsubishi Motors in passenger cars. Work is also under way on commercialization of a system that helps the driver to stay in lane by generating torque in the steering wheel. High costs of cameras and steering actuators will limit the number of vehicle models in which this system can be used in the near term. If camera prices continue to fall and the system is integrated with existing electric power steering components, however, wider adoption will soon become possible.

It is possible that the sensors and actuators used for these forms of driver support can be used to enable collision prediction (mentioned earlier in this paper) and mitigation of collision damage. Their application represents an important area of research.

4.3 Research and development projects

Japan's ASV project is led by the Road Transport Bureau, Ministry of Land, Infrastructure, and Transport. In its first phase (1991 – 1995) and second phase (1996 – 2000), this project enabled the development of a number of valuable advanced safety technologies (mainly for active safety). Second-phase ASVs developed by Mitsubishi Motors are shown in Fig. 13. A major publicized demonstration of ASV technologies was conducted in 2000. The ASV project's third five-year phase, which is focused primarily on promoting adoption of ASV technologies and encompasses an effort to realize driver support systems that use telecommunications technologies, began in October 2001. Mitsubishi Motors is enthusiastically pursuing its third-phase activities, whose goals include the realization of systems that allow vehicles to interact with the road infrastructure.

Japan's AHS, whose development is led by the Road Bureau of the Ministry of Land, Infrastructure, and Transport, is being realized by means of intelligent vehicles (ASVs), intelligent road infrastructure, and road-to-vehicle communication technologies. A vehicle in this system obtains information from the road infrastructure by means of radio communication and provides it to the driver. Items covered by this information include other vehicles (for example, the positions of stationary and slow-moving vehicles on parts of the road ahead that the driver cannot see, of vehicles approaching relatively major roads from relatively minor ones via junctions, and of oncoming vehicles whose path the driver must cross when turning right at junctions) and the radii of curves that the driver will soon have to negotiate. Mitsubishi Motors took part in the AHS proving test in 2000 (Fig. 14) and will begin taking part in a test on actual roads in the summer of 2002.

In Japan and Europe, other research and development projects are aimed at applying vehicle-to-vehicle communication (apart from road-to-vehicle communication) to safety systems. This technology is used primarily when vehicles follow each other with short headway distances, but other applications (for example, accurate monitoring of nearby vehicles' movement; automatic braking for collision avoidance; and alarms

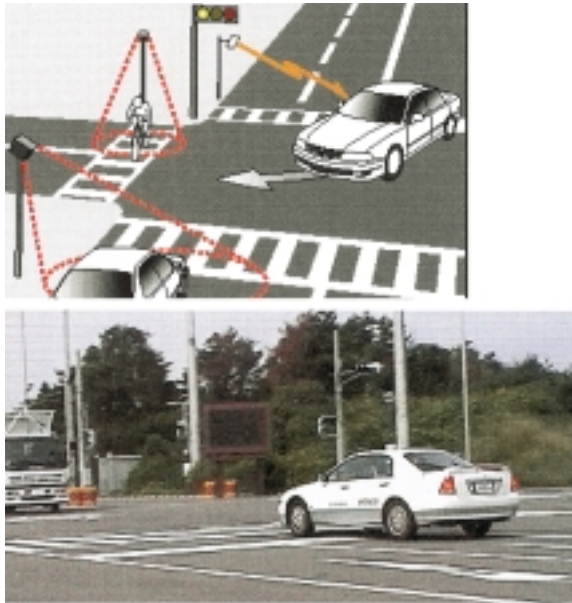


Fig. 14 Test scenario of AHS proving test conducted in 2000 (photo taken at test course of Public Works Research Institute (now National Institute for Land and Infrastructure Management) in Tsukuba City)

to prevent vehicles from hitting motorcycles) are also conceivable. Mitsubishi Motors is pursuing research in this area in conjunction with DaimlerChrysler.

In the future, development and widespread adoption of new technologies must be supplemented by more stringent evaluation of those technologies' cost performance and side effects. In this regard, Mitsubishi Motors is conducting tests of its ITS-ASV (a product of the second phase of Japan's ASV project) on public roads with authorization from Japan's Minister of Land, Infrastructure, and Transport (see page 66). This test vehicle incorporates variable-light-distribution headlamps, lane deviation prevention system, and other technologies that will likely soon be put to widespread commercial use. Data generated by the tests conducted on public roads will be valuable at various levels; they will not only significantly benefit evaluation and improvement of new safety systems but will also help the government in any consequent endeavor to relax safety regulations for road vehicles.

5. Summary

The following are words of traffic accident researchers⁽⁵⁾.

"Ones who are seeking to reduce traffic fatalities must remember that road transportation is merely a system – one conceived for quick, safe, and easy movement of people and commodities – and that, as with any system, there is no limitation that cannot be overcome and no problem for which a remedy cannot be found".

On this basis, those of us involved with vehicle development must never stop pursuing technological advances as we work toward our goal of hugely improved vehicle safety; we must never be fully satisfied with the progress we have made.

References

- (1) N. Rangarajan, R. Eppinger, et al.: "Fundamentals and Elements of the NHTSA", THOR Alpha ATD Design
- (2) <http://www.worldsid.org>
- (3) "Study on Prevention of Accidents Involving Walking Children during Slow Movement of Vehicles", report of 2000 research funded by Sagawa Traffic Foundation, Institute for Traffic Accident Research and Data Analysis, 2001
- (4) "Study on Adaptive Front Lighting System", report of 2000 research commissioned by JAMA, Japan Automobile Research Institute
- (5) Näätänen, R. and Summala, H.: "Road-User Behavior and Traffic Accidents", North-Holland, Amsterdam, 1976



Yoshihiro GOI



Yuusuke KONDO



Isamu NISHIMURA



Tetsushi MIMURO



Keiichi YAMAMOTO



Yasushi CHIKATANI

Development of Virtual Powertrain Model

Masato KUCHITA* Taizo KITADA* Kazuo KIDO**

Abstract

The Virtual Powertrain Model described here was developed for use in predicting the fuel consumption, exhaust emissions and riding comfort of a vehicle in its concept and development stages. All what a user of this code has to do when operating it is to select desired models for the engine, transmission, vehicle, and control system and to combine them together. The model for engine and other basic functional components are formed into packages which are made compatible with model packages of other functional components for easy exchange of model combinations and quick calculation of many combination variations. The models of the individual parts constituting basic functional components are also designed to be compatible with others. A user interface for accessing this computer code provides the user with graphical means of monitoring vehicle's driving conditions and manipulating the vehicle through windows.

Key words: Simulation, Modeling

1. Introduction

Developing an outstanding passenger car is not simply a matter of combining a good engine, a good transmission, and a good chassis and body. It is also important to ensure that every component is optimally balanced with the others and to create control logic that allows every component to extract its maximum potential. Particularly with regard to fuel economy, every hardware component has already been refined to extremely high level, so that the focus of development work aiming at improving fuel economy has been shifted to the selection of component combinations and to control strategies.

To optimize high sophisticated control systems with a high degree of freedom rationally and to study the most suitable combination of components for the target vehicle efficiently, Mitsubishi Motors Corporation (MMC) has developed a Virtual Powertrain Model and has been widely using it on the front line of development work. Thanks to the progress of personal computers (PCs) nowadays, this software has been transferred to PCs from engineering workstations (EWSs) and can be used by everyone.

This paper describes an overview of the computation code, its merits, and examples of its utilization.

2. Overview of Virtual Powertrain Model

2.1 Overall computing system

The basic concept of the Virtual Powertrain Model is to make computation models of each component, such as an engine, a transmission, a vehicle, and an electronic control unit (ECU), in the form of one-package computation models and to create a virtual vehicle on the computer by combining them.

To realize this concept, individual computation mod-

els are subdivided on a unit-by-unit basis and models corresponding to the same functional unit are made interchangeable. The user can create the desired powertrain model by simply combining the models for relevant functional units. And the user can easily alter the specifications of the engine, transmission, and other components and/or replace models with different ones. For example, the user can easily replace an automatic transmission (AT) with a manual transmission (MT) or with a continuously variable transmission (CVT).

Fig. 1 shows the root hierarchy (top layer) of this computation code. This code is roughly divided into three blocks: a physical phenomena block such as an engine, a control block, and a human characteristic block. Each block consists of some subroutines that describe the components of the block. As far as possible, the basic components of the bottom layer are written as combinations of primitive functions such as adders, integrators, and comparators. The driver is modeled to simulate a typical driver's operation of the accelerator and clutch pedals.

The computation code treats one engine combustion event as one time step, and the several time-integrated values of that period are transferred to following blocks. This is the same method that has been used in the same type of computer programs for many years⁽¹⁾⁽²⁾.

Fig. 2 shows the operation window, which contains a speedometer, a tachometer, a transmission shift position indicator, an accelerator indicator, a brake indicator, and a monitor pane showing the target and actual vehicle speeds. The code is capable of using the automatic driving function to simulate driving in accordance with a legally defined driving cycle (for example, Japan's 10-15-mode test cycle or European Union's test cycle) and to predict the resulting fuel economy. If automatic driving is changed to manual driving and the

* Advanced Powertrain Dept., Car Research & Development Office

** MCOR CAE Group

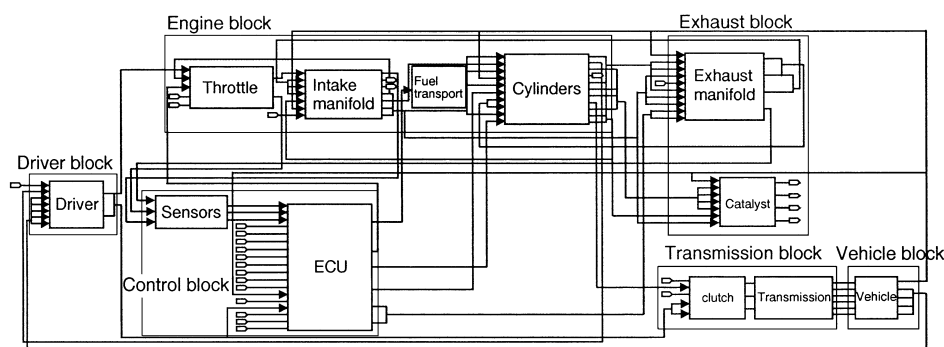


Fig. 1 Root hierarchy of powertrain model

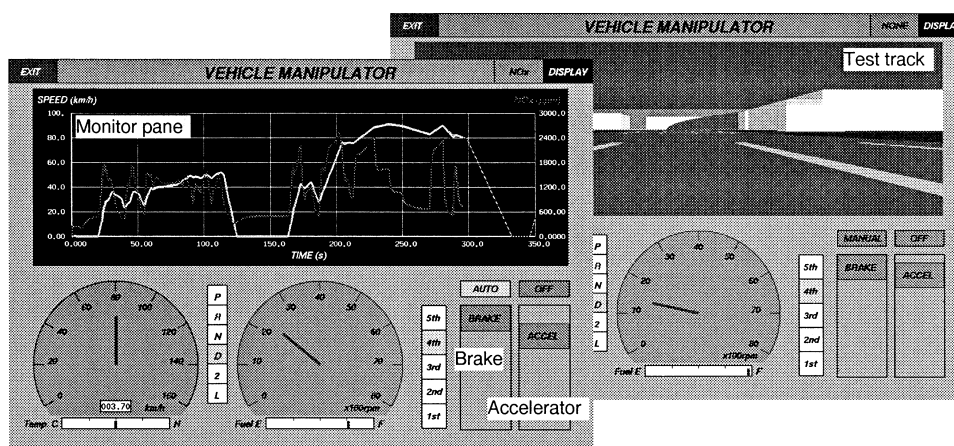


Fig. 2 Operation window of powertrain simulator

computation speed is set to real time, the user can simulate driving by controlling the accelerator and brake pedals using a mouse. Thus, the user can grasp a sensory appreciation of the vehicle's driving feel, although one doesn't involve a real sense of acceleration. Further, switching the monitor pane to a three-dimensional mode, the user can simulate driving while watching a representation of MMC's test track (shown in Fig. 2) and listening to an engine exhaust sound that is synthesized from computation results.

2.2 Engine block

The engine block consists of four elements: a throttle model, an intake manifold model, a fuel adhesion model, and a cylinder model. In the throttle model, the amount of air passing through the throttle is calculated from the intake manifold pressure using Bernoulli's equation. In the intake manifold model, the intake manifold pressure is calculated from the balance of the amount of air entering from the throttle and exiting to the cylinders. In the fuel adhesion model, the fuel transport lag caused by the wall film in the manifold or port is treated as a first order time lag. In the cylinder model, the engine output is determined from an experimental performance map measured during steady-state operation. For taking the influence of the ignition timing and air/fuel ratio on the engine output into account,

a pressure-volume (P-V) cycle diagram is drawn for each combustion event in each cylinder. And the engine output is corrected by the comparison between the indicated pressure calculated from the P-V diagram of the transient condition and that of the steady-state condition. This technique permits, by way of example, the vehicle acceleration to be expressed accurately even with the ignition timing force-retarded to suppress knocking during acceleration.

2.3 Transmission block

The transmission model consists of a clutch and a gearbox. Depending on the combination of models selected, an MT, an AT, or a CVT is composed. Of course, all models for each item have common data input/output formats for interchangeability so the combination can be changed easily. There are two models for the clutch: a mechanical clutch and a hydraulic clutch (torque converter). In the mechanical clutch model used with MTs, shock caused by interruption and resumption of the torque flow and the fuel losses caused by unnecessary revving can be predicted. In the torque converter model used with ATs and CVTs, the output shaft torque is calculated by using a characteristic map to determine the capacity factor and torque ratio from the speed ratio. Furthermore, the torque converter model includes the lock-up clutch model in which full-

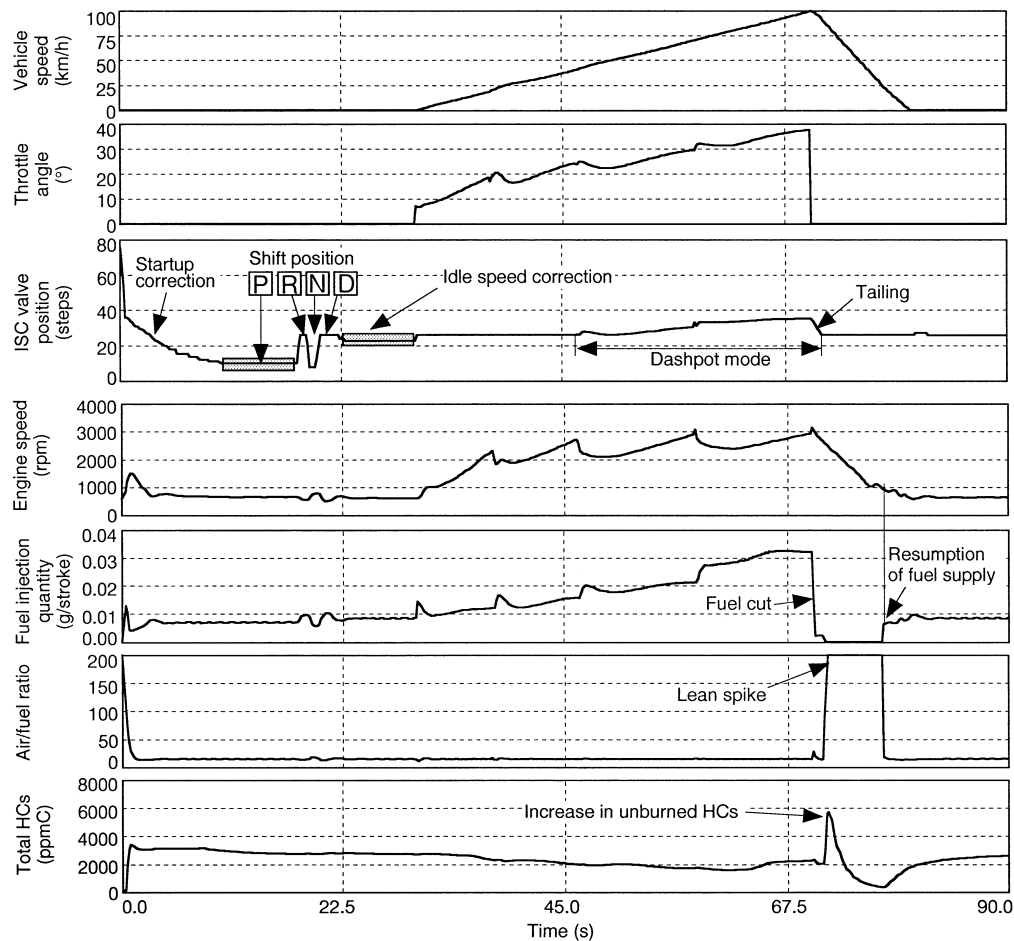


Fig. 3 Example of fuel injection control

ly locked engagement and partially locked engagement conditions can be simulated. Two types of the gearbox models are provided: a discrete ratio gearbox for an MT or an AT and continuously variable ratio gearbox for a CVT.

2.4 Vehicle block

In the vehicle model, the vehicle acceleration is calculated to subtract losses from the powertrain's output torque. These losses are caused by aerodynamic resistance, rolling resistance, the road's hill-climbing resistance, and braking. In addition to a conventional mechanical brake model, a regenerative brake model for electric vehicles (EVs) and hybrid electric vehicles (HEVs) is provided.

2.5 Control block

The major parts of the engine and transmission control are modeled in accordance with its specifications. In the engine ECU model, signals for control of the fuel injection quantity and ignition timing are calculated using signals from a throttle position sensor, a crank angle sensor, an air flow sensor, and an O₂ sensor in all engine operating conditions (including startup and transient conditions).

2.6 Driver block

In the driver model, the accelerator and brake operations are simulated to track the target vehicle speed value using proportional-integral (PI) control, and the PI control coefficients are adjusted to replicate the actions of a typical driver. The clutch operations are also modeled to be capable of expressing the driver's characteristics.

2.7 Other models

A catalyst model that takes warmup into account, an EV model, and an HEV model are provided. Accessory models (an alternator model that takes generation control into account, a starter model, an air conditioner model, and a power steering model) are also provided.

3. Calculation examples

3.1 ECU model calculation

3.1.1 Fuel injection control

Fig. 3 shows the calculation result performed to check the fuel control conditions and effects of fuel cut for a vehicle with a 1.5-liter engine and an AT, when the vehicle rapidly decelerated after smoothly accelerating. The AT shifted up as the vehicle speed increased and the engine speed changed each time. Following the

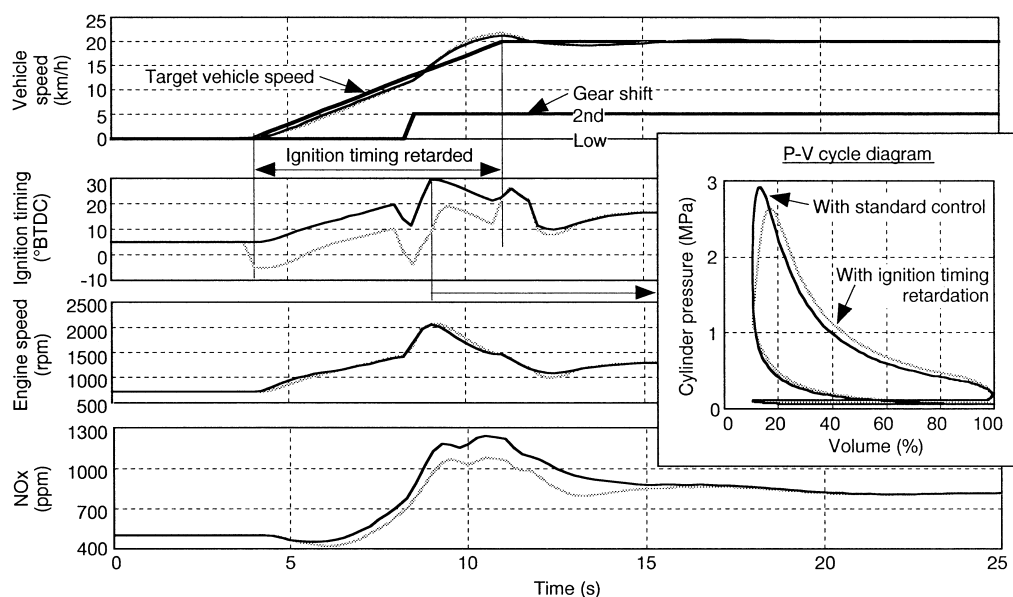


Fig. 4 Example of ignition timing control

change from acceleration to deceleration, fuel cut control took place. When the engine speed dropped to 1000 rpm, the fuel injection restarted. A lean spike occurred owing to the fuel cut. At the same time, because of the lag in transport of fuel that had adhered to the intake ports, unburned hydrocarbon (HC) emissions increased.

Also, the position of the idle speed controller (ISC) valve changed in accordance with the transmission's shift position and feedback correction of the idle speed took place. Tailing of the ISC valve position occurred when the throttle was fully closed during the dashpot control (the ISC valve position control for regulation of the air amount during deceleration).

3.1.2 Ignition timing control

The engine output is basically derived from experimental data. Since the output of a gasoline engine is greatly influenced by the ignition timing, the calculated output is corrected through an engine cycle calculation.

Fig. 4 shows the calculation result corresponding to retardation of the ignition timing by 10° (relative to the standard timing) for prevention of transient knocking during acceleration in the first phase of 10-15-mode operation. As the ignition timing was retarded, the engine output decreased and the vehicle acceleration also decreased. Therefore the driver depressed the accelerator pedal further, and the vehicle speed significantly overshoot the target level. On the other hand, retardation of the ignition timing caused nitrogen oxide (NOx) emissions to decrease.

3.2 10-15-mode calculation

Fig. 5 shows the calculation result performed for 10-15-mode operation of a popular type of car with an AT. Fig. 5 (a) shows the target and actual vehicle speeds. Accelerator was controlled to track the target vehicle speed by means of feedback control, but the

actual vehicle speed slightly exceeded the target vehicle speed. The throttle angle, the engine speed, and the engine output are shown in Fig. 5 (b), (c), and (d) respectively. The engine output value is represented in terms of brake mean effective pressure, which is related to the engine torque and displacement. It can be seen that the engine was mainly operated in the low-speed (up to 2000 rpm) and low-load (up to 0.6 MPa) range in 10-15-mode operation. Fig. 5 (e), (f) respectively show calculated and measured concentrations of NOx emissions. NOx emissions are useful information that gives a solution to minimize exhaust emissions from lean-burn engines. NOx emissions are also derived from experimental data and corrected around the effects of the ignition timing and air/fuel ratio. NOx emissions are greatly influenced by the combustion temperature and air/fuel ratio, so adequate correction logic is required. As shown in Fig. 5 (e), (f), the calculated values corresponded closely to measured values.

Fig. 6 shows the result of analysis of the energy required in the case of Fig. 5. The computer code is capable of representing the amounts of all conditions by numeric values and integrating the values throughout the period of operation, so it is an ideal tool for analysis of factors that affect fuel consumption and for use in efforts to devise fuel economy strategies.

As shown in Fig. 6, the running work employed in 10-15-mode operation consists of the inertial work for accelerating the vehicle, the vehicle's rolling resistance, and the vehicle's aerodynamic resistance. When it is set as 100 %, engine losses (mechanical losses, pumping losses, electrical generation losses, and so on) are 130 %, and drive losses of the AT are added to it, the total value of the losses is 190 %. In other words, propulsion of the vehicle is accompanied by the loss of almost twice as much as energy used for propulsion.

Further, from the calculated energy consumption shown in Fig. 6 for the acceleration, constant-speed,

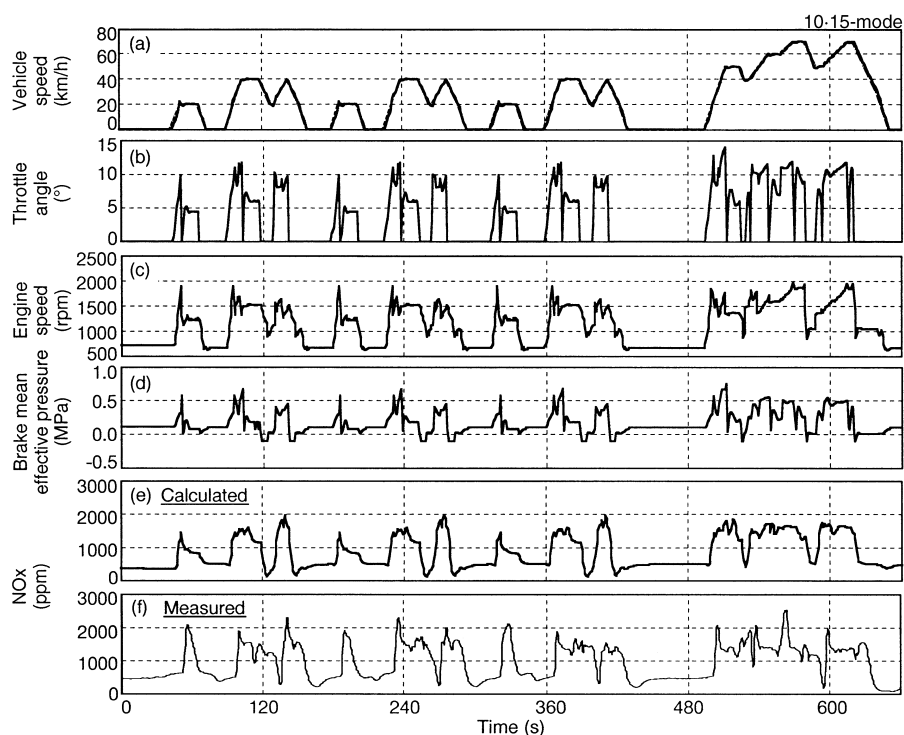


Fig. 5 Example of test driving in 10-15-mode

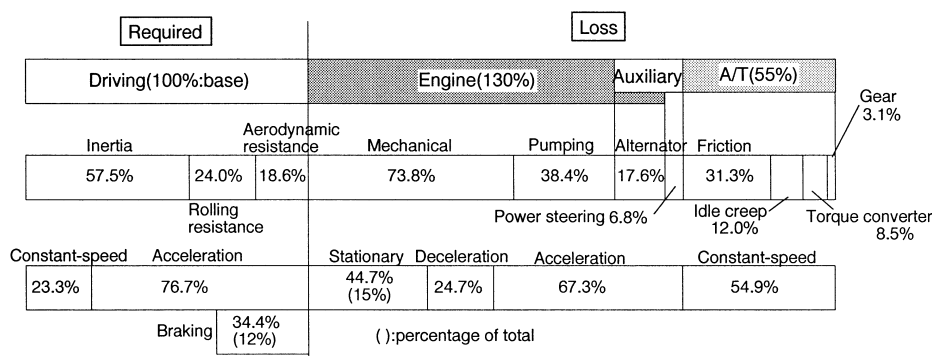


Fig. 6 Energy distribution during 10-15-mode operation of AT car

deceleration, and stationary periods, if the engine stops during the stationary period, 15 % of the total energy can be saved. Also, all of the energy lost in braking amounts to 12 % of the total energy.

3.3 CVT fuel economy and acceleration performance calculation

Since a CVT continuously changes the gear ratio, it can produce smooth acceleration. Also, it can allow the engine speed and load to be kept within the range in which fuel economy is better. Fig. 7 shows the comparison between the engine operating range of a CVT car and that of an AT car during 10-15-mode driving. The dots on the map for the AT car (the left map) were placed according to the engine speed from Fig. 5 (c) as the horizontal axis and the brake mean effective pressure from Fig. 5 (d) as the vertical axis, and plotted at

uniform time intervals. The engine was mainly operated in the low-speed and low-load range in 10-15-mode operation. From the calculation results, the range of engine speed used with the CVT car was even lower than that used with the AT car. The engine output required for propulsion is the same with the CVT car and AT car, so the CVT car's engine runs with higher load (torque) than that of the AT car. As shown in Fig. 7, therefore, the CVT permits the engine to operate in the range where fuel economy is better.

Fig. 8 shows the acceleration characteristics calculated for a CVT car driven in accordance with the same pattern as shown in Fig. 3. It can be seen that the engine speed smoothly changed with the CVT car owing to continuous changes of gear ratio. It can also be seen that, since the CVT permits control of the engine speed arbitrarily, it is possible to run the engine

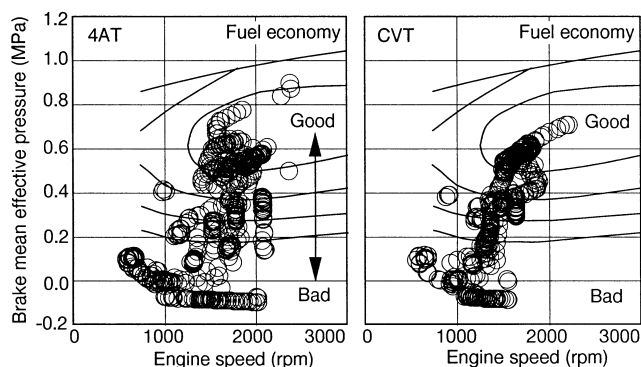


Fig. 7 Operation zones of AT car and CVT car

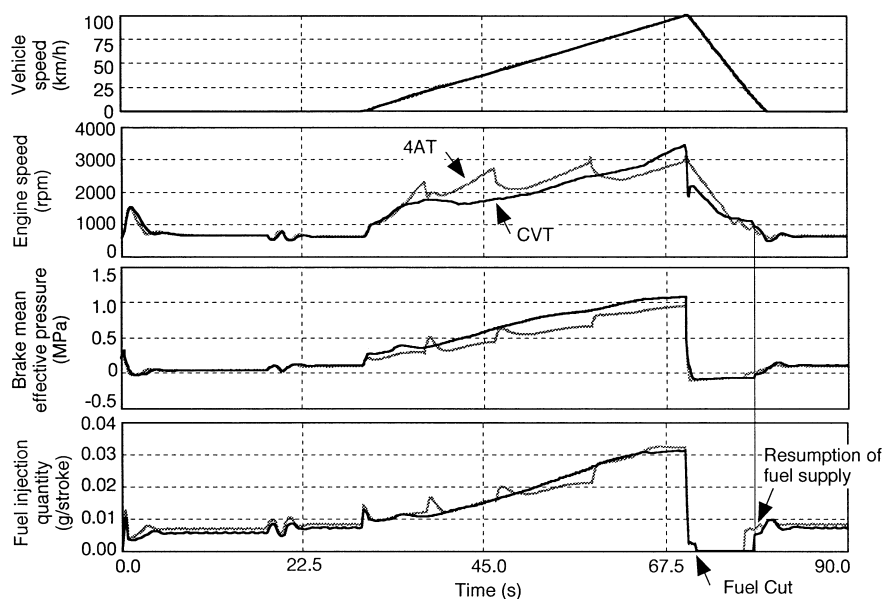


Fig. 8 Acceleration characteristics of CVT car

at lower speed than with the AT and to obtain higher level of torque. Therefore, higher fuel economy can be obtained. Plus, the fuel cut range can be wider for saving fuel because deceleration with the torque converter locked up is possible down to lower vehicle speed with the CVT than with the AT.

3.4 HEV calculation

The greater the degree of freedom in the design of control systems, the more important it is to refine the control concept by means of simulations. An HEV achieves superior fuel economy by using its electric motor to regenerate braking energy, by stopping the engine rather than letting it idle, and by allowing its engine to operate in its more efficient conditions. For the greatest possible benefit, it is essential to develop and employ HEV control logic that takes full advantage of the degree of freedom such as power switching between the engine and motor.

Fig. 9 shows the calculation result performed for an HEV that was controlled to use the motor alone during constant-speed driving under 40 km/h. Fig. 9 (b), (c) respectively show the engine speed and output. Areas

where the engine speed is zero indicate engine stop. Fig. 9 (d) shows the motor output. Positive motor output corresponds to driving, and negative motor output corresponds to generation. Propulsion of the vehicle using the motor alone is indicated by the hatched areas of the figure. It can be seen that the motor was generating mainly during deceleration and was used for driving during constant-speed periods and starting of the engine in the area where positive spikes of motor output appeared. To achieve better fuel economy, the engine load is controlled to 0.4 MPa and higher. Any surplus power (even during acceleration) is used for generation and stored into the battery.

Fig. 9 (e) shows the battery's state of charge (SOC). With an HEV, it is necessary to make fuel economy comparisons without being accompanied by increases and decreases in battery energy. Consequently, it is necessary to make the SOC at the start of vehicle driving and the SOC at the end of vehicle driving identical. In practice, this is achieved by adjusting a starting SOC value.

Fig. 10 shows the engine operating range in the case of Fig. 9. It can be seen from Fig. 10 that the engine was operated only under high-fuel-economy conditions. The average brake thermal efficiency of the engine on the HEV exceeds 30 %, whereas that on the AT car represented in Fig. 7 is approximately 25 %. Fig. 11 shows the result of analysis of the energy balance for the 10-15-mode operation represent-

ed in Fig. 9. As shown, approximately half of the energy supplied for acceleration of the vehicle (inertial work) is recovered by means of regenerative braking and re-used for the power source of propulsion and of the vehicle's electrical equipment. Nevertheless, to operate the engine under high-fuel-economy conditions, this control logic includes the energy cycle that consists of converting the engine's surplus energy to electric energy, keeping it in battery, and using it to drive the vehicle. Therefore the energy losses related to the motor's generating and driving efficiencies occur in this energy reusing cycle.

3.5 Driver characteristics calculation

A comparison of different drivers' habits about accelerator and clutch operations is described here.

Fig. 12 shows the computation result performed for acceleration of an MT car with various levels of accelerator and clutch response. In the result for a driver who operated the accelerator and clutch aggressively, it can be seen that the vehicle speed overshoot the target level at the beginning of acceleration and in the phase where the vehicle made a change from acceleration to con-

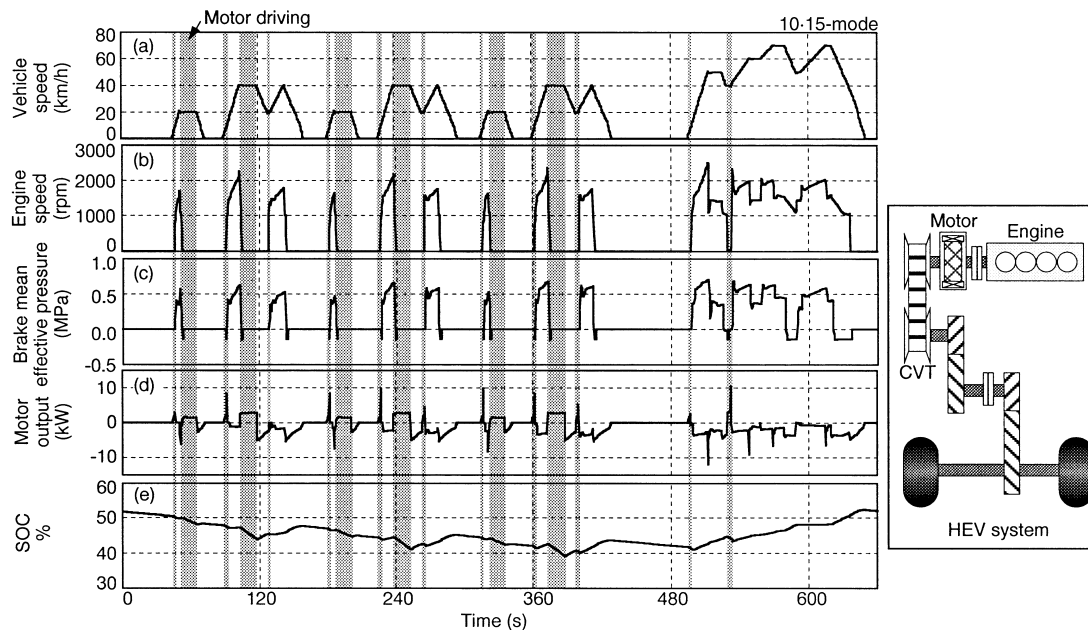


Fig. 9 Example of HEV test driving in 10-15-mode

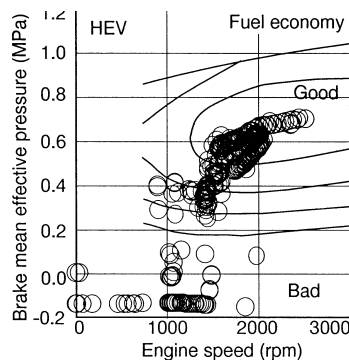


Fig. 10 Operation zone of HEV engine

stant-speed operation. Also, it can be seen that the significant shift shocks which mean projections in acceleration during gear shifts occurred, because the clutch-release time was short and the clutch was engaged before the engine speed had dropped sufficiently. In the result for a driver who operated the accelerator and clutch slowly, it can be seen that the vehicle speed undershot the target level at the beginning of acceleration and that the accelerator pedal was subsequently depressed further to compensate. It can also be seen that the freewheeling occurred during gear shifts, because the clutch was engaged relatively late.

4. Future extension and improvement plan

This simulation program consists of subroutines written in the C programming language. In normal use, subroutines should be combined to create an execution file and input data should be exchanged for the purpose of calculation. However, a user who designs control systems must rewrite the control block (ECU models) to confirm the effect of newly designed control systems.

Most ECU control development is currently performed using Matlab/Simulink^{TM(3)}, so the current C language subroutines are being transferred into S-functions for incorporation into Simulink block diagrams and some of them is being converted into Simulink block diagrams.

An improvement of the engine model to apply to a hardware-in-the-loop simulator (HILS), which can receive signals from an actual ECU and send the calculation results as signals that can be read by the ECU, is also in progress. The improvement includes adoption of an external clock that is necessary for use with a HILS. Furthermore, because it is compulsory to finish the jobs within the designated period between the reference control signals, a new calculation logic is employed. This new logic allocates a task level that is a kind of label classified by the priority to every calculation task, and then the low priority tasks are sometimes skipped when they bump into higher priority tasks.

When measurement data do not exist at the concept stage, engine performance maps can be obtained using an engine simulation code developed by MMC⁽⁴⁾. A program for semi-automatic creation of these maps is also under developing.

5. Summary

Such a computation program that predicts the entire powertrain performance should not be developed by one programmer, because specialized knowledge of every component is needed to make subroutines of them. The best scheme to develop such a program is that each subroutine is developed by relevant experts after the data input/output formats are defined, and then put together like a puzzle to create an entire program that matches the objective. Our hope at MMC is to develop this program into a comprehensive develop-

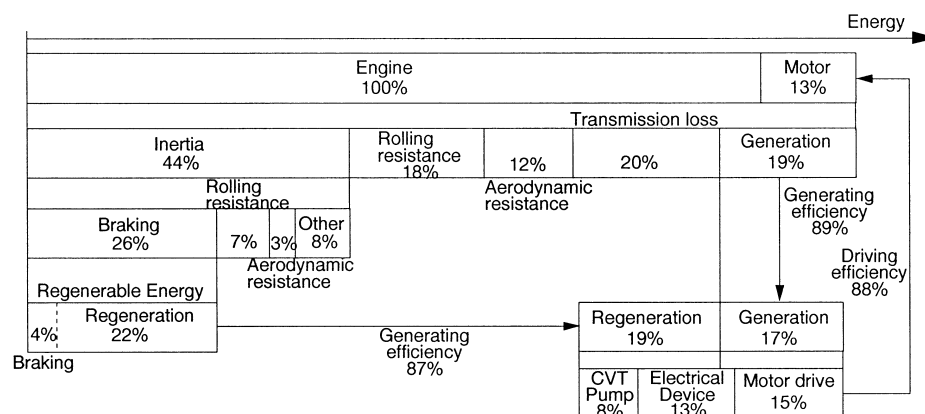


Fig. 11 Energy balance of HEV in 10-15-mode

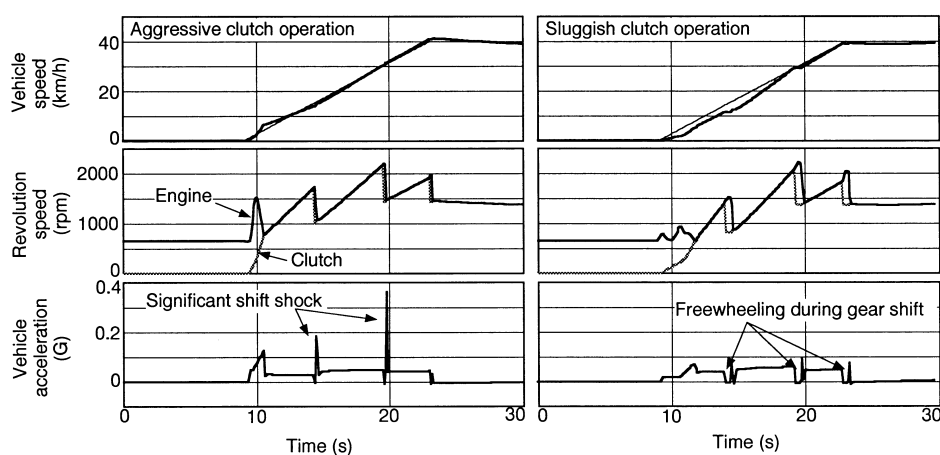


Fig. 12 Clutch operation with different driver models

ment tool. The resulting tool will be an effective means of developing competitive and successful products.

References

- (1) Ando and Motomochi: Internal Combustion Engine, Vol. 27, No. 10, p. 9, October 1988
- (2) Oikawa and Nakagawa: Mitsubishi Heavy Industries Technical Review, Vol. 20, No. 2, March 1983
- (3) Sumiya, Anzai, and Yamashita: Mitsubishi Electric Technical Review, Vol. 74, No. 9, p. 55, 2000
- (4) Kitada, Kuchita, and Ohashi: Mitsubishi Motors Technical Review, No. 11, p. 31, 1999



Masato KUCHITA



Taizo KITADA



Kazuo KIDO

Development of Multivariate Analysis Scheme for Simultaneous Optimization of Heavy-Duty Diesel Engines

Shuhei YONEYA* Masashi YAMAMOTO*
Tatsuya MATSUGUCHI* Yasuaki KUMAGAI*

Abstract

In line with recent increase in the stringency of exhaust emission requirements imposed on diesel engines, MMC is actively introducing electronic control technologies into many components of its products, particularly into the fuel injection system, exhaust gas recirculation system, and variable geometry turbocharger. Electronic control of engine components is very effective in not only reducing exhaust emissions but also in giving flexibility for calibration of the engine performance. However, optimization of electronic control systems involves handling a number of parameters, which renders finding optimum conditions for the systems time-consuming.

Reported in this paper is a statistical analysis scheme to solve this problem in development of electronic control systems that can optimize diesel engines' emission control parameters. The scheme uses as its base the "design of experiments" method which is derived from multivariate analysis. It proved to be effective that this scheme was applied to system optimization studies aiming at reduction in exhaust emissions and fuel consumption. And this scheme also improved parameter analysis under different operating conditions, leading to efficient development of the final systems.

Key words: *Simultaneous Optimization, Exhaust Emissions, Statistical Analysis*

1. Introduction

In order to comply with stringent exhaust emission standards and to respond to eager demands for better fuel consumption, MMC has recently introduced many innovative technologies into the diesel engines of its trucks, including fuel injection systems with a flexible control (such as the common rail system), exhaust gas recirculation systems (EGR), and variable-geometry turbochargers (VG). Electronic control technologies used in these new systems provide the means for increasing the flexibility in optimization of engine performance, but require complicated processes for calibration. If calibration is performed using the conventional "one-factor-at-a-time" method (a parameter study in which each parameter is varied for examination with all other parameters being fixed), engineers encounter the following two problems: (1) uncertainty as to whether or not the calibration results are accurate and optimum, and (2) the calibration process is time-consuming because of the ever-increasing number of parameters.

The multivariate simultaneous optimization scheme is a sort of statistical analysis, that has been developed by Mitsubishi Motors to solve the above-mentioned problems. It is based on the design of experiments⁽¹⁾ which are being widely used in the development of products in many fields. The scheme was used in the calibration of the control systems to optimize exhaust

emissions and fuel consumption of the in-line, six-cylinder, heavy-duty diesel engine equipped with an EGR system and VG to comply with the 1999 exhaust emissions regulation. The scheme consists of two parts. The first part is a multivariate analysis using the design of experiments method in which particular parameters are analyzed for each exhaust gas mode point and, using a prediction formula derived from the results of the analysis, the exhaust gas and fuel consumption characteristics are studied for each mode. The second part is a calculation program using the prediction formula created in the first part in order to obtain the total optimum values of exhaust emissions and fuel consumption to ultimately meet the objective, while taking account of the balance among all the modes on exhaust emissions and engine performance. The following section of this paper details the multivariate simultaneous optimization analysis scheme and its application to an actual case.

2. Experiment planning and analysis using the statistical analysis scheme

2.1 Design of experiment

Electronic technologies are increasingly being introduced for control of engine components with the goal of simultaneously reducing exhaust emissions and improving fuel consumption, and as a result, increasing the number of parameters requiring calibration.

* Engine Test Dept., Truck & Bus Research & Dev. Office

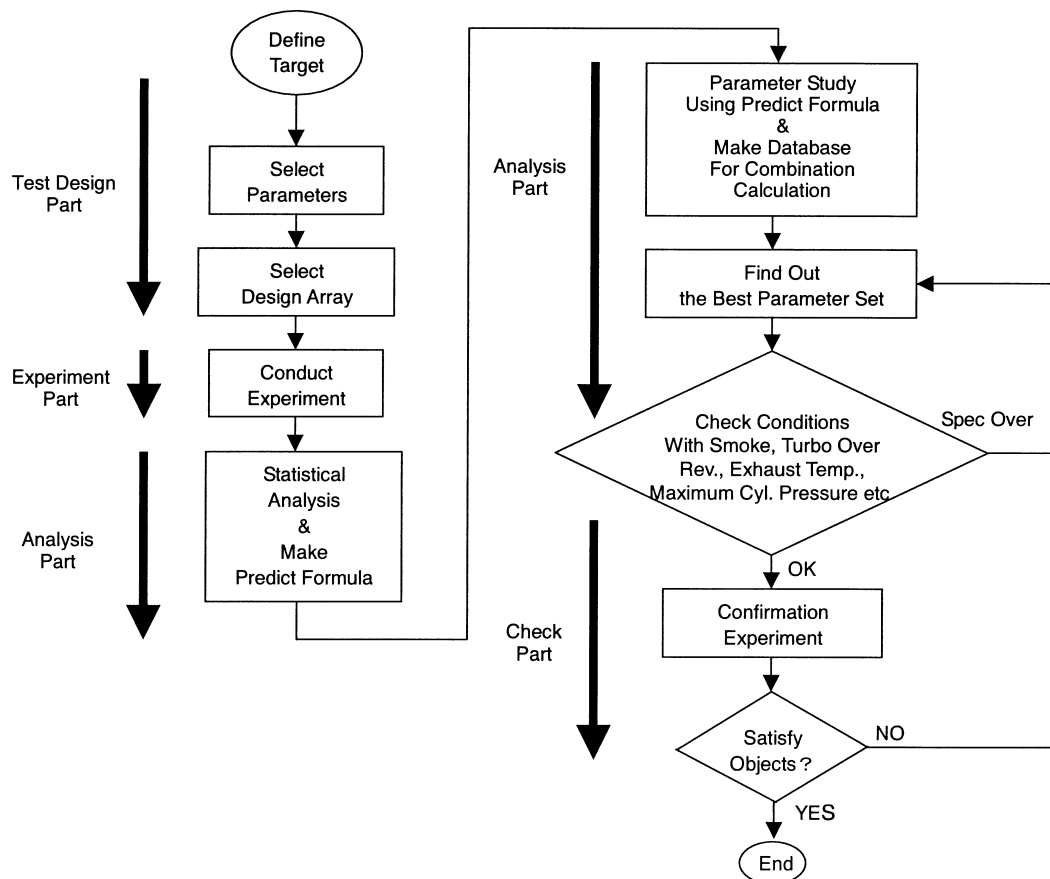


Fig. 1 Flow diagram of the optimization

Calibrating many parameters by repeated experiments using the conventional "one-factor-at-a-time" method is not only inefficient, but also less effective; the method is unsuitable for readily identifying the effect of each parameter and the synergetic or offsetting effects between different parameters (hereinafter collectively called "interaction"), thereby increasing the likelihood of missing the optimum combination of parameters.

The design of experiments method allows, through statistical analysis (primarily the analysis of variance), the calculation of each of the influences and effects that multiple parameters have on experimentally obtained data independently, enabling quantitative evaluation. Another merit of the analysis of variance is that it can provide quantitative representation of not only individual parameters, but also of interactions between parameters, enabling concurrent evaluation of interactions with individual parameters. In particular, the method using an orthogonal design array in the design of experiments effectively solves the problem of an increasing number of test items (the most difficult problem for conventional methods) so that engineers can plan and carry out tests in systematic ways.

2.2 Optimization scheme using design of experiment

Diesel engine exhaust emission tests used in Japan and the European Union consist of 13 different steady state modes. The exhaust emission value is determined by summing the exhaust emission measurements for all of the modes which have been multiplied by the

weighting coefficient specific to each individual mode before the summation. To achieve an optimum combination of exhaust emissions and fuel consumption, it is essential to find an optimum trade-off between factors such as exhaust emissions and fuel consumption, and then to combine parameters so that the total exhaust emission complies with the regulation, while taking account of the balance among modes. Several reports have been made on the application and yielded results of multivariate analysis using the design of experiments method in the development of engines. Nearly all the reported studies focused on engines operating under single conditions^{(2) - (4)}; there were no reports on studies of simultaneous optimization under multiple operating conditions such as those included in the test cycles required by exhaust emission standards.

The multivariate simultaneous optimization scheme described here is an approach developed in order to find the most appropriate combination of parameters for optimizing overall exhaust emissions and fuel consumption, taking account of the balance between multiple operating conditions or modes using the following means and process: experiments and analyses are carried out using the design of experiment; each parameter is quantitatively evaluated; exhaust emissions and fuel consumption are calculated using a prediction formula; and calculation is carried out to find the optimum combination of parameters. This process, from planning of tests to conducting tests and analyses, will be described in accordance with the flow in Fig. 1.

Table 1 Engine specifications

Engine type	6M70T4 (T/C, I/C)
Cyl. bore x stroke	L6, ϕ 135 x 150 (12.9 L)
Max. power, torque	302 kW/2,200 rpm, 1,765 Nm/1,200 rpm
Fuel injection system	Common rail system

Planning of tests

- (1) Determination of test objective (items to be optimized)
- (2) Selection of test parameters and determination of the number of levels

If the number of levels assigned to each parameter is "n", the order of the approximation expression derived becomes "n-1". It is therefore necessary to determine the number of levels that is sufficient to identify the tendency. The level-to-level interval is then determined for each parameter in each mode. In doing so, it is considered that the exhaust temperature, smoke, turbine and engine speed, maximum cylinder pressure, and so forth, have limitations, and the test conditions are kept within a range which does not cause any operational trouble or engine damage.

- (3) Selection of orthogonal design array and parameter layout

Selection of the orthogonal design array depends on the number of levels and number of parameters. Several types of design array are available for use depending on the number of parameters and levels, e.g., L18 and L27 (the number in the name of each orthogonal design array type indicates the number of times tests were carried out for the array). The parameters are assigned to the orthogonal design array using linear graph (a schematic that correlates the relationship between parameters with the row number of the orthogonal design array).

Orthogonal tests

- (4) Tests are carried out in accordance with the orthogonal design array.

Data analysis

- (5) Analysis of variance and creation of prediction formula
Analysis of variance is conducted on the data obtained from the orthogonal tests, at each mode. At the same time, a prediction formula is created using Chebychev's orthogonal polynomial (a type of approximate expression).

- (6) Creation of predicted performance value database
Detailed parameter studies are carried out using the prediction formula in order to create a database of predicted performance value.

- (7) Deduction of optimum parameters
Calculation is carried out using the database of predicted performance value in order to find a combination of parameters that simultaneously optimizes exhaust emissions and fuel consumption.

Verification tests

- (8) The engine, calibrated to the above-mentioned parameter combination, is operated and the calibration is verified for appropriateness. If the calibration includes any discrepancy, the combination-finding calculation of step (7) is performed again.

Table 2 Analysis of variance (9th mode)

Designed parameters	Contribution %		
	NOx	PM	FC
VG vane position	6.37	9.69	1.65
EGR valve lift	41.87	10.93	2.69
Injection timing	15.27	11.52	51.43
Common rail pressure	24.36	27.33	37.40
Injection nozzle diameter	0.18	0.50	1.20
Injection nozzle core angle	1.02	2.11	0.36
VG vane position x EGR valve lift	8.20	8.03	2.58
VG vane position x injection timing	***	***	***
EGR valve lift x injection timing	***	***	***
Error	2.74	29.88	2.69

***: Pooled

3. Application of simultaneous optimization scheme

The multivariate analysis scheme for simultaneous optimization described above was actually applied to tests conducted seeking conformance with the 1999 exhaust emission standards. This will be described below by way of example.

3.1 Optimization objective and parameters tested

The ultimate objective for optimization using the multivariate analysis scheme was to comply with the 1999 exhaust emission regulation in terms of the 13-mode nitrogen oxides (NOx) and particulate matter (PM) emissions, and to simultaneously reduce the fuel consumption (FC). 12.9-liter, in-line, six-cylinder diesel engine with intercooled turbocharger was used for the tests and analysis (see **Table 1**). Six parameters were selected for optimization testing: the fuel injection timing, common rail pressure, VG vane position and EGR valve lift as the electronic-control-related parameters, and the injection nozzle hole diameter and injection hole angle as the parameters fixed during the mechanical design stage (six parameters in total). Each parameter was given three levels of the same intervals so that a second-order approximation could be obtained, and the parameters with different levels were assigned on L27 orthogonal design array. Tests were then conducted 27 times as the 13-mode exhaust emission test according to the orthogonal design array. By using the design of experiment, the tests were performed only 27 times for all the necessary parameter studies, which otherwise would have required tests for all combinations of the parameters (i.e., $3^6 = 729$ times). The parameters were allocated so that interactions between the VG vane position, EGR valve lift and fuel injection timing were also considered. The schematic (or linear graph) representing the parameter allocation is shown in **Fig. 2**.

3.2 Analysis of variance (analysis and studies at each mode)

After conducting the 27 tests according to the parameter allocation on the orthogonal design array, an analysis of variance was carried out for each mode. **Table**

L27 Orthogonal design array

	1	2	3	4	5	6	7	8	9	10	11	12	13
	VG	EGR	VG*EGR	VG*EGR	IT	VG*IT	VG*IT	EGR*IT	RP	ND	EGR*IT	NCA	ERR
1	1	1	1	1	1	1	1	1	1	1	1	1	1
2	1	1	1	1	2	2	2	2	2	2	2	2	2
3	1	1	1	1	3	3	3	3	3	3	3	3	3
4	1	2	2	2	1	1	1	2	2	2	3	3	3
5	1	2	2	2	2	2	2	3	3	3	1	1	1
6	1	2	2	2	3	3	3	1	1	1	2	2	2
7	1	3	3	3	1	1	1	3	3	3	2	2	2
8	1	3	3	3	2	2	2	1	1	1	3	3	3
9	1	3	3	3	3	3	3	2	2	2	1	1	1
10	2	1	2	3	1	2	3	1	2	3	1	2	3
11	2	1	2	3	2	3	1	2	3	1	2	3	1
12	2	1	2	3	3	1	2	3	1	2	3	1	2
13	2	2	3	1	1	2	3	2	3	1	3	1	2
14	2	2	3	1	2	3	1	3	1	2	1	2	3
15	2	2	3	1	3	1	2	1	2	3	2	3	1
16	2	3	1	2	1	2	3	3	1	2	2	3	1
17	2	3	1	2	2	3	1	1	2	3	3	1	2
18	2	3	1	2	3	1	2	2	3	1	1	2	3
19	3	1	3	2	1	3	2	1	3	2	1	3	2
20	3	1	3	2	2	1	3	2	1	3	2	1	3
21	3	1	3	2	3	2	1	3	2	1	3	2	1
22	3	2	1	3	1	3	2	2	1	3	3	2	1
23	3	2	1	3	2	1	3	3	2	1	1	3	2
24	3	2	1	3	3	2	1	1	3	2	2	1	3
25	3	3	2	1	1	3	2	3	2	1	2	1	3
26	3	3	2	1	2	1	3	1	3	2	3	2	1
27	3	3	2	1	3	2	1	2	1	3	1	3	2

	Level		
	1	2	3
VG vane position (VG)	1	2	3
EGR valve lift (EGR) mm	0	3	6
Injection Timing (IT) °BTDC	0	5	10
Rail Pressure (RP) MPa	70	90	110
Nozzle Diameter (ND) mm	0.2	0.22	0.24
Nozzle Cone Angle (NCA) °	154	157	160

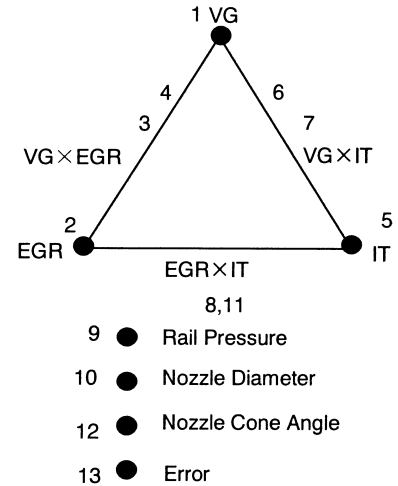


Fig. 2 L27 orthogonal design array with linear graph

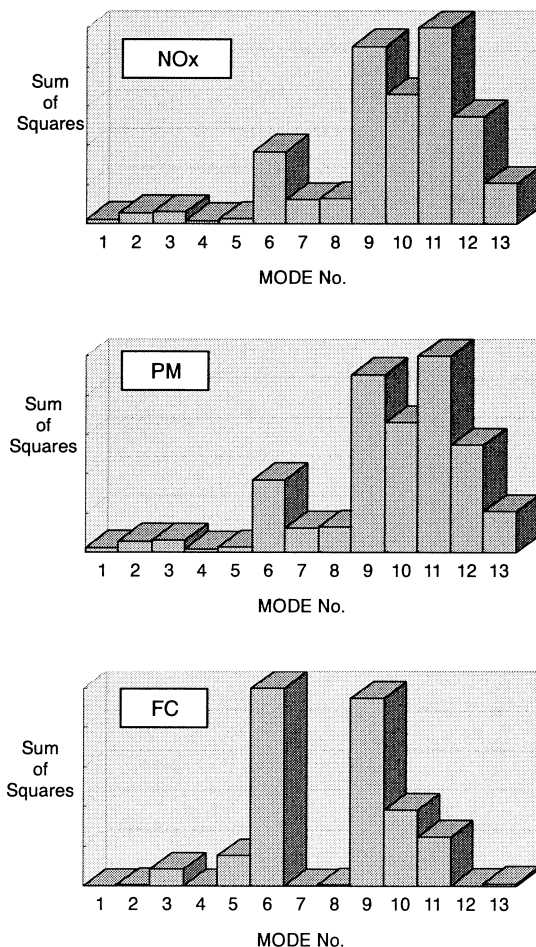


Fig. 3 Comparison of alteration of emissions and fuel consumption between modes

2 shows the analysis results (contribution of each parameter) for the ninth mode. The following are inferred from the results: the common rail pressure and fuel injection timing substantially contribute to NOx, PM and fuel consumption; the EGR valve lift and the interaction between the VG vane position and EGR valve lift (expressed as "VG vane position x EGR valve lift" hereinafter and in Table 2) also contribute significantly to NOx and PM emissions; the other parameters contribute only slightly. The results of the test also show that the two interactions, "VG vane position x fuel injection timing" and "EGR valve lift x fuel injection timing", contribute very slightly. The large contribution by the interaction "VG vane position x EGR valve lift" can be explained by the following: with the tested engine, EGR gas is introduced into the EGR system when the turbine inlet pressure is increased by throttling the VG vane; the EGR operation is therefore closely related with the VG vane position. Thus, the analysis of variance is adequately capable of quantifying interactions between parameters.

Fig. 3 compares the "total variations" of emissions (NOx and PM) and fuel consumption between modes. The total variation refers to the sum of the square of deviation of the data obtained from the orthogonal design array experiment. The total deviation increases, as variation by each parameter changes largely within the range adopted in the orthogonal design array experiment. Therefore, by comparing the total variations of different modes, it is possible to find the modes that would contribute most significantly to reduction of exhaust emissions and fuel consumption. In the orthogonal experiments discussed here, use of uniform

Target data : y
 Total data Average : μ
 Parameter : A, B
 Average of Levels : A_m, B_m
 Number of Levels : a, b
 Interval of Levels : h_A, h_B

A_k, B_n : Sum of data [$A(B)$ level = $k(n)$]
 AB_{kn} : Sum of data [A level = k , B level = n]
 k, n : Level
 i, j : Order number
 r : Number of data

$$y = \mu + K_{A1}(A - A_m) + K_{A2}\left[(A - A_m)^2 - \frac{(a^2 - 1)h_A^2}{12}\right] \\ + K_{B1}(B - B_m) + K_{B2}\left[(B - B_m)^2 - \frac{(b^2 - 1)h_B^2}{12}\right] \\ + K_{AB}(A - A_m)(B - B_m)$$

$$K_{Ai} = \frac{(W_1A_1 + W_2A_2 + \dots + W_nA_n)}{r \cdot \lambda S \cdot h_A^i}$$

$$K_{Bi} = \frac{(W_1B_1 + W_2B_2 + \dots + W_nB_n)}{r \cdot \lambda S \cdot h_B^i}$$

$$K_{AB} = \frac{\sum_k W_k^i \left[\sum_n W_n^j (AB_{kn}) \right]}{[r \cdot (\lambda S)_A \cdot h_A^i \cdot (\lambda S)_B \cdot h_B^j]}$$

Fig. 4 Explanation of predicted formula

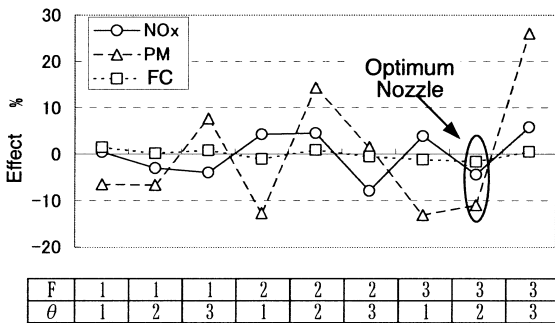


Fig. 5 Effect of injection nozzle specification on emissions and fuel consumption

intervals in setting the level of each parameter enabled the total variation of all the modes to be compared on the same basis. Namely, the difference in the total variation among modes corresponds exactly to the difference in sensitivity of the parameters, so that the graphs can provide the means for finding the mode that are most advantageous for each performance value. As seen from the graphs, the sixth mode and the ninth through twelfth modes have greater variation with regard to NOx and PM emissions, and the sixth mode and ninth through eleventh modes have greater variation with regard to fuel consumption. This indicates that, for example, if each parameter were varied in the twelfth mode, the NOx and PM emissions could be lowered without adversely affecting fuel consumption. Detailed study of the balance among modes leads to overall concurrent optimization of exhaust emissions and fuel consumption.

3.3 Creation of prediction formula and parameter studies

With the design of experiment, a prediction formula that uses Chebychev's orthogonal polynomial (see Fig. 4) can be obtained through conducting orthogonal

experiments. This formula includes an interaction term, therefore it is capable of taking account of interaction between the VG vane position and EGR valve lift that is calculated in the analysis of variance. This prediction formula was applied to each exhaust emission mode point in order to perform further detailed parameter studies, which could not be achieved with experiments using an actual engine, and a database containing predicted exhaust emissions and fuel consumption for each mode was created. The prediction database data were then combined for every mode in order to calculate the exhaust emissions and fuel consumption of that mode. The combination calculation was carried out using the predicted values after setting target values for exhaust gas temperature, turbine speed, cylinder pressure and other engine's durability-related factors to certain values. Within the limitations thus established, parameter combinations that met the target were calculated for final optimization.

4. Exhaust emissions optimization calculation

4.1 Selection of injection nozzle parameters

The injection nozzle parameters are invariable throughout the 13-mode tests. For this reason, it is necessary to determine each nozzle parameter value after recognizing how each parameter affects emissions and fuel consumption. Fig. 5 is a factor-effect diagram that shows the effects of each parameter on NOx, PM and fuel consumption for nine different nozzle specifications (three injection hole diameters "F" x three injection hole angles "θ"). Plotted on the y-axis are the deviations (expressed in percentages) from the average of the data obtained through the orthogonal experiments conducted 27 times. The deviations below the zero line represent drops in the emission or fuel consumption value. As is evident from the graph, the fuel injection nozzle

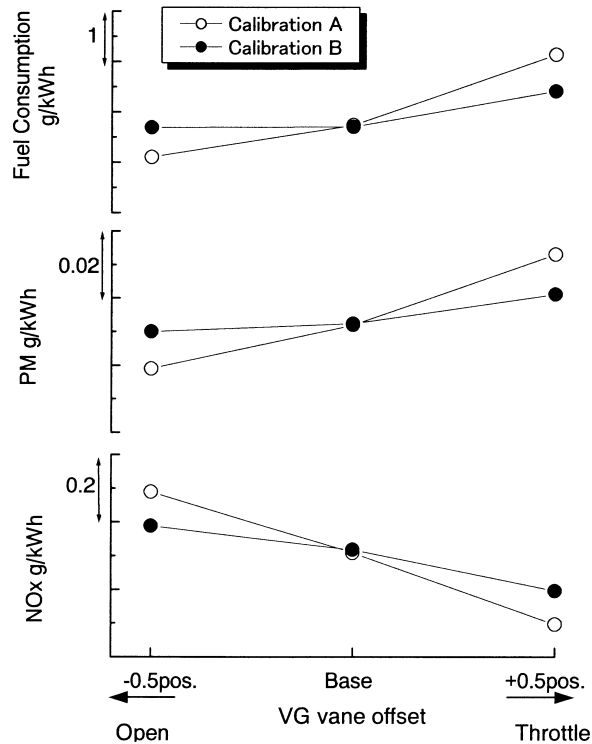


Fig. 6 Analysis of characteristics between Calibration A and Calibration B

specification that shows negative deviations for all of the NOx, PM and fuel consumption values is the “F3 · θ_2 ” specification. This specification was thus selected as the optimum nozzle specification and used in the 13-mode exhaust emissions optimization calculation in order to calibrate each control parameter for compliance with the exhaust emissions regulation.

4.2 Mode-by-mode characteristics evaluation

Two different calibration approaches were found as a result of the optimization calculation. One is a parameter set (A) that can obtain low exhaust emissions and fuel consumption by a throttling VG vane position, high EGR, and advanced injection timing. The other parameter set (B) consists of a more opened VG vane position, low EGR, matching with injection timing and common rail pressure. It is difficult to judge either one superior by only comparing the exhaust emission levels achieved. An appropriate method for evaluation was to assess the characteristics resulting from variation by the VG vane setting which was one of the major factors that affected exhaust emissions and fuel consumption. Two approaches were evaluated as follows: calculation was carried out for both approaches with the VG vane position offset by ± 0.5 , and the resulting NOx, PM and fuel consumption values were compared (Fig. 6). The results of Calibration A showed sensitivity to variation in the VG vane setting for all of NOx and PM emissions and fuel consumption, which means that the approach would also be sensitive to variations resulting from the production process. The conclusion derived from the calculation was that the parameter set (B) is a superior

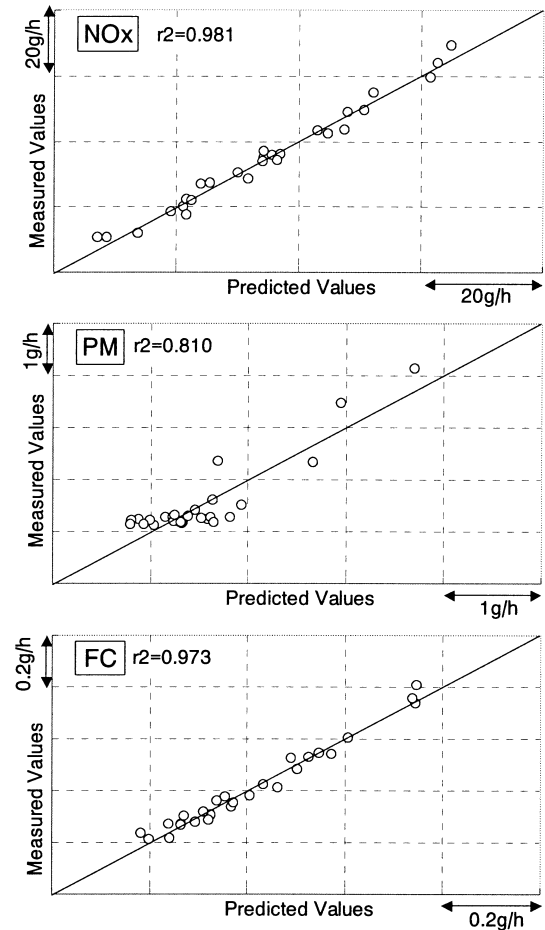


Fig. 7 Correlation between predicted and measured values (ninth mode)

method to the parameter set (A). This method makes it possible to optimize the parameters, including deviation, and also to determine control intervals from the deviation range to predicted values. Next, the optimum parameter values from parameter set (B) were used for verification tests with the engine.

4.3 Verification test on engine

Before verifying calculation results using the actual engine, the prediction accuracy of the prediction formula used in the parameter studies was examined. Fig. 7 shows the correlation of the predicted values with the measured values for the ninth mode. The correlation coefficients for NOx and fuel consumptions (0.981 and 0.973, respectively) were high enough for the exhaust emission optimization calculation to be regarded as valid. The correlation coefficient for PM was 0.810, which is rather lower than the other two items. However, this level of accuracy is considered sufficient for judging the qualitative tendency of PM emission.

Next, optimization calculation was carried out using Calibration B with the “F3 · θ_2 ” specification determined as the fuel injection nozzles. The results were compared with measurements obtained from experiments on the actual engine. The result of the verification is shown in Fig. 8. The calculated NOx and fuel consumption val-

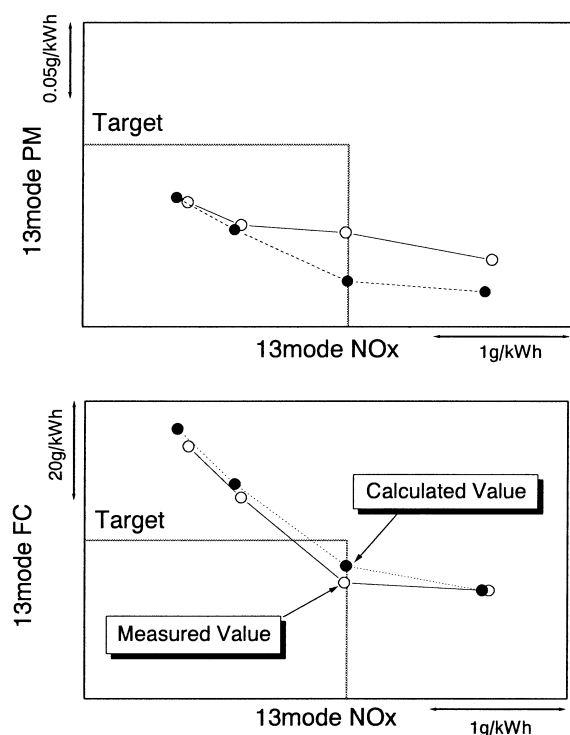


Fig. 8 Comparison of predicted and measured emissions and fuel consumption

ues agreed closely with the actual measurements and were at levels satisfying the 1999 exhaust emission regulation. The PM values, as described above in the discussion on prediction accuracy, included some discrepancy between calculated and measured values and actual measurements. This may have resulted from the following: orthogonal experiments were carried out for each mode separately, and the engine operation condition before the mode tests had greater influence on PM measurements than on NOx and fuel consumption measurements. Another error may be caused through predicting PM values from smoke and hydrocarbon values.

Through the above-mentioned verification process, it was confirmed that the simultaneous optimization scheme is capable of predicting the exhaust emissions and fuel consumption fairly accurately and can successfully shorten the time required for emission and fuel consumption optimization.

5. Summary

A scheme based on the design of experiment was developed for use in simultaneous optimization of diesel engine parameters and, from the results of its actual application to optimization of exhaust emissions and fuel consumption, the following conclusions were drawn:

- (1) Quantitatively determining the influence (contribution) that each parameter has on exhaust emissions

and fuel consumption can provide guidelines for selecting an approach for calibration.

- (2) A prediction formula created by applying the design of experiment to each exhaust emission mode point enables detailed parameter studies to be conducted without actual measurements. Through calculation using the results of the parameter studies, exhaust emissions and fuel consumption can be optimized overall.
- (3) Parameter studies using the prediction formula enable the prediction of exhaust emissions and fuel consumption when each factor varies, which has characteristics that are less influenced by deviation (or that are advantageous to productivity).
- (4) A multivariate simultaneous optimization scheme method has been successfully established, which can be carried out efficiently in a short period, by applying the design of experiments.

References

- (1) Taguchi, G.: "Design of Experiments", Third Ed., Maruzen
- (2) Hunter, C. E. et al.: "Simultaneous Optimization of Diesel Engine Parameters for Low Emissions Using Taguchi Method", SAE Paper 902075
- (3) Hchschwarzer, H. et al.: "Fully Automatic Determination and Optimization of Engine Control Characteristics", SAE Paper 920255
- (4) O'Conner, J. F., White, C. L., and Charnley, M. R.: "Optimizing CFD Prediction of Diesel Engine Combustion and Emissions Using Design of Experiments; Comparison with Engine Measurements", SAE Paper 982458
- (5) M. Yamamoto, S. Yoneya, T. Matsuguchi, Y. Kumagai: "Optimization of Heavy-Duty Diesel Engine Parameters for Low Exhaust Emissions Using the Design of Experiments", SAE Paper 2002-01-1148



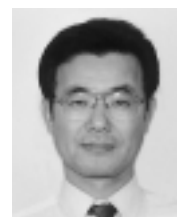
Shuhei YONEYA



Masashi YAMAMOTO



Tatsuya MATSUGUCHI



Yasuaki KUMAGAI

Development of New Index Capable of Optimally Representing Automobile Aerodynamic Noise

Hisafumi DOI* Masaru KOIKE**

Abstract

Sound pressure level, or dB(A), is usually used as an index to represent the amount of noise when comparing the aerodynamic noise generated in a certain vehicle model with that of another. The result of such a comparison, however, is sometimes inconsistent with the result of a comparison based on human auditory feeling. The discrepancy results from difference in quality between aerodynamic noises; certain high decibel noises are not always noisy to the ear and the reverse is also true. To resolve this discrepancy, a new noise representing index has been developed. The index is an outcome of a system that uses a dummy head capable of reflecting changes in acoustic fields as if a human body were present and a processing system that combines the dummy head's outputs appropriately with a psychological acoustic index that has taken into account the nonlinearity of human auditory sense and other relevant factors. The new index shows remarkably improved consistency with human auditory feeling and the system can provide an effective means in developing vehicles in which drivers and passengers feel real quietness.

Key words: *Wind Tunnel, Acoustics, Noise*

1. Introduction

The level of aerodynamic noise increases in proportion to the sixth power of vehicle speed, while noise of other origins increase in proportion to approximately the fourth power of vehicle speed. This explains why aerodynamic noise is predominant over other noises when a vehicle is running at high speed. Progress in engine- and road-noise insulation technologies has also made aerodynamic noise more conspicuous than other noises. Researchers are therefore keen to find ways to reduce the generation of turbulence, which is the origin of aerodynamic noise, and to improve sound-insulation measures for reducing noise in the cabin.

Despite the importance of research into air-flow smoothening technology and efficient sound-insulating methods, the sound pressure level currently used as an index to represent aerodynamic noise in such research is not always consistent with the degree of noisiness to the ears of drivers and passengers because the tone of noise varies from vehicle to vehicle.

The reason why the sound quality of aerodynamic noise differs between vehicles can be seen in the diversity of its sources, which include turbulence that occurs around door mirrors and front pillars, outflow of air through gaps around doors, resonance that occurs in cavities, air-flow-induced vibration of panels, aeolian tone resulting from Karman vortices, etc.⁽¹⁾, each contributing to aerodynamic noise in different degrees.

The factor that causes the difference in the degree of noisiness of noise between vehicles is not only the above-mentioned differences in sound quality but also the balance with other noises, such as road noise⁽²⁾. In

particular, in a vehicle with large road noise, aerodynamic noise tends to be less noisy to the ear.

The factor that contributes the most to the increase in noisiness of noise is not necessarily the sound component whose frequency corresponds to the highest sound pressure level. For this reason, it is essential for effective improvement of the cabin acoustical environment to clearly identify the frequency components that truly make the quality bad to the ear, and to use the results to devise appropriate measures.

There are various types of sound quality evaluation indices that have been proposed by researchers in psychoacoustics fields, but the indices proposed so far are not universal to the immense variety of sounds, ranging from sharp jet engine noise to the rustling sound of air conditioners. The current status of qualitative evaluation of noise is such that a specific index is developed for application to a specific category of noise.

Various sound quality evaluation approaches have also been attempted for the aerodynamic noise of vehicles^{(2) - (5)}, and the development of an evaluation method based on objective human auditory feeling tests is currently in progress.

This paper reports on research conducted by MMC with the goal of establishing a psychoacoustic index appropriate for evaluating aerodynamic noise experienced in the cabins of vehicles in wind tunnel tests. In this research, noise measurement was carried out using a dummy head which was capable of simulating the acoustic field surrounding the driver (which will vary depending on whether the driver is present or not), and the sound-collecting effects at the position of human ears. Through test data processing, a set of psychoa-

* Performance Testing Dept., Car Research & Dev. Office

** Studio Packaging Engin. Dept., Car Research & Dev. Office

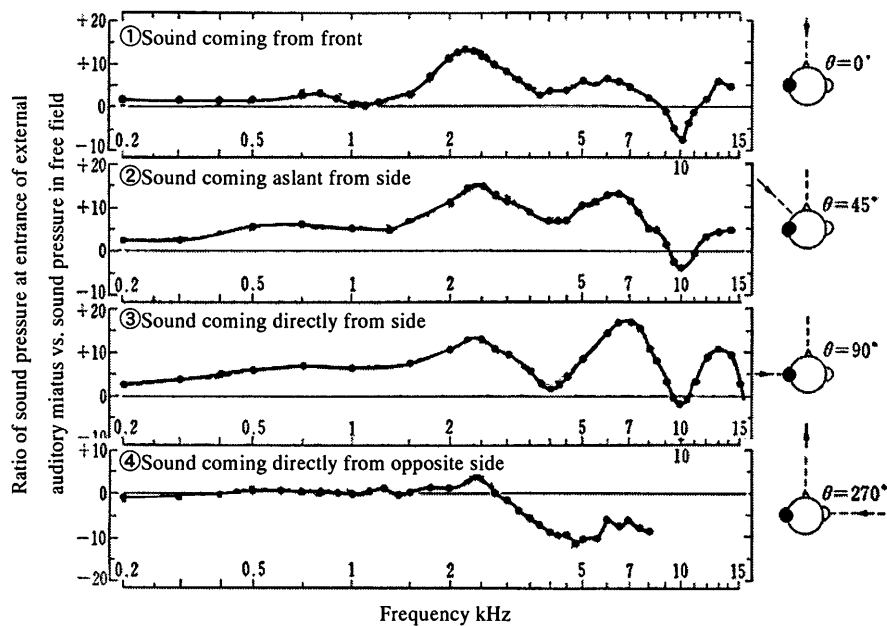


Fig. 1 Change in acoustic field caused by the presence of a human body

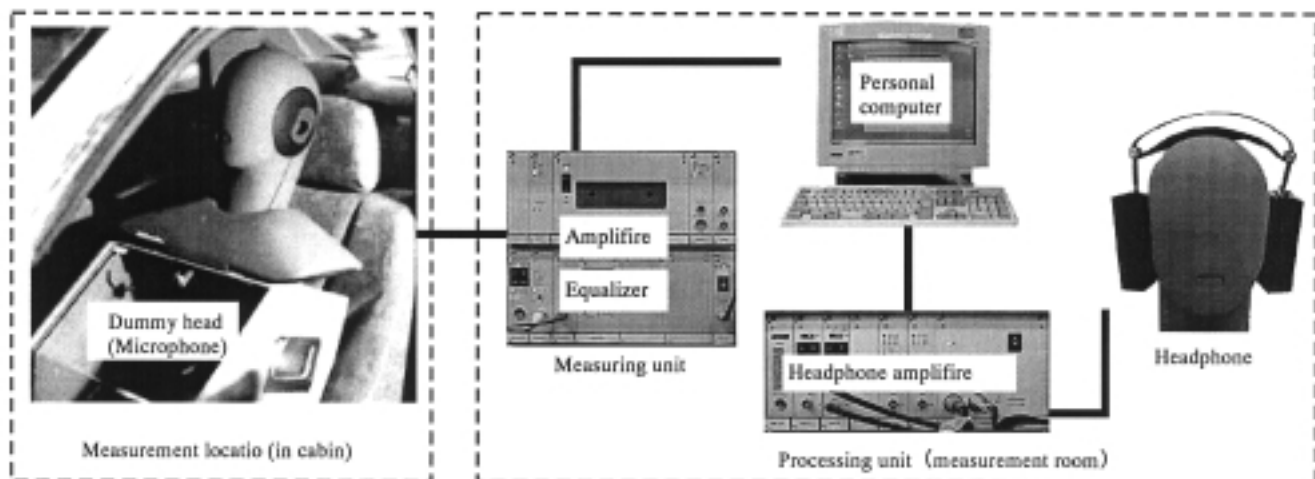


Fig. 2 Dummy-head noise measurement system

oustic indices most appropriate for evaluating aerodynamic noise was selected from among various indices by conducting verification tests on numerous types of vehicles. The new index set proved to be far more consistent with human auditory feeling than with the A-weighted sound pressure level, which is a conventionally used index that is based on sound pressure measurements midpoint between the front seats. The new index set was then actually applied to the noise-improvement tests of a vehicle under development, and it could successfully identify the specific frequency component of noise that constituted the largest factor of noisiness, thereby enabling efficient countermeasures to be taken.

2. Test method

The physical quantity of noise that has been conventionally used by engineers to evaluate aerodynamic

noise is the sound pressure level that is measured through a microphone installed midpoint between the front seats. The acoustic field, however, is different depending on whether or not the presence of a human head is assumed. Fig. 1 shows the differences between sound pressure levels measured at the entrance of external auditory meatus of one human ear and levels measured with an ordinary microphone, using the microphone-measured levels as the reference. As seen from the diagram, the sound pressure level at the position of the human ear is amplified when the frequency of the sound is around 3 kHz or 6 kHz, and may reach a level as high as 10 dB⁽⁶⁾, although the amplitude depends on the direction from which the sound travels to reach the ear.

In view of the above facts, we introduced a dummy head and the data processing system shown in Fig. 2 in order to collect data that would correspond to human auditory feeling. The dummy head was installed inside

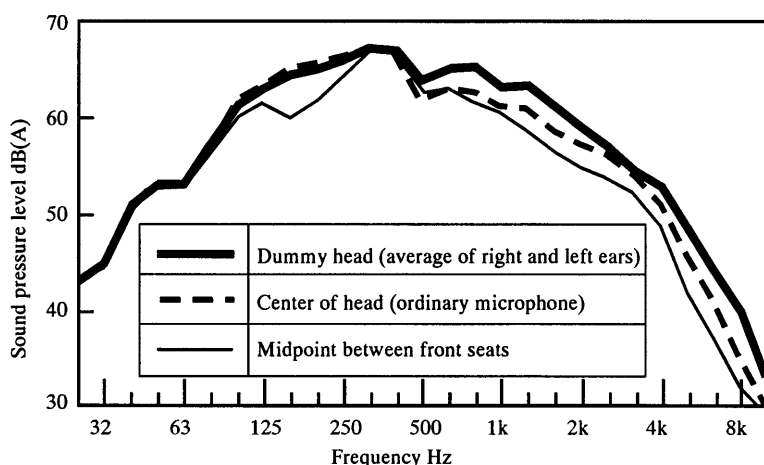


Fig. 3 Sound pressure levels measured using dummy head and those measured using a microphone

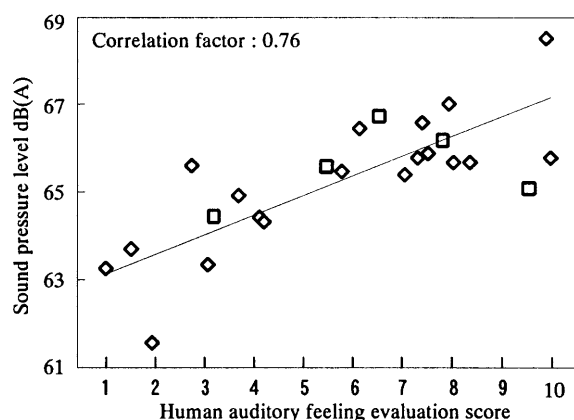


Fig. 4 Correlation between sound pressure levels and human auditory feeling

each of the vehicles placed in the wind tunnel, and the sound signals coming out of the dummy head were sent to a personal computer via an amplifier and stored as time-based waveforms. The stored data could later be retrieved for frequency analysis and could also be reproduced into sound that could be heard using headphones, in order to compare it with the noise of another vehicle. The dummy head used in the tests was a German Head Acoustics' product.

Fig. 3 compares the sound pressure levels measured using the dummy head and those measured using an ordinary microphone, both installed in a vehicle that was placed in the wind tunnel. As seen from the graph, the dummy-head measurements differ significantly from the ordinary microphone measurements in the frequency zone of 500 Hz and higher. These results are consistent with the difference in the sound pressure acting on a human ear depending on the sound-incoming direction shown in Fig. 1. The likely reasons for the difference are as follows: the 500-Hz and higher-frequency components of the noise heard in a vehicle's cabin are generated in the areas around the front and center pillars and the door mirror which are all located diagonally in front of or on the side of the driver.

Fig. 1 shows that the high-frequency components of the sound from these directions are amplified and this explains why the dummy-head outputs are higher than the ordinary microphone outputs, as shown in Fig. 3.

3. Approach used for quantifying human auditory feeling

In order to identify the correlation between physical quantities (such as the sound pressure level) and human auditory feeling, the following approach was used for quantifying the human auditory feeling. Different types of vehicles were placed in a wind tunnel one at a time; the dummy head shown in Fig. 2 was installed in the front seat of each vehicle; and the aerodynamic

noise was recorded with the wind tunnel's mainstream velocity set at 120 km/h. Noise recording was carried out on 29 vehicles which included recent models of randomly selected luxury cars and compact class cars.

It is known that among the factors that constitute quality of aerodynamic noise, "loudness", "sharpness" and "fluctuation" are predominant, and other factors are far smaller in their degree of contribution⁽⁵⁾. This means that the human auditory feeling of the aerodynamic noise can be expressed one-dimensionally by the weightiness and the balance of the three factors. The human auditory feeling perceived in each test vehicle was then quantified by using "paired comparison method". The paired comparison method is a means for objectively quantifying the human auditory feeling, in which an evaluating person compares a pair of sounds and selects the less noisy one, then repeats the process for all the sound pairs. The pair comparison was carried out by 12 persons and their evaluation results were summed in order to determine the evaluation score for each sound. The number of vehicles used for the test was 29, therefore the number of pairs amounted to 406. In order to carry out the evaluation efficiently, one person performed comparisons for all 406 pairs and the pairs with evident differences were excluded from the comparison. Eleven persons then carried out comparisons for all of the remaining pairs.

4. Correlation between human auditory feeling and sound pressure level

Fig. 4 shows the correlation between the human auditory feeling quantified using the method described in the preceding section, and the sound pressure levels (conventionally used noise evaluation index) measured using a microphone located midpoint between the front seats. Plotted on the x-axis are the evaluation scores of the human auditory feeling that are assigned to individual vehicles such that the feeling of the vehicle evaluated as being the worst is given the score of 1 and that evaluated as being the best is given the score of 10; the

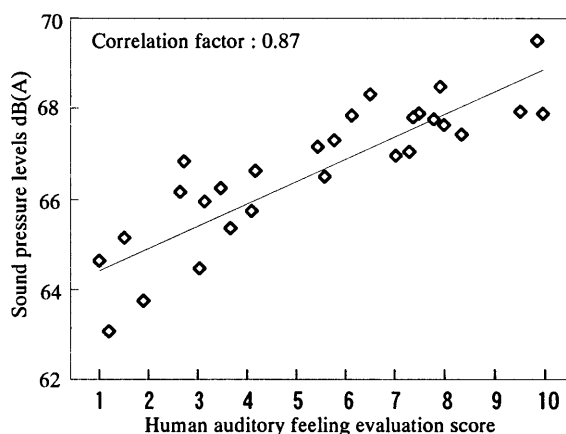


Fig. 5 Correlation between dummy-head-detected sound pressure levels (average of both ears) and human auditory feeling

quantified feeling levels between them are given scores of nine different ranks (this also applies to the x-axis of Figs. 5 and 8). If the graph shows feeling evaluation and sound pressure level data clustering on the same line, these two types of data correlate well with each other. The graph, however, indicates the presence of many vehicles whose data are scattered from the line. This means that there are vehicles whose pressure level is low but the auditory feeling is evaluated as being bad, and vice versa. The correlation between the sound pressure level and human feeling for this case is 0.76.

5. Effects of measurement using dummy head

Because the sound pressure levels measured using an ordinary microphone showed poor correlation with the evaluation scores of human auditory feeling as described above, sound pressure level data obtained from a dummy head were used for the correlation study instead of the ordinary microphone data, in expectation of finding a physical quantity that corresponds better to human auditory feeling.

Fig. 5 shows how the evaluation scores of human auditory feeling correlate with the averages of the sound pressure levels detected by the dummy head's right and left ears. The correlation attained was 0.87, which is significantly higher than that of the case in the preceding section. This improvement can be explained by the fact that the acoustic field formed around the dummy head and the other conditions accompanying its presence, brought the frequency distribution of the measured sound closer to that experienced by human ears than when measurement was made using an ordinary microphone.

6. Introduction of psychoacoustic indices

In an attempt to create an index with an even higher correlation with human auditory feeling, various psychoacoustic indices were examined for appropriateness. The psychoacoustic indices known to be relevant

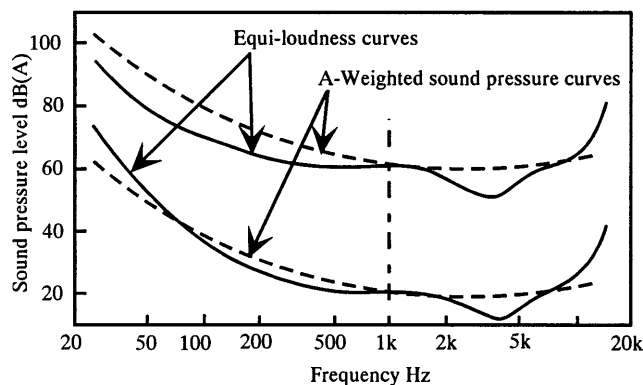


Fig. 6 Equi-loudness curves and A-weighted sound pressure curves

to aerodynamic noise are the following:

- (1) Loudness
- (2) Sharpness
- (3) Roughness
- (4) Fluctuation strength

The conventionally used A-weighted sound pressure level (hereinafter referred to as "A-weighting") is a sound-evaluating index that consists of sound pressure levels of various frequencies obtained through measurement, and corrected using a human-auditory-feeling-based factor whose amount is constant irrespective of the sound pressure level. However, the amount subjected to the correction varies with the sound pressure level and frequency. The resulting non-linearity of feeling is taken into consideration in the case of the "loudness" index. Fig. 6 compares both indices: the "loudness" and the A-weighting.

Since the A-weighting of every frequency is given the same amount of correction, the two A-weighting curves (broken lines) in the diagram have the same shape. The two "loudness" curves, on the other hand, have different shapes because they reflect the non-linearity of the acoustic sensation; their frequency characteristics are different from each other as they are different in sound pressure level. This means that the same noise of a certain frequency and sound pressure level may be evaluated quite differently depending on whether the "loudness" index is used or the A-weighting is used.

In addition to non-linearity, the loudness index also takes into account the masking effect, which is a sound cancellation effect that takes place between adjacent frequency bands. A conceptual diagram of the masking effect is shown in Fig. 7. In this diagram, the shaded part corresponds to the silent zone resulting from the masking effect when a sound of 1 kHz (160 Hz in band width) and 60 dB is being generated. Therefore, a sound of 2 kHz in frequency and 10 dB in sound pressure level is not taken into account with "loudness" because such a sound is not heard.

As described above, "loudness" is an index that reflects both the non-linearity of human sensation and the masking effect.

The "sharpness" index is the same as the "loud-

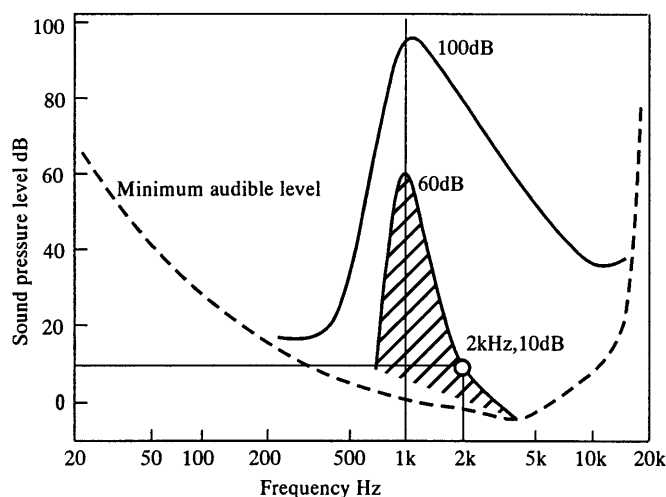


Fig. 7 Masking effect of neighboring frequency bands

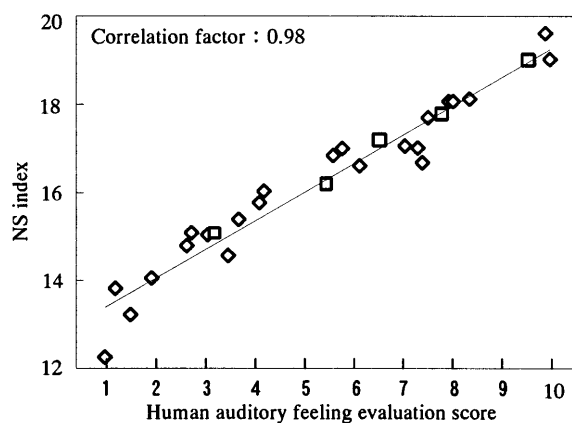


Fig. 8 Correlation between NS index and human auditory feeling

ness" index except that greater weighting is added to high-frequency components of sound. "Roughness" and "fluctuation" are both indices that express fluctuation. Detailed explanations of these two indices are omitted from this paper.

The index numbers of the above-mentioned four indices were individually calculated from the sound recorded using the dummy head; they were multiplied by their respective weight factors, and they were summed in an attempt to establish a new trial evaluation index. The weight factors were selected such that the new index showed the maximum correlation with the evaluation scores obtained from the human auditory feeling tests mentioned in previous section. As a result of this selection, it was determined that only the "loudness" and "sharpness" indices were to be incorporated into the new index and the "roughness" and "fluctuation" indices were rejected because they did not significantly contribute to the evaluation of aerodynamic noise.

The "loudness" (represented by N) and "sharpness" (represented by S) index values were then combined into a new evaluation index (named "NS index") by

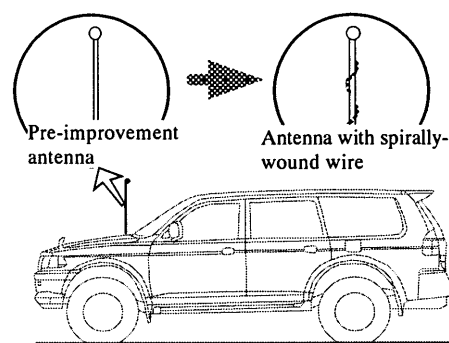


Fig. 9 Pole antenna

means of multiple regression analysis. Fig. 8 shows the correlation between the NS index values and the evaluation scores allotted to individual vehicles through the human auditory feeling tests. From this diagram, it is evident that the data obtained from both quantifying processes cluster on the same line more than they do in Figs. 4 and 5. This index shows a very high correlation with human feeling of 0.98.

Meanwhile, it is quite likely that the contribution of the "roughness" and "fluctuation" strengths to noise evaluation was judged to be low because the aerodynamic data were collected through tests conducted in a wind tunnel where aerodynamic conditions involved rather small fluctuations. In actual road driving, natural winds will cause much greater fluctuations to aerodynamic conditions, implying that the strength of the "fluctuation" index has a more important contribution to noise evaluation than with wind tunnel testing. Unfortunately, natural winds fluctuate every moment, making it difficult to obtain relevant data with good repeatability. For this reason, the discussion in this paper is limited to the range that is covered in the wind tunnel tests.

7. Application of the new index to the development of new vehicles

The new NS index described in the preceding section was applied to actual car development. This section describes one of the achievements accomplished through the use of this index, in which the index could help identify an aeolian tone noise from the pole antenna (see Fig. 9). Subsequently, generation of the noise was restricted by using a wire spirally wrapped around the antenna. The diameter of wire is 0.2 times of diameter of antenna.

Fig. 10 shows the sound pressure spectrum derived from a measurement carried out using an ordinary microphone installed midpoint between the front seats of a vehicle. From the diagram, it can be seen that the frequency of the aeolian tone noise is 2.5 kHz and its sound pressure level has been lowered by the measure taken. However, it is not certain from the results of this type of measurement whether or not the pre-improvement sound pressure level of this 2.5-kHz component should be given priority over others with higher sound

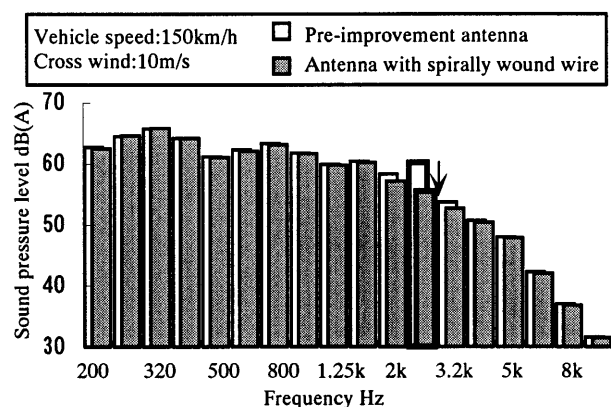


Fig. 10 Sound pressure spectrum

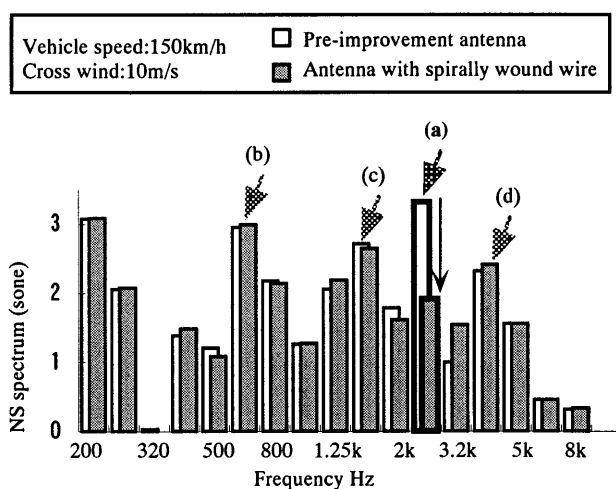


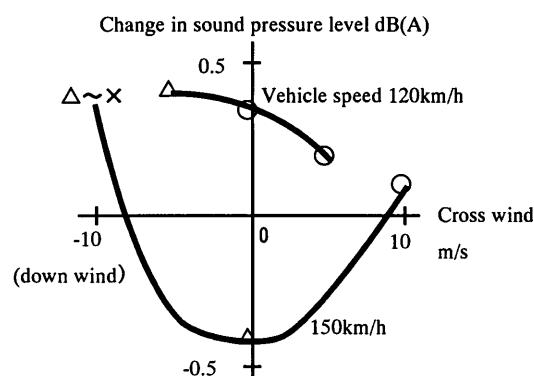
Fig. 11 NS spectrum

pressure levels when taking preventive measures. **Fig. 11** shows the sound pressure spectrum obtained using dummy-head measurements and analyzing them using the NS index. This diagram clearly indicates that the pre-improvement sound pressure level of the 2.5-kHz component is the highest and should be dealt with first. As seen from the diagram, the sound pressure of that component is reduced to a level lower than those of the components of other frequencies, verifying that the noise-reducing measure is effective.

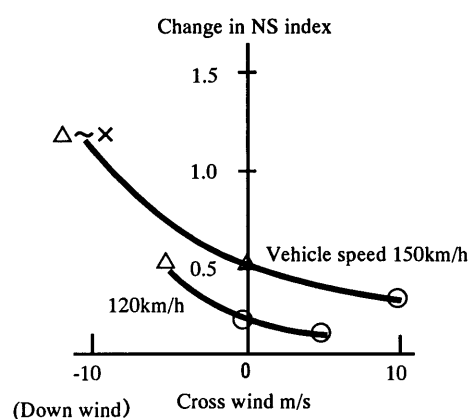
Both **Figs. 10** and **11** correspond to a wind tunnel test setting in which the mainstream velocity and the vehicle's yaw angle to the mainstream are adjusted such that the vehicle speed is 150 km/h and side-wind velocity is 10 m/s. The noise evaluation result, however, is different depending on the direction of the side wind. **Fig. 12** shows changes in the sound pressure level, NS index number and human auditory feeling that resulted from the addition of a pole antenna (without spiral wire). The "human feeling" here is different from that referred to in **Figs. 4, 5** and **8**; it concerns rating of noisiness of sound to the ear only, with respect to the antenna-induced noise.

Part (a) of Fig. 12, which corresponds to measurement with an ordinary microphone and noise evalua-

Symbol	Human feeling
○	Not noisy
△	Somewhat noisy
×	Noisy



(a) Sound pressure levels measured with ordinary microphone



(b) NS index measured with dummy head

Fig. 12 Change in sound pressure level, NS index and human auditory feeling caused by the addition of pole antenna

tion representation by the sound pressure level, shows inconsistency between the change in the sound pressure level and that in the human feeling, both caused by a change in the side wind. On the other hand, the change in the NS index number and that in the human feeling shown in part (b) of Fig. 12 correlate well with each other.

8. Summary

- (1) Aerodynamic noise was recorded using a dummy head for each of the tested vehicles; the recorded noise was then listened to and compared with another to rank all the vehicles in terms of evaluation of noise by human auditory feeling. The results showed that the ranking obtained in this manner often did not agree with that represented by the A-weighted sound pressure level index, which was based on ordinary microphone measurements.

- (2) Psychoacoustic indices were applied to the creation of a spectrum of the sound measured using a dummy head instead of the above-mentioned sound pressure level index. The newly created index showed significantly improved correlation with the evaluation based on human auditory feeling.
- (3) The new index (NS index) was used in the development of a new vehicle in order to deal with an aeolian tone noise problem generating from a pole antenna. The index was able to identify the noise as the problem that dominated the others. The measure taken to solve the problem actually reduced the noise (or made it less noticeable than the others).
- (4) The above-mentioned result proved the effectiveness of the NS index in finding a specific frequency component of noise that should be dealt with first priority in an aerodynamic noise-improvement activity.
- (5) MMC has constructed a system that includes a database storing dummy-head-recorded noise data and corresponding NS indices, and allows engineers to hear and compare noises quickly and easily. The company is utilizing the system in the development of new models.

References

- (1) Koike, M.: "Aerodynamic Noise of Passenger Cars – Diversity of Mechanisms", Mitsubishi Motors Technical Review (Japanese edition), NO. 11, 1999
- (2) Hoshino et al: "Evaluation of Noise Balance in Cabin", Proceedings of JSAE Convention, No. 953, p. 181, May 1995
- (3) Hoshino, K.: "Overall Evaluation Method for Wind Noise Based on a Sensual Evaluation Structure", Proceedings of JSAE Convention, No. 112-00, 20005448, 2000
- (4) Hoshino, K.: "Evaluation of Wind Noise Taking Auditory Sense Masking and Directional Sensation into Account", Proceedings of JSAE Convention, No. 982, p. 119, May 1998
- (5) Murata, O.: "Evaluation of Cabin Noise Tone during Cruising", Proceedings of JSAE Convention, No. 942, p. 145, May 1994
- (6) Sakai, H. (Editor): "Auditory Sense and Acoustic Psychology", p. 8, Corona Publishing Co.



Hisafumi DOI



Masaru KOIKE

Design of Air Conditioning System Using CFD Combined with Refrigeration Cycle Simulator

Toshio TAKEUCHI* Naoya KAKISHITA* Itsuhei KOHRI*

Abstract

Finding optimum layout of the condenser and other air conditioning system components in a vehicle is as essential as optimizing specifications of each system component to ensure adequate cooling performance of the system under a variety of conditions. This paper concerns a mathematical scheme that was developed for the use in finding an optimum layout of air conditioning system components. The scheme consists of an analysis model for engine compartment thermal flow that utilizes computational fluid dynamics (CFD) code and a refrigeration cycle simulator that is based on the thermal dynamic heat balance of air conditioner refrigerant. Described here are the concept of the scheme and examples of its application to development of vehicles.

Key words: Air Conditioning, Computer Aided Engineering, Numerical Analysis

1. Introduction

The recent widespread use of three-dimensional computer-aided design (CAD) applications has enabled automotive engineers to use computer-aided engineering (CAE) tools for predicting the performance of a vehicle from various aspects in the early stages of its development. One of the main reasons for this is that CAE, which used to be merely a qualitative prediction means, now allows even quantitative evaluations to be performed.

A vehicle's air conditioning system is one item that automotive manufactures must develop in close liaison with component makers. The design of the cooling unit and ducts, for example, is inseparably linked with the cabin equipment design and layout; the compressor and condenser greatly influence the design of the component layout in the engine compartment. The development of air conditioning system components themselves and the design of their layout in the vehicle and basic vehicle structure, therefore, would be most efficient if all of them could be carried out concurrently. Computer fluid dynamics (CFD) analysis is a recent achievement of CAE technology that is finding growing application in the air conditioning field to enable such concurrent development to be performed through simulation. To date, CFD has mainly been used by air conditioner manufactures to analyze the airflow of air conditioners in isolation, or by automotive manufactures to analyze defroster performance and interior airflows; in other words, it has been applied most frequently to in-cabin component layout and event analyses^{(1) - (3)} but has rarely been used to analyze component layout in the engine compartment.

One of the challenges in the development of trucks and buses is the more stringent requirements on controlling the engine compartment thermal environment

so that the products will comply with future tougher emission and noise standards. These requirements must be met by, for example, optimizing the specifications and location of the condenser. The aerodynamics and thermodynamics research team at MMC has therefore recently developed a cooling performance prediction scheme consisting of a refrigeration cycle simulator that calculates the thermal dynamic heat balance of the refrigerant in an air conditioner and a CFD-based code that simulates thermal flow in the engine compartment⁽⁴⁾. This paper will first discuss the method of calculating the dynamic characteristics of the refrigeration cycle under the system's daily operating conditions, and will then outline the analysis of engine compartment thermal flows⁽⁵⁾⁽⁶⁾ to predict the temperatures of the cooling air flow through the condenser. Finally, a case of applying this scheme in the actual development of a vehicle, in which the scheme was shown to be valid and useful for qualitative predictions, will be described.

2. Refrigeration cycle simulator

The heat balance of refrigerant (refrigeration cycle) must be calculated from the operational characteristics of the compressor, evaporator and condenser before the air conditioning system's performance can be calculated. As the air conditioner on a vehicle is used under a variety of conditions, prediction calculations using only bench-test-based basic performance data provided by the air conditioner manufacture are inaccurate for some conditions.

To be able to predict air conditioning performance under different vehicle operating conditions, the research team has constructed a refrigeration cycle simulator that uses systematically collected and simplified bench-test data for calculation⁽⁷⁾. This section describes the method used for formulating an algebraic model

* Vehicle Research Dept., Truck & Bus Research & Dev. Office

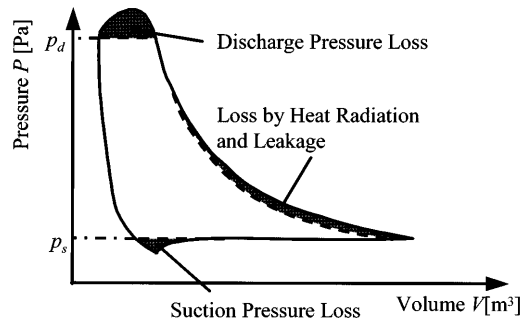


Fig. 1 P-V diagram

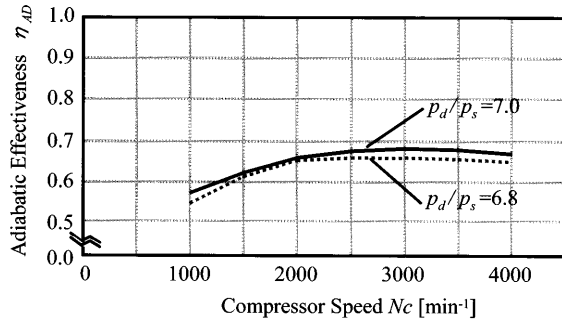


Fig. 2 Adiabatic effectiveness

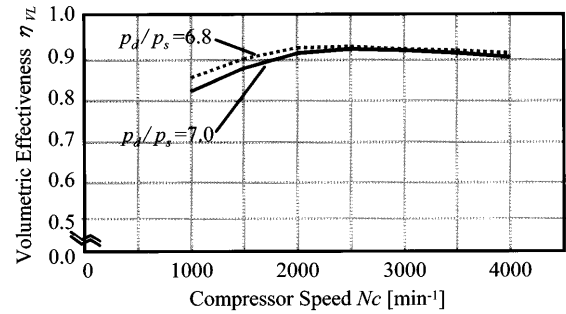


Fig. 3 Volumetric effectiveness

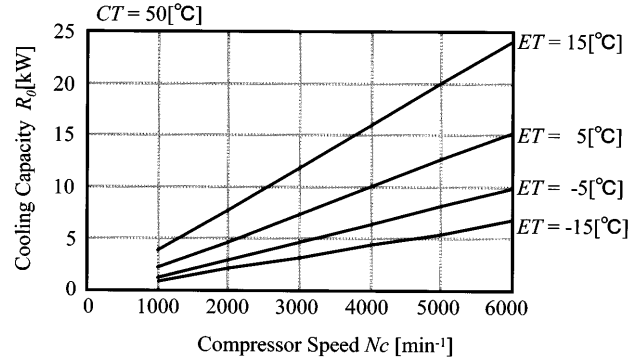


Fig. 4 Standard bench test data (cooling capacity)

that expresses air conditioning characteristics using a minimum number of parameters. The method is based on the previously established theory for calculating the thermal equilibrium point in a refrigeration cycle⁽⁸⁾.

2.1 Formulation of compressor characteristics model

The characteristics of a compressor are represented by compression work (power) W and cooling capacity R . During compressor operation, a cycle consisting of adiabatic compression, discharge, adiabatic expansion, and suction is repeated. Each cycle involves pressure losses during the suction and discharge events and refrigerant losses due to internal leakage⁽⁹⁾ (Fig. 1). These losses are represented by adiabatic compression effectiveness η_{AD} and volumetric effectiveness η_{VL} , and are quantities specific to each compressor (Figs. 2 and 3). The W and R characteristics are expressed using η_{AD} and η_{VL} as functions of the following four parameters: compressor inlet refrigerant temperature T_s , discharge and suction pressures P_d and P_s , and speed Nc of the compressor⁽¹⁾.

The W and R to be evaluated here are those of the compressor mounted on a vehicle, so to obtain W and R under actual operating environments, it was decided to use the results of studies on the theoretical relationship between the effectiveness η_{AD} and η_{VL} and the amounts W and R as a basis (as proposed previously by the authors, reference⁽⁷⁾) and to use the characteristics W_0 and R_0 measured under a reference condition rather than using η_{AD} and η_{VL} as explicit functions. Specifically, W and R are expressed using the equations below, taking into consideration the fact that the characteristics of W and R are subject to change, under the influence of superheated temperature ΔT_{SH} and sub-

cooled temperature ΔT_{SC} , from the reference condition (represented by W_0 and R_0 in the equations) where the density of the refrigerant is free from superheated temperature ΔT_{SH} and subcooled temperature ΔT_{SC} :

$$W = f_W(ET, \Delta T_{SH}) \cdot W_0(ET, CT, Nc) \quad (1)$$

$$R = f_R(ET, CT, \Delta T_{SH}, \Delta T_{SC}) \cdot R_0(ET, CT, Nc) \quad (2)$$

Thus, W and R can be expressed without using η_{AD} and η_{VL} by using the following three parameters: evaporator temperature ET , condenser temperature CT and compressor speed Nc . W_0 and R_0 are separately determined as characteristics subordinate to the compressor speed Nc from the data obtained through systematically conducted bench tests (Figs. 4 and 5), and, in environments involving superheated and subcooled temperature, they are determined through prediction using equations (1) and (2) above.

2.2 Formulation of evaporator heat exchange performance model

At the outlet of the evaporator, refrigerant must be in a state of superheated vapor to prevent liquid refrigerant from entering the compressor. To ensure this, the expansion valve detects the temperature at the outlet of the evaporator and controls the flow rate of refrigerant such that ΔT_{SH} remains appropriate. As a result, the refrigerant in the evaporator is maintained in a partly two phase (gas-liquid) state and a partly single phase (superheated vapor) state (Fig. 6). Assume here that the whole evaporator volume is 1 and that the part occupied by superheated vapor corresponds to a ratio of α , then the value of α should change as ΔT_{SH} changes due

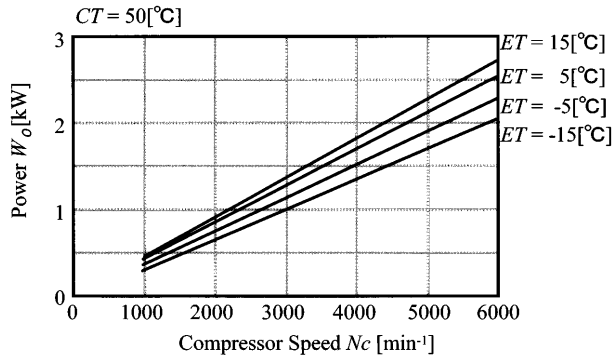


Fig. 5 Standard bench test data (power)

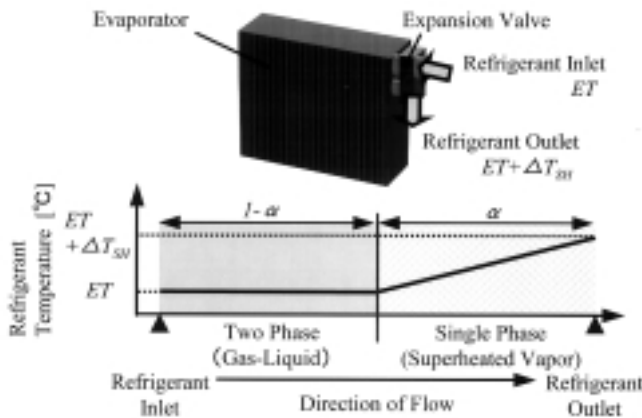


Fig. 6 Phase change of refrigerant in evaporator

to variations in operating conditions. This necessitates consideration of the heat exchange performance which reflects changes in the value of α . In the methods of obtaining the exchanged heat quantity that have been reported by air conditioner manufactures, local heat values are calculated by applying calculations to different parts constituting the flow path of refrigerant, which are defined by detailed shapes such as fins and tubes⁽¹⁰⁾⁽¹¹⁾. On the other hand, automotive manufactures require the exchanged heat values of an evaporator on a vehicle, as in the case of a compressor. To meet this need, a simplified heat exchange performance model is formulated.

In an open circuit system, the evaporator's heat exchange performance depends on the mass flow rates \dot{m}_{EA} and \dot{m}_R of air and refrigerant, the temperatures of air and refrigerant (evaporation temperature) T_A and ET , and the two phase region ratio α . Knowing that the expansion valve controls ΔT_{SH} to maintain it nearly constant and that the refrigeration cycle depends on the components of the air conditioning system which forms a closed circuit, α can be defined by parameters \dot{m}_{EA} and \dot{m}_R provided the compressor and condenser form components of a closed-circuit system like that in a vehicle. This is because the expansion valve controls \dot{m}_R depending on \dot{m}_{EA} in order to maintain ΔT_{SH} constant. This is expressed by the equation given below, in which the change in the two phase region ratio is represented by the heat exchange characteristic f_{QE} which

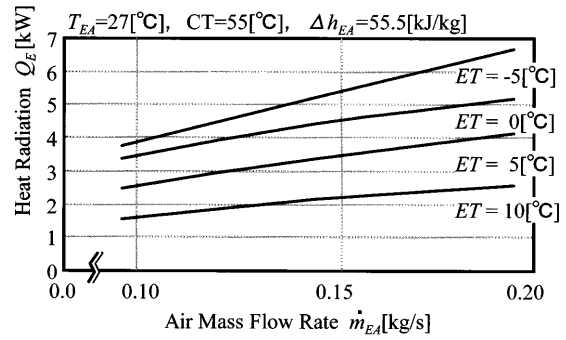


Fig. 7 Heat exchange performance (evaporator)

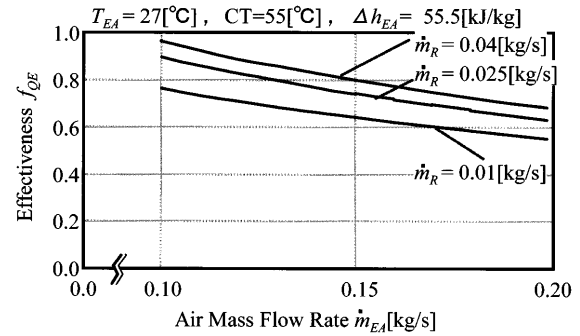


Fig. 8 Heat exchange characteristics (evaporator)

corresponds to the difference in enthalpy between air and the fin Δh_{EA} , and is considered as a function of the mass flow rates \dot{m}_{EA} and \dot{m}_R of the air and refrigerant, respectively.

$$Q_E \equiv \dot{m}_{EA} \cdot f_{QE}(\dot{m}_{EA}, \dot{m}_R) \cdot \Delta h_{EA} \quad (3)$$

The heat exchange characteristic f_{QE} is calculated by obtaining the evaporator's heat exchange performance Q_E from ET and CT obtained through a systematically conducted bench test (Fig. 7) and solving equation (3) for \dot{m}_{EA} and \dot{m}_R (see Fig. 8).

2.3 Formulation of condenser heat exchange performance model

Superheated vapor refrigerant discharged from the compressor quickly condenses at the inlet of the condenser, but the degree of sub cooled ΔT_{SC} at the outlet is not so large; this suggests that CT is constant inside the condenser and so it is appropriate to express the condenser's heat exchange performance Q_C by the heat exchange characteristic f_{QC} with regard to the temperature difference between refrigerant and air ΔT_{CA} . Provided CT is constant, the heat exchange performance is considered to be independent of the refrigerant flow rate \dot{m}_R ; consequently, f_{QC} can be expressed as a function of the mass flow rate \dot{m}_{CA} . If the heat capacity flow rate of air is represented by C_{CA} , then

$$Q_{CA} = C_{CA} \cdot f_{QC}(\dot{m}_{CA}) \cdot \Delta T_{CA} \quad (4)$$

The heat exchange characteristic f_{QC} can be derived by obtaining the heat exchange performance of the con-

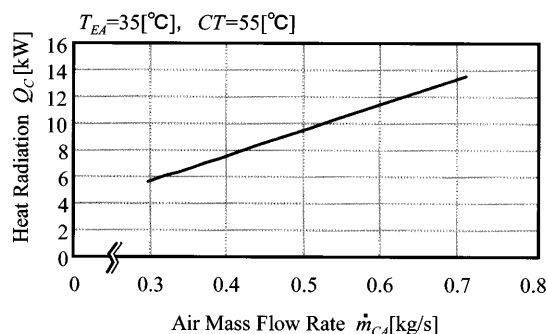


Fig. 9 Heat exchange performance (condenser)

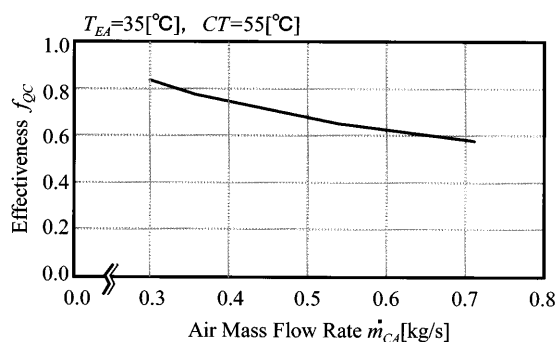


Fig. 10 Heat exchange characteristics (condenser)

denser (Fig. 9) from bench test data and then solving equation (4) for the flow rate (Fig. 10).

2.4 Calculation process of refrigeration cycle

The thermal equilibrium point during operation of the air conditioning system is calculated by repeating the calculations of steps ① to ③ below using as parameters the abovementioned bench-test-based performance data and also the vapor and condensation temperatures (Fig. 11).

- ① Certain ET and CT temperatures are assumed for a compressor speed of N_c which is to be studied, corrections corresponding to superheated temperature ΔT_{SH} and sub cooled ΔT_{SC} are made to W_0 and R_0 , then the compression work (power) W and cooling capacity R of the compressor in operation are derived (equations (1) and (2); part (A) of Fig. 11).
- ② With the evaporator, the evaporation temperature ET' at which Q_E balances with R is derived through inverse operation from the thermal properties of the cooling air flow and refrigerant and the heat exchange characteristics of evaporator f_{QE} (equation (3)). If the obtained ET' is different from the initially assumed ET , then ET is corrected and then the process returns to step ① (parts (A) and (B) of Fig. 11).
- ③ With the condenser, the condensation temperature CT' at which the condensation capacity Q reaches equilibrium ($Q = R + W$) is calculated through inverse operation from the thermal properties of the cooling air flow and refrigerant and the heat exchange characteristics of condenser f_{QC} (equation (4)). Like the calculation with the evaporator, if CT'

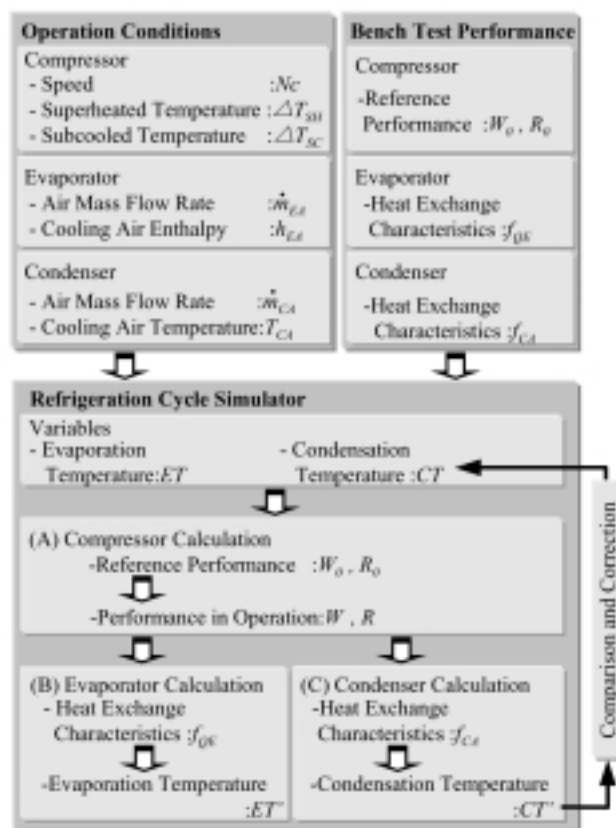


Fig. 11 Refrigeration cycle simulator

is different from CT , the CT is corrected and calculation is performed again starting with step ① (parts (A) and (C) of Fig. 11).

2.5 Verification of refrigeration cycle simulator

Fig. 12 compares the calculated cooling capacity R , compressor work (power) W , and low and high refrigerant pressures P_H and P_L with the experimentally obtained ones for an air conditioning system on a light-duty truck running at a speed of V_h (compressor speed of N_c). In the calculation carried out for this comparison, the inputs of air-related conditions – the conditions not related to the heat exchanger (i.e., air flow rate, air temperature and humidity) – are those obtained through experiments in order to evaluate the accuracy of outputs of the refrigeration cycle simulator itself. The calculated results show a slight increase in the difference from the experimentally obtained results in higher V_h ranges, but the accuracy of all the calculation results is acceptable for practical purposes, proving that the refrigeration cycle simulator can adequately predict the performance of an air conditioning system, provided air-related conditions are given. The cause of the increase in error in higher V_h ranges may be attributable to pressure losses that may have occurred due to lubricants in the refrigerant tube and compressor.

3. CFD analysis of airflow and thermal fields around condenser

This section discusses the computational tool devel-

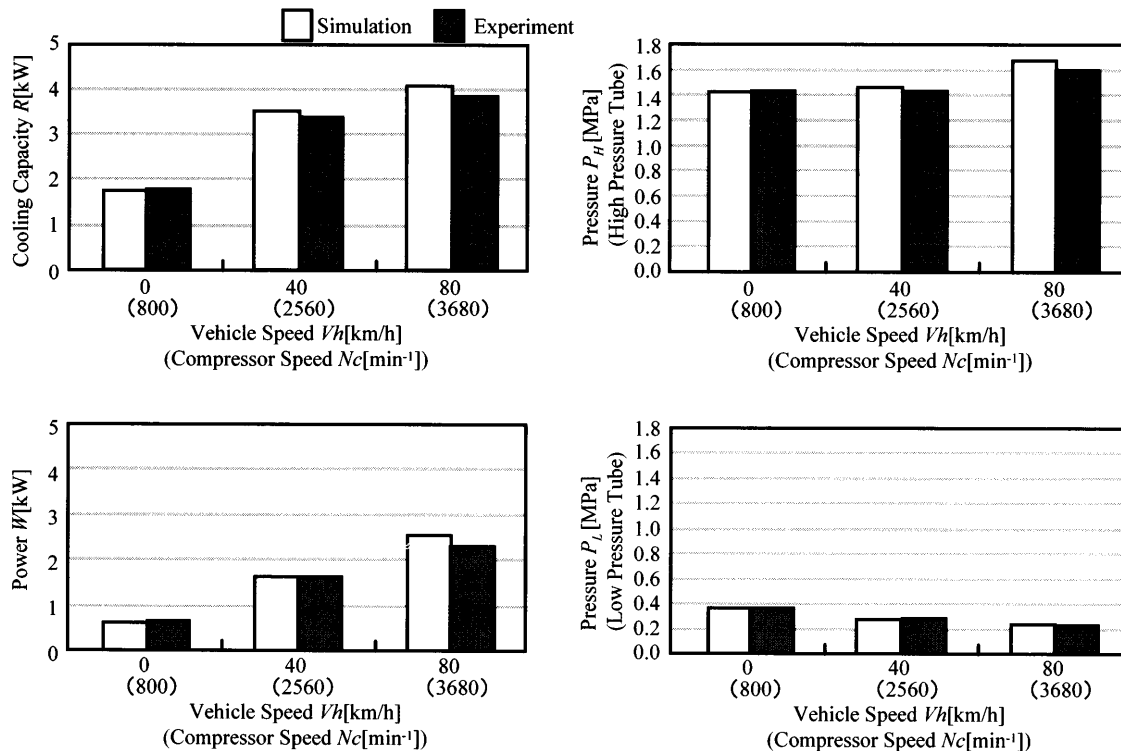


Fig. 12 Comparison between Simulator and Experiment

oped for simulating the airflow and thermal fields around the condenser for use in studies of component layout in the engine compartment. The heat exchange performance of the condenser is significantly affected by the turbulence involved in the air flow through and over components arranged in complicated configurations, as well as the heat released from engine cooling system components in the engine compartment. Therefore, the simulation of the condition of air around the condenser must consider the layout of components and the heat balance with regard to the engine cooling system. In developing the computational tool, the engine cooling performance prediction scheme that was previously reported by the authors⁽⁵⁾⁽⁶⁾ is used for calculating the heat balance in the engine cooling system.

3.1 Heat balance in engine cooling system

The concept of the scheme used for calculating the heat balance in the engine cooling system will be described below, referring to Fig. 13. First, the engine output is obtained by giving necessary driving conditions (second quadrant). The curve in the third quadrant shows the characteristic of the engine power loss resulting from cooling which is necessary for the engine to operate normally and is represented by the heat quantity corresponding to each engine output. Reference values for the engine power loss characteristic are separately obtained from bench test measurements. Once the reference characteristic values have

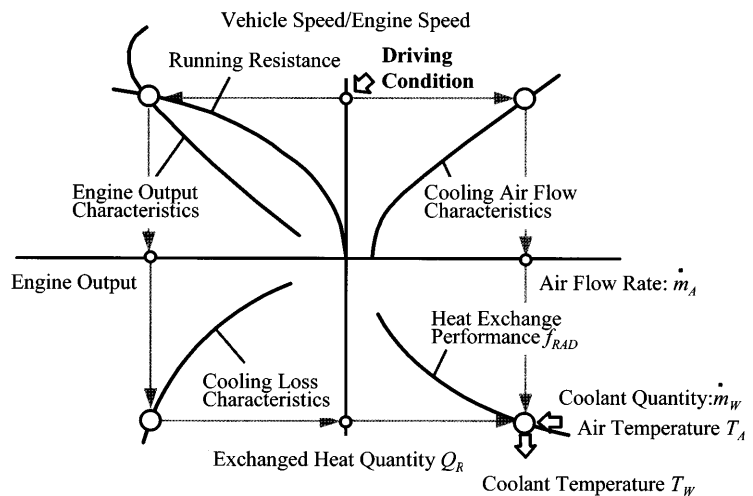


Fig. 13 Heat balance in engine cooling system

been established, the necessary heat quantity to be exchanged by the radiator can be determined by giving an engine output. Meanwhile, the performance of the cooling fan of a truck's engine depends on the engine speed as the fan is directly driven by the engine. If, in addition to the fan performance, the pressure loss characteristic of the engine compartment ventilation system and the temperature rise characteristic of the incoming air are given, the cooling air flow rate and air temperature can be determined (first quadrant). The exchanged heat quantity Q_{RAD} can then be expressed as a function of coolant temperature T_W , coolant quantity \dot{m}_W , cooling air flow rate \dot{m}_A , and air temperature T_A as follows:

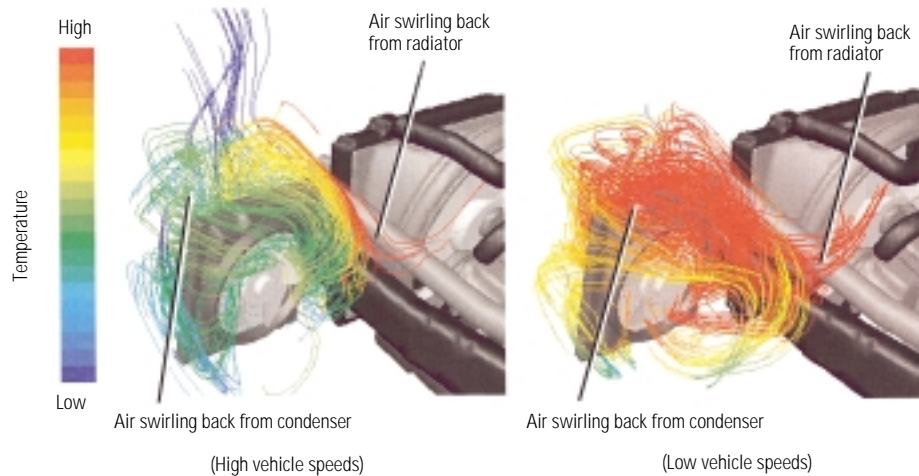


Fig. 14 Airflow and thermal fields around condenser

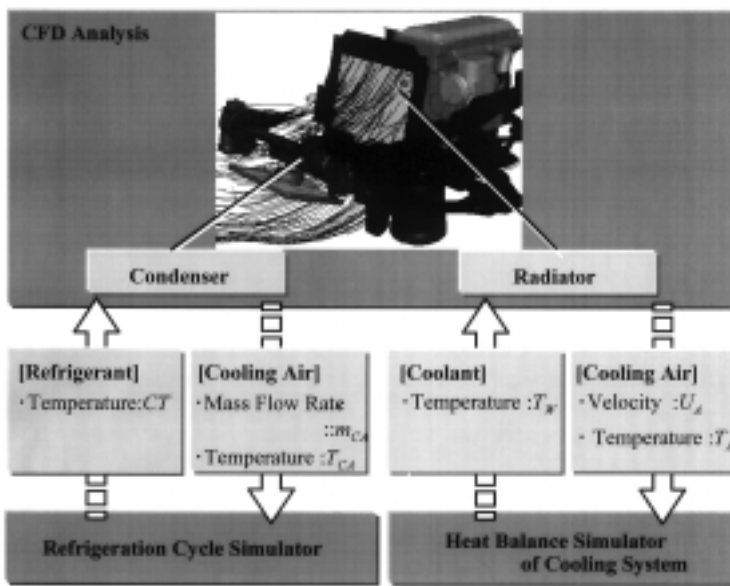


Fig. 15 General flow of cooling performance calculation

$$Q_{RAD} = f_{RAD} (\dot{m}_A, \dot{m}_W, T_A, T_W) \quad (5)$$

Among the abovementioned parameters, T_A and \dot{m}_A can be obtained using the first quadrant. The \dot{m}_W parameter can be obtained based on the water pump characteristic from the engine speed. The radiator exchanged heat quantity Q_{RAD} has already been obtained using the third quadrant. This means that T_W in a state of thermal equilibrium can be calculated through an inverse operation, provided the heat exchange performance of radiator f_{RAD} is given (fourth quadrant). The temperature thus obtained represents the thermal equilibrium point of the engine cooling system.

The heat balance calculation of the engine cooling system involves calculating the result of interaction between the abovementioned element factors using a one-dimensional model. However, a CFD analysis is used for calculating the heat transport of the cooling air flow through the engine compartment (handled in the

first quadrant) as it significantly affects the cooling performance of the radiator and condenser and involves predicting the flow and thermal fields, which requires highly accurate calculations. The one-dimensional code for the calculation of the coolant system and the CFD analysis code for the calculation of the cooling air system are thus combined and used for predicting the coolant temperature through repeated calculation.

3.2 CFD analysis of airflow and thermal fields around condenser

In actual vehicles, part of the high-temperature air which has passed through heat exchangers such as the condenser and radiator often swirls back to the front surface of the heat exchangers; for this reason, the air temperature distribution at the inlet of each heat exchanger must be precisely predicted. The CFD analysis code, therefore, is designed to use as inputs the refrigerant temperature (condensation temperature) or coolant temperature inside the heat exchangers so that the temperatures of the air at the front of each heat exchanger, including that of swirling-back air, can be obtained. Fig. 14 is an example of the calculated effects of the air swirling back to the front of the condenser. This example shows that the temperature at the front of the condenser of an air conditioning system varies with the vehicle speed due to a change in the swirling back air even if the specifications of the system are the same.

4. Cooling performance prediction scheme

Fig. 15 shows an outline of the air conditioning performance prediction scheme formed by combining the refrigeration cycle simulator and the code for calculating the engine cooling system heat balance. With this scheme, the air temperatures in front of the condenser and radiator are first calculated for each temperature of the refrigerant and coolant in these heat exchangers.

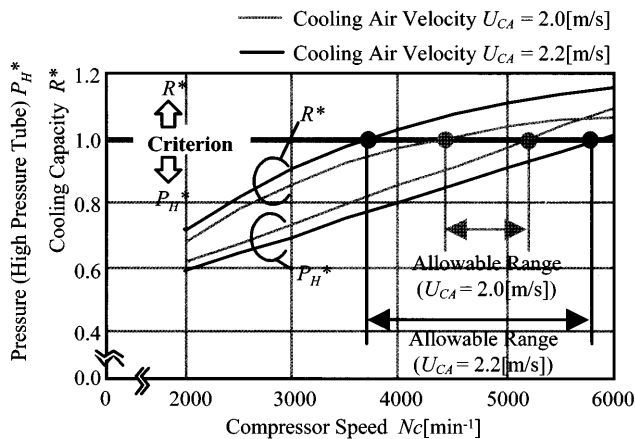


Fig. 16 Cooling capacity and refrigerant pressures

Next, the temperatures of the refrigerant and coolant are calculated back using the air temperatures in front of the condenser and radiator thus obtained and also the outcomes of the refrigeration cycle simulator and heat balance calculation of the engine cooling system. This process is carried out repeatedly until the solution of the coolant temperature converges and the air conditioning performance is finally predicted.

5. Application of cooling performance prediction scheme

This section describes, in comparison with the experimental measurements, the results of the cooling performance prediction obtained by applying the abovementioned scheme to the analysis model of a vehicle under development.

5.1 Cooling capacity R and refrigerant pressure P_H

In general, the higher the compressor speed N_c and condenser cooling air velocity U_{CA} , the higher the cooling capacity of the air conditioning system. On the other hand, the pressure of the high-pressure refrigerant P_H decreases when U_{CA} increases although it increases as N_c becomes higher. In the graph of Fig. 16, the ratio between R and P_H (represented by R^* and P_H^* , respectively) when the criterion is assumed to be 1.0 is plotted on the vertical axis. It is desirable that R should account for a larger part (or P_H for a smaller part) of the target cooling capacity, so $R^* \geq 1.0$ and $P_H^* \leq 1.0$ hold true. The graph shows that the allowable compressor speeds that satisfy this condition largely depend on U_{CA} values obtained through CFD analysis in order to satisfy all the relevant conditions.

5.2 Specifications of study subject

Fig. 17 shows the analysis model of a front under mounted condenser on a light-duty truck used for the study. With a front under mounted condenser, U_{CA} is generally insufficient. As a measure to increase the U_{CA} level, the addition of wind deflectors A and B are considered since relocating the condenser is not feasible due to truck restrictions such as minimum ground clearance and approach angle.

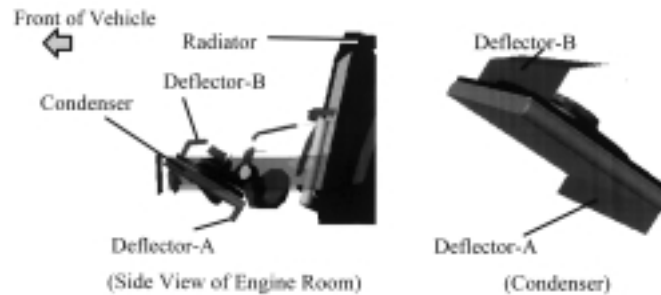


Fig. 17 CFD analysis model

5.3 Calculation results and their evaluation

A comparison of path lines of airflow corresponding to trucks with and without the wind deflectors in Fig. 18 shows that the deflector A guides air appropriately to increase airflow passing under the bumper (part ①) and the deflector B successfully controls the swirling back of the air which has passed the condenser (part ②). The distribution of cooling air velocity U_{CA} at the front of the condenser and that of temperature T_{CA} both reflect the airflow representation by path lines (parts ③ and ④), showing an approximately 25 % improvement in the average cooling air velocity and an approximately 4 % improvement in the air temperature in front of the condenser. Fig. 19 shows improvements achieved in the airflow and thermal fields in terms of R and P_H . The errors in the calculated results from the experimental results are approximately 5 % for R and approximately 3 % for P_H , both of which are acceptable practical levels for the accuracy expected in a predictive calculation.

6. Summary

- (1) In order to make it possible to concurrently study the performance of an air conditioning system and appropriateness of the arrangement of its components during the development of a vehicle's air conditioning system, a mathematical scheme has been constructed by combining the refrigeration cycle simulator and the engine compartment thermal flow analysis code (CFD analysis code).
- (2) The refrigeration cycle simulator formulates simplified models of air conditioning system characteristics and carries out calculations through rearrangement using systematically obtained bench-test performance data.
- (3) With the CFD analysis, a computational code is constructed which allows complicated airflow and thermal fields around the condenser to be calculated considering the heat balance in the engine cooling system.
- (4) As a result of applying the mathematical scheme to performance prediction in the actual development of a vehicle, it has been confirmed that the scheme can predict the cooling performance of an air conditioning system with acceptable accuracy for practical purposes.

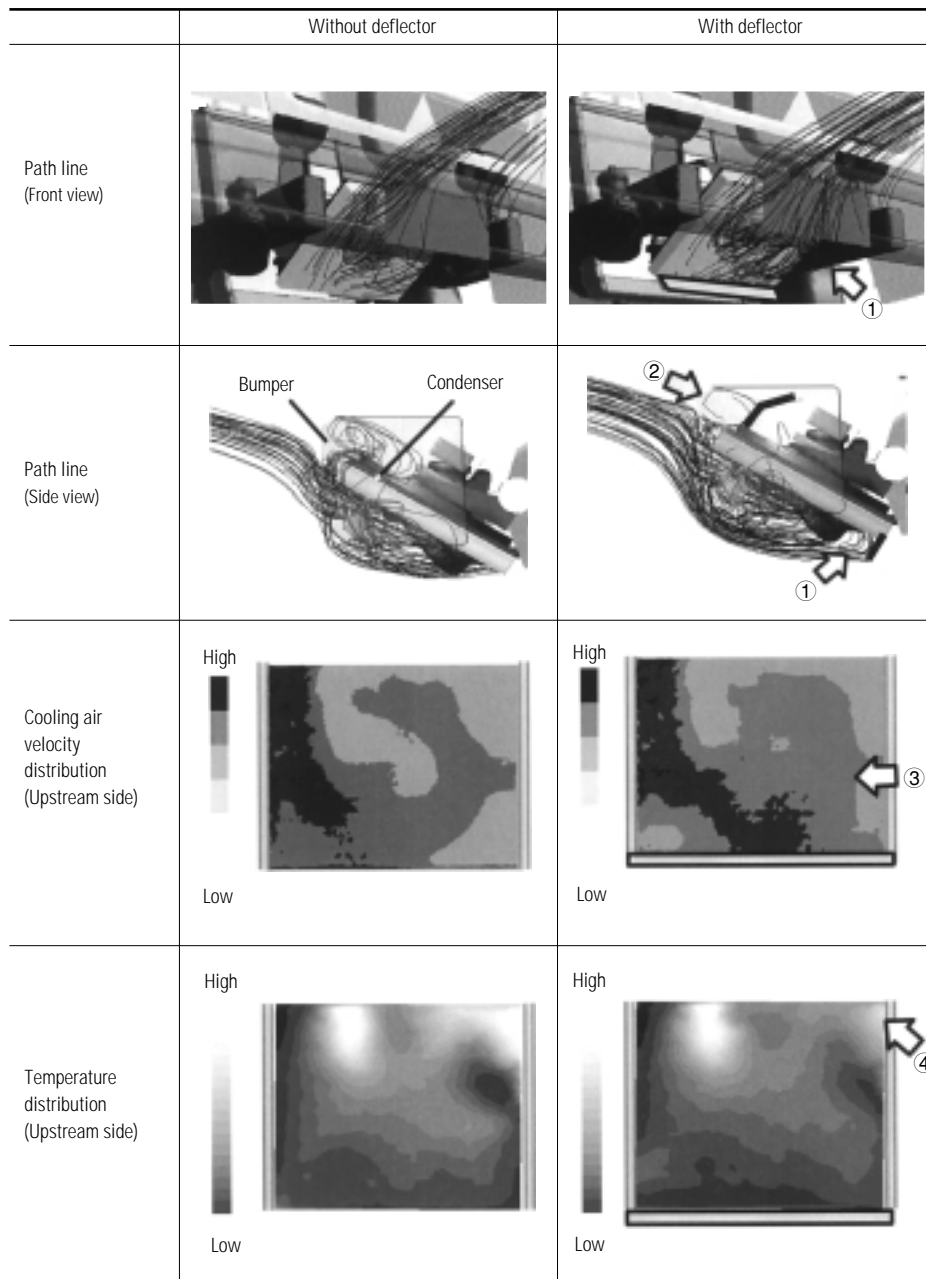


Fig. 18 Airflow and thermal fields

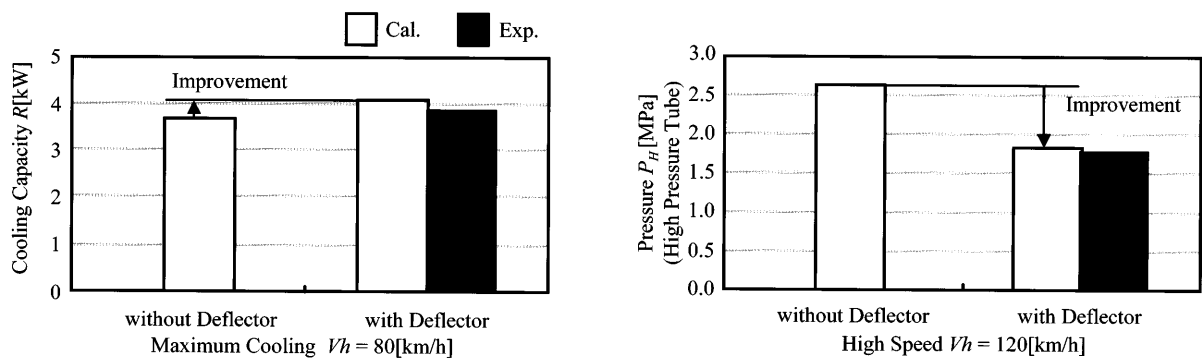


Fig. 19 Comparison between Prediction and Experiment

References

- (1) Huang D. C., Oker E., Yang S. L., and Arici: A Dynamic Computer-Aided Engineering Model for Automobile Climate Control System Simulation and Application Part 1: A/C Component Simulations and Integration, SAE Paper 1990-01-1195, 1990
- (2) Eisenhour R. S., Kawakami K., and Tsunada N.: HVAC System Analysis Method for Testing, SAE Paper 960684, 1996
- (3) Kitada, Asano and Kamihara: Development of Car Air Conditioner Basic Performance Simulator, Proceedings of JSAE Convention, 20005538, 2000
- (4) Takeuchi T., Kakishita N., and Kohri I.: The Prediction of Refrigeration Cycle Performance with Front End Air Flow CFD Analysis of an Automotive Air Conditioner, SAE Paper 2002-01-0512, 2002
- (5) Takeuchi, T. and Kohri I.: Development of Prediction Method of Engine Cooling Performance, JSAE Proceedings, 20005312, 2000
- (6) Kohri I., Takeuchi T., and Matsunuma Y.: Computational Design of Commercial Vehicle for Reconciling Aerodynamics and Engine Cooling Performance, FISITA, F2000H248, 2000
- (7) Takeuchi T., Kakishita N., and Kohri I.: Development of Method for Predicting Performance of Air Conditioner on a Truck, Proceedings of JSAE Convention, 20016068, 2001
- (8) Sakai: Analysis of Thermal Equilibrium Point in Air Conditioning Refrigerator, JSME Paper No. 246, Vol. 33, 1967
- (9) Kenichi F.: "Car Air Conditioners", Sankaido
- (10) Marthur G. D.: Performance of Serpentine Heat Exchanger, SAE Paper 980057, 1998
- (11) Lee K. H. and Won J.-P.: Thermal Design Study of a High Performance Evaporator for the Automotive Air Conditioner, SAE Paper 1999-01-1191, 1990



Toshio TAKEUCHI



Naoya KAKISHITA



Itsuhei KOHRI

Development of 4M42T Engine for Powering Light-Duty Trucks for European Market

Masaaki UENO* Kenichi KOBAYASHI* Nobuya OSAKI*
Masao KAGENISHI** Eiichi KOUJINA** Yasuaki KUMAGAI**

Abstract

The 4M42T is an in-line four-cylinder diesel engine with an intercooled turbocharger. It was developed for powering the light-duty trucks that are sold in the European market. The engine incorporates a direct injection system, DOHC 4-valve mechanism, cooled EGR system and electronically controlled high-pressure, distributor-type injection pump. It features low exhaust emissions and fuel consumption, operates with little smoke, and produces low noise. The engine meets the EURO 3 emission standard.

Key words: Diesel Engine, Performance, Emission, Fuel Injection

1. Introduction

In recent years, the environmental need for lower exhaust emissions and noise and the economic need for lower fuel consumption have been increasingly acute. At the same time, the European market for light-duty trucks has been in need of engines with superior high-speed performance and low fuel consumption to help meet demand for improved transportation efficiency and faster distribution of goods.

To meet these needs, Mitsubishi Motors Corporation (MMC) developed the 4M42T four-in-line, turbocharged, intercooled, diesel engine and in February 2001 began offering it with Europe-specification CANTER trucks.

The development targets and technological features of the 4M42T engine are described in this paper.

2. Development targets

The 4M42T engine is based on the 4M40T engine, which is highly regarded in Europe owing to its high reliability. MMC developed the 4M42T engine to serve as one of the main models in the light-duty-truck segment of its engine series. Specific development targets were as follows:

(1) Exhaust emissions

MMC aimed to achieve compliance with the EURO 3 emission standard and to achieve virtually smokeless operation.

(2) Output performance

MMC aimed to realize some of the highest levels of output and torque in the class.

(3) Economy

MMC sought to achieve one of the highest levels of fuel consumption in the class by means of improved

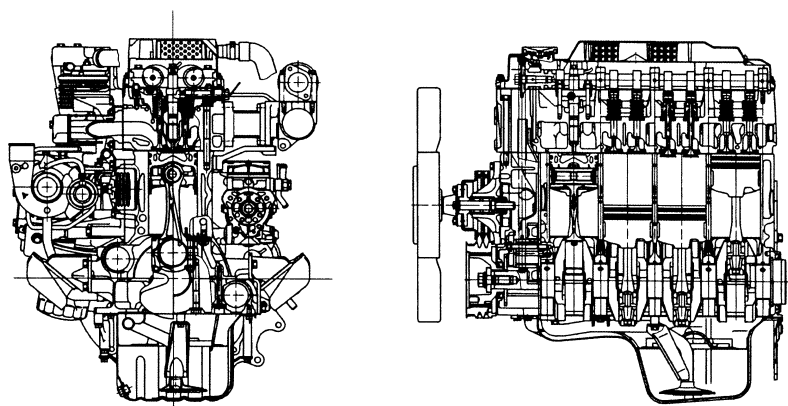


Fig. 1 Sectional views of 4M42T engine

combustion (realized using a direct injection system, dual overhead camshafts with four valves per cylinder, and centrally positioned injector nozzles) and by means of optimized intake and exhaust systems.

(4) Noise

MMC aimed to satisfy the 1999 European Union noise regulations and to minimize idling noise.

(5) Reliability

MMC aimed to give the engine sufficient quality and durability for fault-free operation throughout the life of the vehicle and to make maintenance easy.

3. Major specifications

Compared with the earlier 4M40T engine, the 4M42T engine has a longer stroke and a concomitantly higher displacement. Also, the 4M42T engine has newly designed components made necessary by the adoption of a direct injection system.

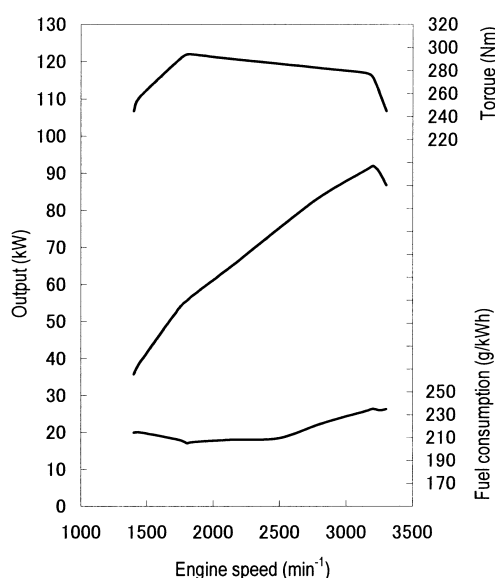
The major engine specifications are shown in Table 1. Sectional views of the engine are shown in Fig. 1, and the engine's performance curves are shown in Fig. 2.

* Engine Design Dept., Truck & Bus Research & Dev. Office

** Engine Testing Dept., Truck & Bus Research & Dev. Office

Table 1 Specifications of 4M42T engine

Model	4M42T	
Type	Direct-injection; four-cycle	
No. of cylinders	4	
Displacement (cc)	2,977	
Bore x stroke (mm)	φ 95 x 105	
Max. output (kW/min ⁻¹)	92/3,200	
Max. torque (Nm/min ⁻¹)	294/1,800	
Compression ratio	18.5	
Combustion chambers	Re-entrant-type	
Valve mechanism	Dual overhead camshafts (driven by timing chain) two intake valves and two exhaust valves per cylinder	
Injection system	High-pressure, distributor-type injection pump (Bosch VP44)	
Forced induction	Turbocharger with intercooler	

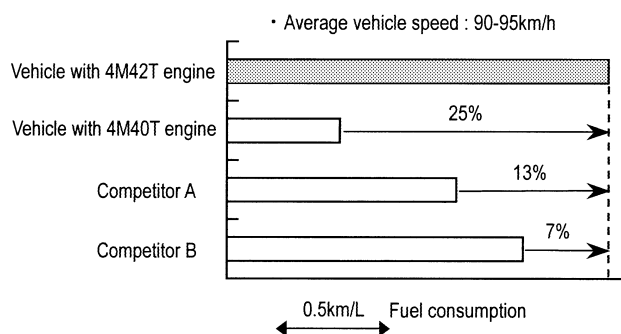
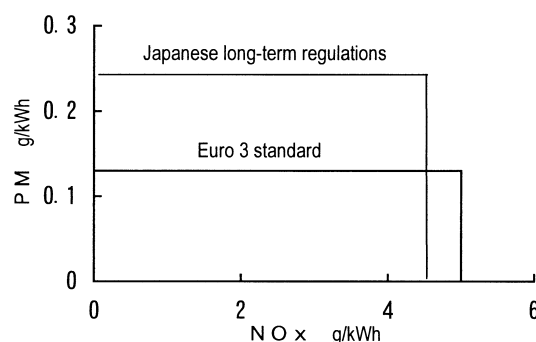
**Fig. 2 Performance curves of 4M42T engine**

4. Technological features

4.1 Performance and exhaust emissions

MMC made the 4M42T engine one of the cleanest-running, highest-performing engines in the class partly by adopting a direct injection system, dual overhead camshafts with four valves per cylinder, a cooled EGR system, an electronically controlled, high-pressure, distributor-type injection pump, and other advanced technologies and partly by optimally tuning each component. At the same time, MMC achieved high-speed fuel efficiency 25 % better than that of a vehicle with the earlier 4M40T engine (Fig. 3).

Fig. 4 shows exhaust-emission standards. As shown, the EURO 3 standard is comparable with Japan's long-term regulations with regard to emissions of nitrogen oxides (NOx) but significantly more stringent (by a margin of 48 %) with regard to emissions of

**Fig. 3 Superior high-speed fuel consumption of vehicle with 4M42T engine****Fig. 4 EURO 3 emission standard**

particulate matter (PM).

4.1.1 Injection system

The injection system uses an electronically controlled, high-pressure, distributor-type injection pump (Bosch VP44) to realize high-pressure injection at 140 MPa. Combined with a minimized nozzle-hole area, the high-pressure injection pump realizes a finely atomized fuel spray and thus promotes mixing of the fuel and air for minimal emissions of black smoke. Further, the cooled EGR system minimizes emissions of NOx while suppressing increases in emissions of black smoke.

Fail-safe functionality is realized by duplication of important signal lines and by control logic that performs self-diagnosis and, when necessary, switches to a backup mode.

4.1.2 Intake and exhaust systems

MMC adopted the cooled EGR system (Fig. 5) to simultaneously reduce NOx emissions and fuel consumption. A water-type cooler reduces the temperature of recirculated exhaust gases before they enter the intake system, thereby maximizing the EGR rate while suppressing increases in PM emissions. At the same time, advanced fuel-injection timing significantly improves fuel consumption. A further advantage of the advanced fuel-injection timing is that they make an oxidation catalyst unnecessary and thus improves productivity (Fig. 6).

A swirl-supported combustion system, which is

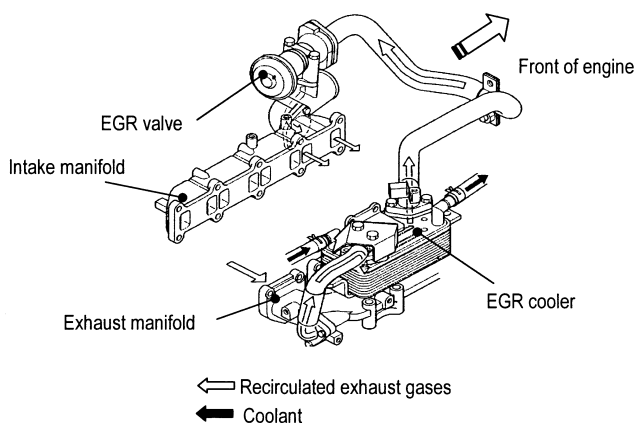


Fig. 5 Layout of cooled EGR system

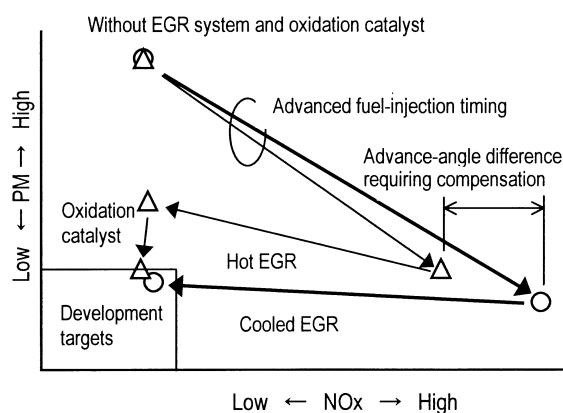


Fig. 6 Effects of cooled EGR system

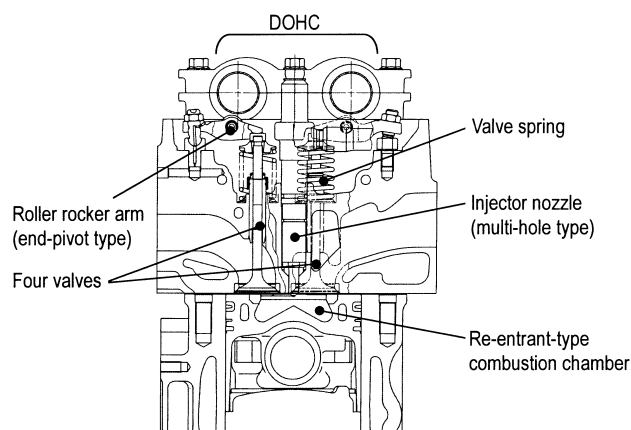


Fig. 7 Configuration of valve mechanism and shape of combustion chamber

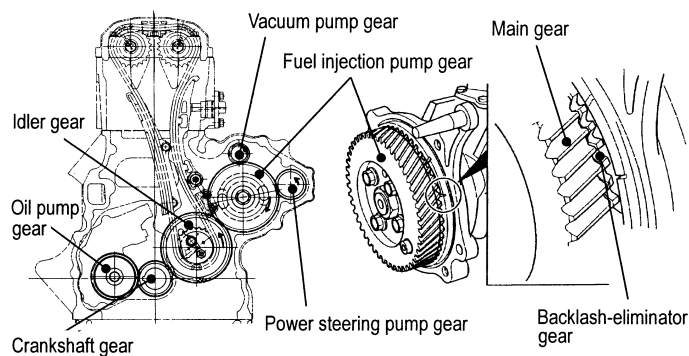


Fig. 8 Construction of backlash-eliminator gear

made possible by the use of two intake ports per cylinder, realizes efficient combustion over the entire range of engine speeds.

Further, the intercooler is a high-capacity type that was developed specifically for the 4M42T engine.

4.1.3 Valve system

Each cylinder has two intake valves and two exhaust valves, which are actuated by means of end-pivot-type roller rocker arms. The cylinder bore was made as large as possible to permit an intake-valves diameter of 30 mm and an exhaust-valve diameter of 28 mm. Also, the intake air volume was maximized by means of optimized valve timing and concomitantly superior valve-system characteristics. The valve springs each have an oval cross section and two unequal pitches to suppress surging at high engine speeds. Consequently, the valve system operates smoothly, precisely, and reliably up to high engine speeds (Fig. 7).

4.2 Noise reduction

(1) Low running speeds

The maximum speed of the 4M42T engine is 20 % lower than that of the earlier 4M40T engine. Combustion noise and mechanical noise are lower, and

fuel consumption and reliability are higher, accordingly.

(2) Mechanical quietness

To help minimize mechanical noise, the injection-pump gear is supplemented by a backlash-eliminator gear (Fig. 8) that minimizes meshing noise at all speeds. Also, a one-piece ladder-frame-type main-bearing cap (as used with the earlier 4M40T engine) is employed for low noise and vibration and for manufacturing convenience.

Other features including offset piston pins, anti-vibration bolts, reinforcing ribs on the timing-gear case, and various covers further suppress noise, making the 4M42T engine significantly quieter than earlier 4M40T engine (Fig. 9).

4.3 Cold startability

The electronically controlled, high-pressure, distributor-type injection pump optimally controls the advance angle and injection quantity during cold starting. Synergy between this operation and engine's high compression ratio enhances cold startability and significantly reduces emissions of white smoke after startup.

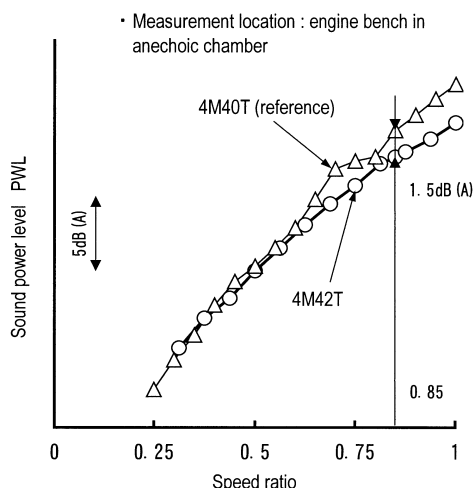


Fig. 9 Reduction in engine noise

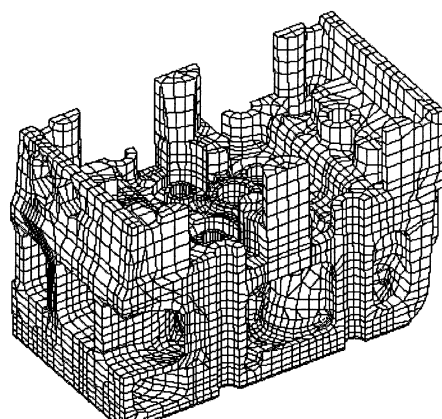


Fig. 10 Finite-element model of cylinder head

4.4 Reliability

Design revisions (described hereafter) were made to ensure sufficient strength for the high combustion pressures caused by direct injection.

To enable the piston pins to withstand the increased cylinder-pressure loading applied to the pistons, surface pressures and deformation were minimized by means of an increased piston-pin size.

Aluminium alloy was adopted for the cylinder head, and the structure of the cylinder head was optimized in accordance with the results of stress analysis. A finite-element model of the cylinder head is shown in Fig. 10.

Special aluminum alloy was employed for the pistons. A cooling channel was added to each piston, and fiber-reinforced metal was employed at the entrance of the combustion chamber.

5. Summary

By employing a direct injection system, a cooled EGR system, an electronically controlled, high-pressure, distributor-type injection pump, and other technologies with the 4M42T engine, MMC achieved its development

targets and realized a highly attractive product.

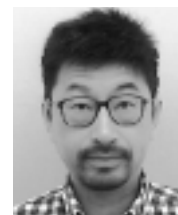
We shall listen to the views of users and developers with a view to making further improvements.



Masaaki UENO



Kenichi KOBAYASHI



Nobuya OSAKI



Masao KAGENISHI



Eiichi KOUJINA



Yasuaki KUMAGAI

Use of Recycled Plastic as Truck and Bus Component Material

Hideo OHTA* Hiromi TOHNO* Tai URUJI*

Abstract

An effort to effectively utilize recycled materials and develop new plastic recycling technology, a study was carried out to find a method that enables using recycled plastic as material of truck components.

As the result of the study, it is now possible for recycled plastic materials from painted passenger-car bumpers to be used as material for production of trucks' black exterior parts. The study also includes establishing a method to use paint-free materials recycled from other industries for those interior and exterior parts in which use of recycled plastic materials from painted bumpers is not acceptable due to paint on pellets.

Keywords: *Recycling, Environment, Plastic*

1. Introduction

As with other companies, Mitsubishi Motors has recognized the fact that protection of the environment is a crucial business activity, and accordingly, efforts are being made to reduce the levels of environmentally unfriendly materials – such as the lead, mercury, and cadmium as used in automobile components – and also to promote the usage of recycled materials in order that environment-related problems may be tackled. Although a large amount of metal, plastic, rubber, and other depletion type resources are used in automobiles, when considered from the point-of-view of recycled material utilization, it can be seen that plastic has inferior recycling properties to those of metals, and furthermore, development of the corresponding technologies is not progressing at the desired rate. Accordingly, the usage both of polypropylene (PP) which has been recycled from passenger car bumpers and of recycled materials from other industries was studied in order that the effective usage of recycled materials could be promoted and that the corresponding recycling technologies could be established. The following provides a summary report regarding this study project.

2. Utilization study for recycled bumper materials

2.1 Recycling material recovery and regeneration methods

Passenger car bumpers which have been removed during replacement by dealers are used in this project, and these are manufactured from PP. These removed bumpers are collected at recovery sites by dealers, and after other materials (i.e., brackets, bolts, etc.) have been removed, they are re-pelletized by a secondary material dealer and are provided to vendors in the form

of recycled material. The majority of bumpers manufactured in recent years have been provided with coatings, and in situations where recycled materials from which these coatings have not been removed are used, segments of the coating can be present on the surface of the components manufactured from recycled bumper materials, thus impairing the overall appearance. Although technologies for removing coating segments during re-pelletizing are available, these remain comparatively expensive, and therefore, this study dealt with the usage of recycled materials from which coating has not been removed.

2.2 Physical properties of recycled materials and studied components

(1) Effect of mixing ratios on material properties and appearance

In order that a suitable mixing ratio for the recycled materials could be determined, materials manufactured with a range of different mixing ratios were subjected to physical property measurement and to investigation of the effect on appearance. Specifically, recycled material mixing ratios of 100 %, 50 %, and 30 % were evaluated. As shown in **Fig. 1**, change in the mixing ratio has no marked effect on the physical properties of the materials; it can also be seen that as the recycled material's mixing ratio becomes higher, the appearance degrades as a result of the effect of coating segments. In addition, when components manufactured from recycled materials are themselves provided with coating, segments of the original coating remain visible on the coated surface of the new products, thus continuing to impair appearance. For this reason, it was determined that the usage of recycled materials for components to be coated is not possible.

(2) Variations in recycled material fluidity (MFR^{*1})

In accordance with the reduction in thickness of

* Material Engin. Dept., Truck & Bus Research & Dev. Office

bumper material which began in 1997, materials with higher levels of fluidity during molding are being implemented at an increasing rate. For this reason, it is considered that the portion of recovered materials with high MFR values will continue to increase in the future, and this is expected to have an effect on both physical properties and dimensions (i.e., shrinkage rate variation). Accordingly, two different types of recycling material with MFR values of 17 and 35 respectively were used in the following evaluation. Specifically, the MFR 17 material has the lowest levels of field recovery, and the MFR 35 material is currently being used as a virgin raw material.

*1: When the melt flow rate (MFR) is higher, the level of viscosity will be lower and liquidity will be higher. Units: g/10 minutes

(3) Components to use recycled materials

Since recycled bumper materials are black in color and usage with coated materials is impossible when the original coating is not removed, components which may use the recycled materials are limited to those which are black and unpainted. **Table 1** shows the components selected for use of recycled materials so that these conditions may be satisfied (all of these are injection-molded components). These were then categorized into classes A through C in accordance with usage requirements, and an investigation into recycled material usage was carried out based on the required characteristics.

2.3 Usage study results

Since those components from Class A are not subject to severe appearance-related requirements, studies were carried out with a recycled material blending ratio of 100 %, and this allowed the component's performance requirements to be satisfied (**Table 2**). Furthermore, the degree of dimensional stability of this material is equivalent to that of the current virgin raw materials, and it was therefore determined that this material is suitable for recycling. **Fig. 2** illustrates an upper shield panel which was manufactured from this material.

In the case of the air cleaner case from Class B (**Fig. 3**), sealability and other strength-related demands are relatively strict, and PP-GF 20 is currently being used as the virgin raw material. Accordingly, evaluation of performance requirements was carried out using a PP-GF 30 base with 50 % (GF 15 %) and 30 % (GF 20 %) ratios of recycled material blending. The results of this evaluation showed that, although the material with 50 % (GF 15 %) blending did not satisfy the property require-

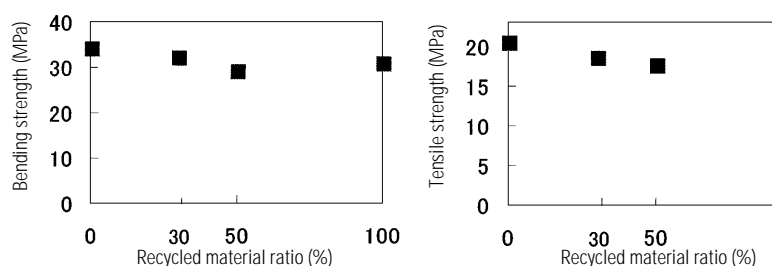


Fig. 1 Physical properties of materials with differing recycled material ratios

Table 1 Components using recycled bumper materials

	Required properties	Study component	Recycled material ratio (%)
Class A	Appearance is not important	Upper shield panel	100
		Lower shield panel	
		Cab side cover	
Class B	Material which strength is required (PP-GF 20)	Air cleaner case	30
Class C	Appearance is relatively important	Dust cover	50
		Tilt control cover	
		10 other components	

Table 2 Evaluation results for Class A components

	Upper and lower shield panels		Cab side cover
Progressive weather resistance	○	○	○
Vibration resistance	○	○	○
Humidity and heat cycle resistance	○	○	○
Impact resistance	○	○	○

(Same results for MFR17 and MFR35)

ments of tensile strength and wear resistance testing, these were satisfied by the 30 % (GF 20 %) material. This material was also determined to be suitable for recycling (**Table 3**).

Since appearance of the Class C components is relatively important factor, evaluation was carried out using a recycled material blending ratio of 50 %. However, coating segments resulted in poor appearance, and it was determined, that application of recycled materials would not be possible in this case.

3. Usage study for recycled materials from other industries

3.1 Recycling material recovery and regeneration methods

In the evaluation of possible usage of recycled materials from other industries, this project adopted container-case recycled materials for study. The term "container-case recycled materials" refers to the recycled materials from cases used to hold containers of beer, soft drinks, milk, and the like. Since these cases are put to use in severe environments, PP with excellent physical properties are used in their manufacture. For this reason, the material from those cases which have exceeded their field-service life or which have become dam-

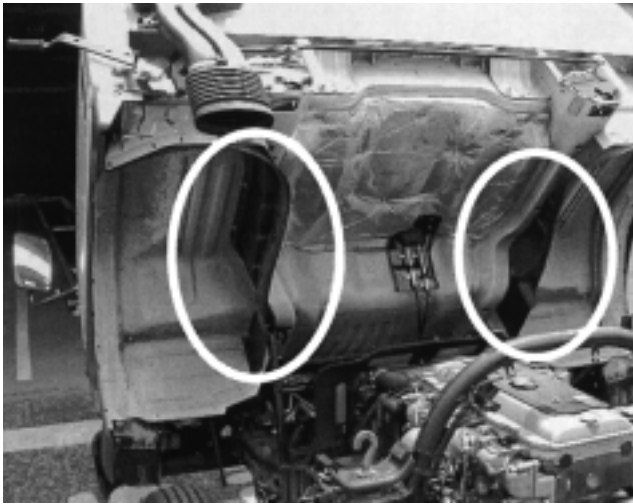


Fig. 2 Upper shield panel

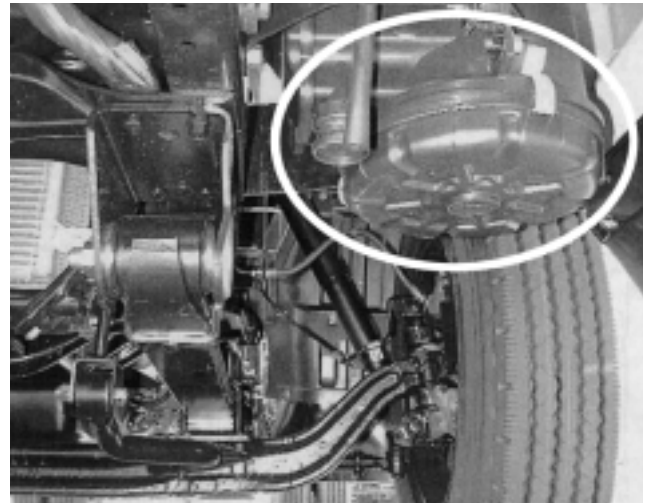


Fig. 3 Air cleaner case

aged is still suitable for use, and this is recycled in the same way as for bumper materials. Due to container-case requirements, a wide range of different colored materials become mixed upon recycling, and carbon or some other pigment is generally added at the re-pelletizing stage to ensure that the resulting material is black.

3.2 Physical properties of recycled materials and studied components

(1) Effect on color tone

Adding black coloring to container-case recycled material of a specified color by the secondary material dealer before the delivery of this material to the component manufacturer, is complex in nature, and therefore, it poses an obstacle to the assurance of supply material. Accordingly, it will be necessary to determine a means of control whereby black material may be achieved within a specific color-tone range regardless of the original material color and the mixture ratio. For this reason, a study was undertaken to determine the effect which the color of original container-cases has on the finished component's color tone.

The container-case recycle materials recovered by secondary material dealers are mainly red, blue, white and mixture of them in color. Carbon was added to each of these colored materials to tint them black. Then, a color difference meter was used to measure the color difference (E^*) between the black-colored recycled material and black virgin raw material. In order that an appropriate ratio for mixture of carbon may be found, recycled material samples added with carbon at ratios of 1 %, 2 %, 5 %, and 6 % were prepared. The results are shown in Fig. 4.

A color difference (ΔE) of 1.5 or less was determined to be insignificant in a visual sense. It was confirmed that such a degree of color difference resulted from a carbon mixture ratio of 1 %, and that, between the sample containing 5 % of carbon and the one containing more carbon, there was almost no change in color difference. Accordingly, it was determined that a carbon mixture amount of between 1 % and 5 % would be suit-

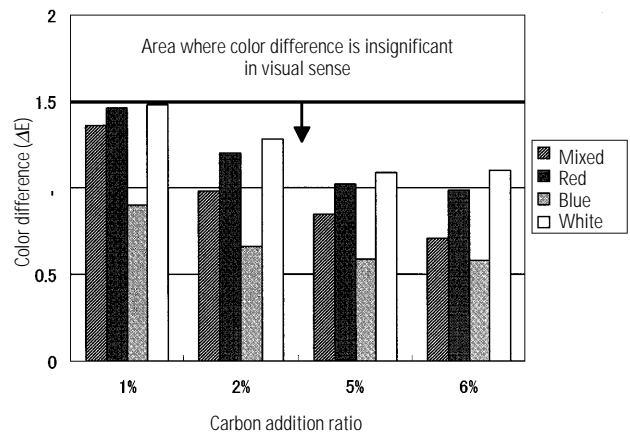
Table 3 Evaluation results for air cleaner case Class B parts

	Component with 50 % recycled material (GF 15 %)	Component with 30 % recycled material (GF 20 %)
Heat/aging resistance	○	○
Tensile test	×	○
Sealability	○	○
Wear resistance	×	○

(Same results for MFR17 and MFR35)

○: acceptable

×: unacceptable

Fig. 4 Carbon addition ratios and change in container material color (ΔE)

able. In the study conducted, components produced from mixed color materials with 2 % carbon added were used.

*2: The color difference ΔE is a quantitative representation of the degree by which a color varies from a base color.

(2) Suitable components and recycled material properties

A study was undertaken to evaluate the usage of recycled container-case material – a recycled material not affected by coating segments – and this was done

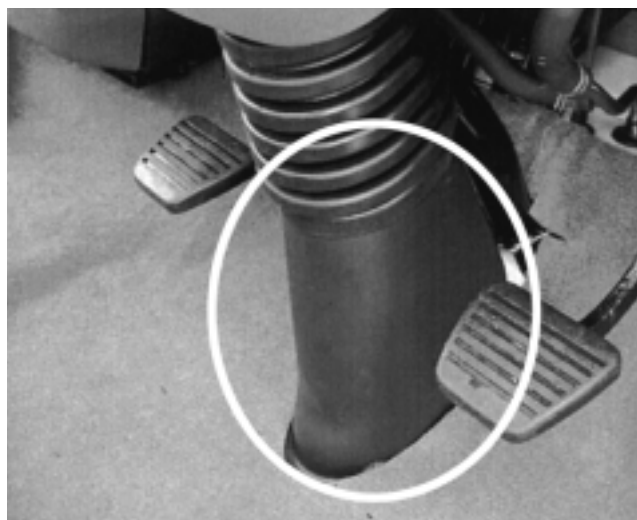
Table 4 Physical property comparison for recycled container-case material and current virgin raw material

Material grade	Recycled container-case material	Current virgin raw material I	Current virgin raw material II	Current virgin raw material III
Produced component	—	Dust cover	Tilt control cover	Side gate board
MFR (g/10 minutes)	10	40	30	1.5
Bending strength (MPa)	30	37	33	—
Elastic modulus in bending (MPa)	1,130	1,400	1,180	980
Tensile yield strength (MPa)	27	29	26	27
Izod impact strength (at 23 °C) (kJ/m ²)	8	7	8	18
Load deflection temperature (at 0.45 MPa) (°C)	110	125	120	—

Table 5 Evaluation results for Class C components

Produced component		Dust cover	Tilt control cover
Evaluation item			
Resistance to heat cycles		○	—
Progressive weather resistance		○	○
Vibration resistance		○	○
Humidity and heat cycle resistance		—	○
Fogging resistance		○	—
Anti-static	Surface resistivity	×	—
	Dust adherence	○	—
Flame resistance		○	—

○: acceptable
 ×: unacceptable

**Fig. 5 Dust cover**

by applying the material to Class C components with which coating segments impaired the appearance in the above-mentioned bumper material study. Furthermore, a study was also conducted by applying the material to the extrusion-formed, side gate boards of medium-duty trucks, for which black PP virgin raw material is currently used. The physical properties of the virgin raw materials used in the components under study and of the recycled container-case material are shown in **Table 4**. With the exception of the MFR value, there are no sig-

nificant differences in these properties, and it is therefore considered that no problems will exist other than those associated with moldability; however, it was decided that judgement on possible usage should be made based on the component's required properties.

3.3 Study results

(1) Injection-molded components

Since container-case material is not affected by coating, evaluation was carried out with a recycled material mixture ratio of 100 %. No problems associated with moldability were identified, and the results of evaluation of the required performance are shown in **Table 5**. The dust cover (**Fig. 5**) failed to satisfy electrostatic requirements; however, the adherence of dust was identical to the trouble-free level of the current virgin raw material. All performance requirements were satisfied for the tilt control cover. Consequently, this material was determined to be suitable for the usage.

(2) Extrusion-formed components

Large differences in MFR exist between the recycled container-case material and the current virgin raw material. Since side gate boards (**Fig. 6**) are manufactured by extrusion forming, it can be foreseen that moldability is adversely affected by low MFR of the recycled material. Accordingly, confirmation of moldability was carried out using 50 % and 30 % recycled material mixture ratios. Although this property did not stabilize for the 50 % mixture ratio, adequate stability was achieved for the 30 % mixture ratio, and evaluation was therefore carried out using a component manufactured with this



Fig. 6 Side gate board (medium-duty truck)

Table 6 Dimension and weight accuracy of side gate board

Measurement item		Standard value	30 % recycled material product	Current virgin raw material product
Total width	(mm)	338.0 – 341.0	339.2	338.7
Thickness	(mm)	22.0 – 23.0	22.5	22.5
Central shrink	(mm)	1 mm or less for every 50 mm	0.7	0.6
Unit mass	(kg/m)	2.24 – 2.76	2.60	2.54

material.

All product dimensions were found to be in conformance with standard values (Table 6), and furthermore, since product properties are equivalent to those of components manufactured from the current virgin raw material, it was determined that this material is suitable for the usage (Table 7).

Table 7 Physical properties of side gate board

Test item		30 % recycled material product	Current virgin raw material product
Three-point bending test	Bending strength (MPa)	13.5	13.1
	Elastic modulus in bending (MPa)	351	333
Compression test	Compression strength (MPa)	4	4
Coefficient of linear expansion	20 – 80 °C (x 10E-5/°C)	15.7	16.3

4. Summary

Through the study described so far, the technology required for usage of recycled materials for PP components has technically been established. Using this technology, approximately 20 tons per month of recycled materials are being used for components of trucks and busses alone. The enactment of Japanese vehicle recycling legislation will give rise to a need for more effective and practical recycling activities, and it will also become necessary to carry out further research into the usage of recycled materials. It is therefore intended to focus on plastic materials other than PP in the future in order that expanded usage of recycled materials may be promoted.

We would like to express our sincere gratitude to all persons from Mitsubishi Motors and other companies who helped in the advancement of this research.



Hideo OHTA



Hiromi TOHNO



Tai URUJI

Molding of Cylinder Head Materials by the Lost-Wax Casting Process Using a Gypsum Mold

Hiroshi KANESHIGE*

Abstract

A resin cylinder head model was produced using a rapid prototype producing system. The resin model was used in the lost-wax casting process instead of a wax model. The casting molded by this method was as precise in both shape and dimensions as a casting produced using a metal mold. This paper describes the manufacturing process of cylinder head material using this method in detail.

Key words: Gypsum Mold, Lost-Wax Casting, Rapid Prototyping

1. Introduction

Cylinder heads are relatively large in size and the molds used for casting them feature complicated core shapes. Traditionally, cylinder heads and similarly complicated castings have been produced by manufacturing wooden patterns that model the shape of the required product, creating sand-molds which are the inverse of the wooden patterns, combining these to form a casting cavity, and finally pouring aluminum or some other molten metal into this cavity to produce the required casting. Creation of wooden patterns in this process requires a considerable amount of time as it involves time-consuming jobs such as designing casting plans and making wooden pattern manufacturing data.

In recent years, machinery manufacturers have market-released a wide variety of rapid prototyping machines which use three-dimensional, computer-aided design data in the creation of the models, and these machines are being put to use in the field of electrical appliances to make resin case prototypes and, in the field of automobiles, to create models of small resin components in order that development periods may be shortened. Meanwhile, it is possible to use models produced using these machines as lost-wax models from which gypsum molds may be created, and this method is actually applied to the production of small cast-component test samples. However, it is generally standard for accuracy attainable by this method to be restricted

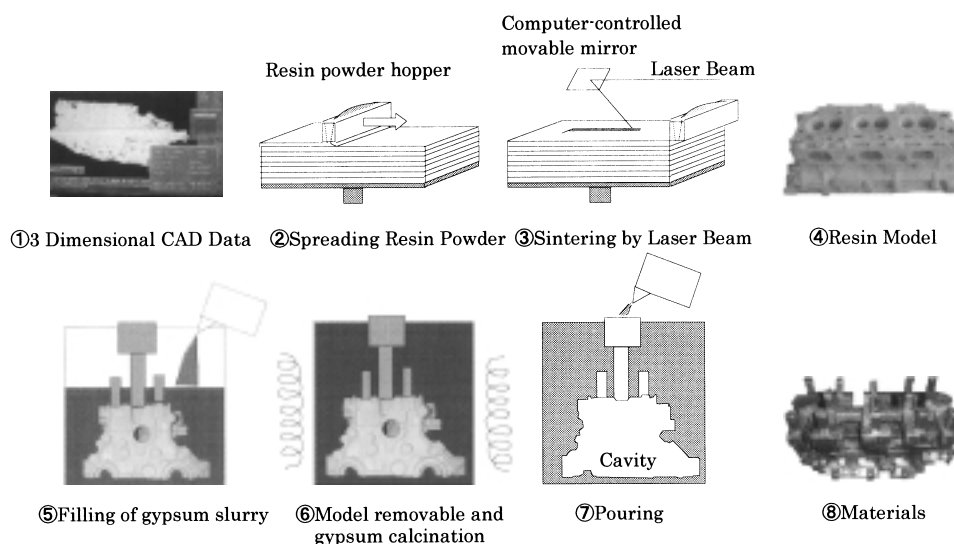


Fig. 1 Main process steps

to a level of approximately ± 1 mm when it is used in the production of cylinder heads or other similarly complicated components with weights in excess of 10 kg. For this reason, this process has not been used for the production of cylinder head materials whose intake and exhaust ports require an accuracy of ± 0.5 mm. Recently, Mitsubishi Motors successfully resolved this accuracy-related problems by forming individually the parts of a resin model and devising measures for limiting deformation encountered in the production of gypsum molds. This paper will introduce the new method that has been established to rapidly produce advance materials of cylinder heads in small quantities to the same accuracy as available with metal molds.

2. Method overview

Fig. 1 presents an overview of the above-mentioned process. In this process, three-dimensional computer-

* Powertrain Production Engin. Dept., Car Production Strategy & Planning Office

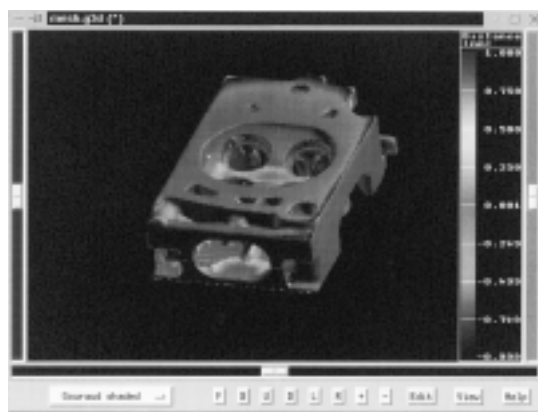


Fig. 2 Results of dimensional measurement on divided polystyrene resin model

aided design data are used to create a resin model (part ① of Fig. 1). First of all, a laminate of fine polystyrene powder is laid down with an arbitrary thickness on a platform (Part ② of Fig. 1). Next, a laser beam is scanned across the surface of the resin powder layer in accordance with slice-shape data which has been obtained by correcting the desired shape data with the shrinkage rates for both resin model forming and casting, and the resin powder is thus sintered (Part ③ of Fig. 1). When the first layer has been completely sintered, another thin layer of fine plastic powder is formed, and laser beam scanning is again used to sinter the layer, thus forming a new sintered layer on top of the first sintered layer. By repeating this layer-forming procedure, a resin model is formed (Part ④ of Fig. 1). Next, sprues, heads, and chillers are added to this resin model, and wax is then applied to the model to improve the adhesion of the resin model and the gypsum slurry.

Following this, the resin model is setup within a depressurized molding flask, and gypsum slurry is then poured into the molding flask and allowed to harden (Part ⑤ of Fig. 1). Next, the gypsum mold is removed from the molding flask, and by placing this into an oven, the resin model can be melted and removed, and the gypsum mold can be calcined (Part ⑥ of Fig. 1). The mold is then cooled down to the pouring temperature, and molten aluminum is poured into the mold (Part ⑦ in Fig. 1). After cooling and mold removing, the casting is subjected to solution treatment to modify the metal structure of the combustion chamber walls, and then artificial hardening treatment (T6) is carried out, thus completing the cylinder-head material (Part ⑧ of Fig. 1).

3. Measures for assurance of dimensional accuracy

3.1 Resin model forming

One-piece resin model forming was initially tried, but the cleaning of polystyrene from the water chamber was extremely troublesome; accordingly, it was decided to form the resin model in two pieces, one parted from the other at the water chamber. Warping of the joint surfaces of these separately formed models was corrected using sand paper, and they were joined

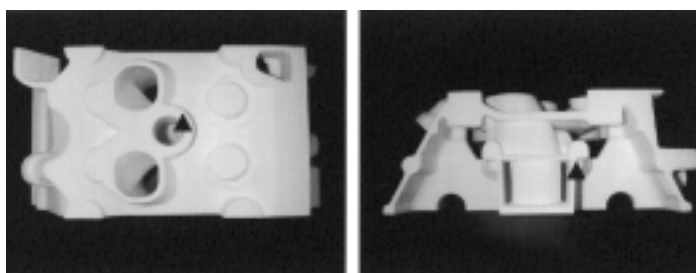


Fig. 3 Forming into shells of thick-wall portions

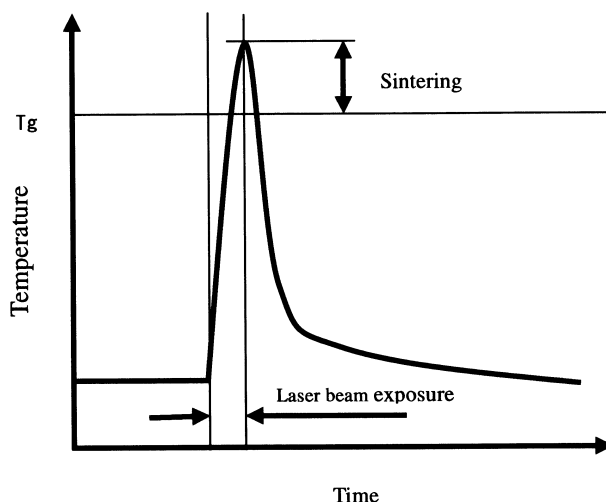


Fig. 4 Heating pattern of resin powder sintering

together using a polyvinyl-acetate emulsion type adhesive. The shape dimensions of the assembled model were measured using a three-dimensional measurement device, which revealed that shrinkage of material at thick-wall sections led to warping of the entire model. It was concluded that this resulted from the buildup of heat from radiated laser beam in thick-wall sections, thus raising the sintering temperatures at these sections and leading to a larger degree of shrinkage than occurring in thinner sections. The following solution was devised in order to resolve this problem.

(1) Separated polystyrene model forming

In order to reduce the total amount of incoming laser beam during forming, the forming of the model was further subdivided by parting it not only at the water chamber but also between combustion chambers by providing joint margins. The separation surfaces were corrected while maintaining the flatness and perpendicularity of the joint sections thereby matching the accuracy of the port-to-port pitch to the target value. Fig. 2 presents the results of dimensional measurements on the separated polystyrene model.

(2) Application of shell structure in thick-wall sections

Shells structure was applied in sections with thick-walls in order to restrict the localized build up of heat which can occur at these locations. Fig. 3 presents a separated polystyrene model in which shell structure has been adopted in such sections.

(3) Optimization of laser sintering temperature

Fig. 4 illustrates the pattern of heating during the

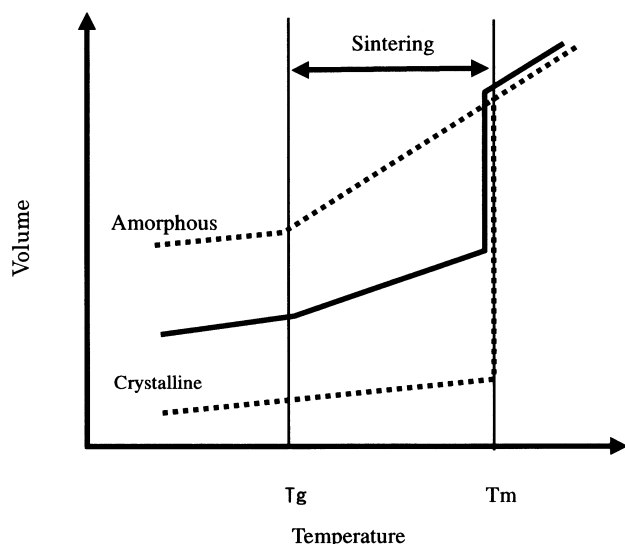


Fig. 5 Thermal expansion of resin

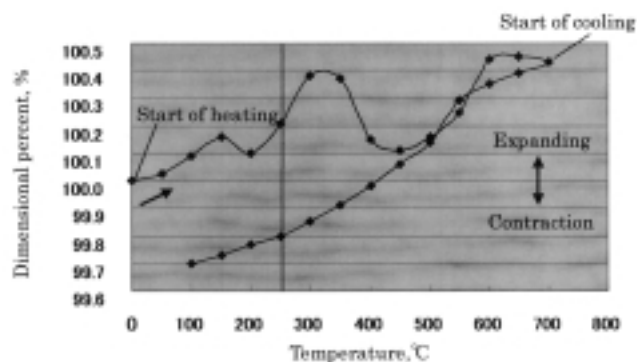


Fig. 6 Expansion and contraction that takes place during formation of gypsum mold





Two-piece resin mold		$\pm 1.6 \text{ mm}$
Six piece resin mold		$\pm 0.9 \text{ mm}$
+inclusion of shell structure in resin mold		$\pm 0.6 \text{ mm}$
+Optimization of sintering temperature, etc.		$\pm 0.4 \text{ mm}$

Fig. 7 Accuracy in length of materials produced by different methods

sintering of the fine resin powder. If the laminated sections of fine polystyrene powder layers are preheated using an infrared lamp at just below the glass-transition temperature and then exposed to the laser beam, the temperature of the plastic powder will rise to the range between the glass-transition temperature and the melting point, and sintering of the resin powder will take place. As shown in Fig. 5, the rate of thermal expansion is considerably high for resins at a temperature above the glass-transition temperature; accordingly, disparity in the sintering temperature contributes greatly to deformation. Furthermore, the physical properties of the resin powder varies from lot to lot, and it is therefore necessary to adjust the pre-heating temperature, laser output, and laser scanning speed to the optimum values for each individual one. Accordingly, the pre-heating temperature for the fine polystyrene powder was dropped by approximately 80 °C from the initial setting of 84 °C, and fine tuning of this temperature was carried out for each individual lot. As a result it was possible to always assure a dimensional accuracy of the resin model to within $\pm 0.4 \text{ mm}$.

3.2 Lost-wax casting with a gypsum mold

The principal cause of deformation during lost-wax casting process using a gypsum mold is the temperature variation that occurs during the melting and

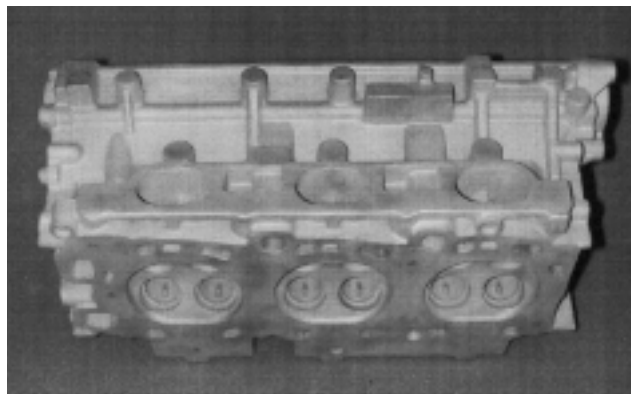


Fig. 8 Finished material

removal of resin model, during sintering of the gypsum mold, and during the cooling of the sintered mold to the pouring temperature. In the case of cooling of the mold in particular, large-scale shrinkage takes place; consequently, cooling was carried out in the oven over a period of at least two hours in order to prevent deformation of the gypsum mold. Fig. 6 shows the expansion and contraction that takes place during the formation of the gypsum mold.

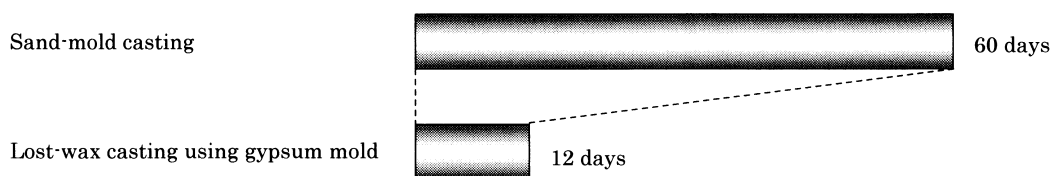


Fig. 9 Comparison of manufacturing periods

4. Dimensional accuracy

Fig. 7 presents a comparison of the contribution to improved dimensional accuracy as achieved using each of the improvement measures. The required dimensional precision of ± 0.5 mm was achieved for the position (and shapes) of the air intake and exhaust ports in the final product. Fig. 8 provides a photograph of the finished casting.

5. Man-hour and cost comparison

Fig. 9 compares the man-hours required for the gypsum mold, lost-wax process with those for sand-mold process. With the conventional sand-mold method, a period of 60 days is required for wooden pattern manufacture and other tasks before the first product can be obtained; however, when using this new method, the first casting can be obtained after 12 days, thus allowing the development period to be reduced by 48 days.

In the case of cylinder-head materials, the cost involved in producing six units by the gypsum mold lost-wax process is equivalent to that involved in producing one unit by the sand-mold process. It is considered that this process can be adopted for the prototype production in advance of sand-mold casting.

6. Summary

The lost-wax casting method using a gypsum mold has made it possible for cylinder head test samples that are large in size and relatively complicated in core shape to be manufactured with a high degree of dimensional accuracy. Using materials produced by this method, designers can develop cylinder heads efficiently as they can test and check engine performance for a wide range of different port shapes before proceeding to sand-mold casting. From now on, this project will involve the studying of issues such as the reduction of costs for fine resin powder in hope that this method can be applied to testing where larger number of samples are required. Finally, all the project members would like to express their sincere gratitude to all persons from Mitsubishi and other companies who helped in the advancement of this research.



Hiroshi KANESHIGE

Development of New PAJERO Rally Car for Paris-Dakar Rally

Yoshihiko OTOTAKE* Shuusuke INAGAKI*



Fig. 1 New PAJERO rally car at 2001 Paris-Dakar Rally finishing line

The rally version of a new Mitsubishi PAJERO model competed in the Paris-Dakar Rally for the first time in 2000 and achieved third place overall. It achieved an even better result – overall victory – in the Paris-Dakar Rally the following year.

1. The Paris-Dakar Rally

The Paris-Dakar is a long-distance off-road rally that began in 1979. It takes place on a huge scale; the 10,000 km course begins in Europe in mid-winter conditions and continues into Africa through demanding environments including mountains, rocks, mud, deserts, dunes, and savanna. Competing teams take nearly three weeks to cover the course, camping along the way. For teams and vehicles alike, the Paris-Dakar is a supremely severe test.

The PAJERO has competed in the Paris-Dakar every year since 1983 (the year following its launch) and has achieved outstanding results including six overall victories.

2. Concept of new PAJERO rally car

With the PAJERO rally car, Mitsubishi Motors Corporation (MMC) took advantage of the production model's superior features to achieve outstanding competitiveness and reliability. Key features are as follows:

- Four-wheel independent suspension (and concomitantly superior handling stability and roadholding)

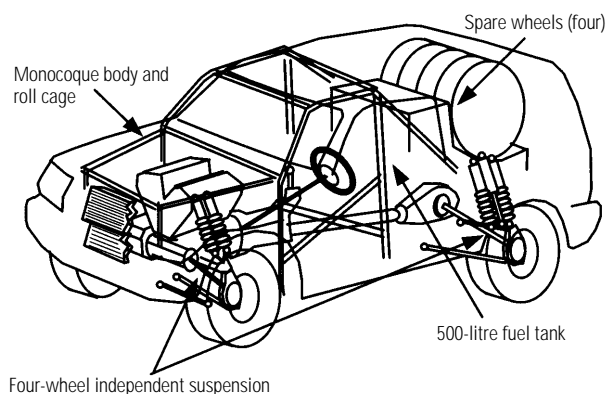


Fig. 2 Major features of new PAJERO rally car



Fig. 3 Driving scene

- Light, highly rigid monocoque body
- Long wheelbase (and concomitantly superior stability and load capacity)
- Engine and drivetrain employing proven components

3. Engine

The Paris-Dakar rules permit a competing vehicle's engine to be replaced with another one provided it is used by the same manufacturer in the same vehicle family, so MMC employed the powerful 6G74 MIVEC engine, which has proven itself in the PAJERO EVOLUTION. The rules do not permit the adopted engine's internal parts to be modified, and they require the

* Vehicle Testing Dept., Car Research & Dev. Office

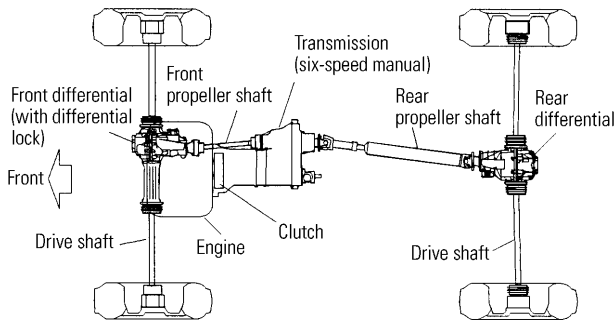
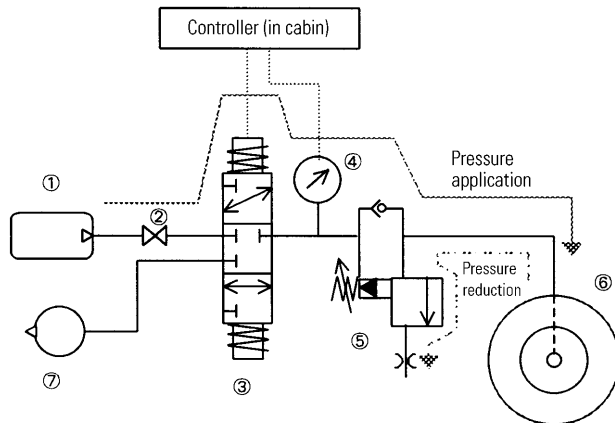


Fig. 4 Drivetrain configuration



- ① High-pressure air tank
- ② Regulator
- ③ Solenoid valve
- ④ Pressure sensor
- ⑤ Selector valve (fitted on wheel)
- ⑥ Tire
- ⑦ Vacuum pressure source

The controller adjusts the tire pressure to the desired level by activating the solenoid valve in accordance with information from a pressure gauge. Parts ③, ④, and ⑤ are provided separately for each wheel, so each tire pressure is controlled independently of the others.

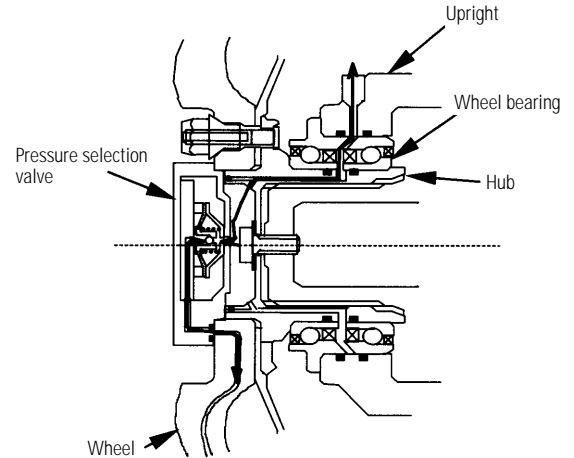
Fig. 5 Tire pressure control system

engine's intake air volume to be limited by a restrictor. MMC increased the respective capacities of the radiator and oil cooler in the cooling system to enable high-load operation for long periods at low vehicle speeds.

4. Drivetrain

The drivetrain is configured for full-time four-wheel drive. For superior traction and reliability, it employs viscous-coupling-unit front and center differentials and a mechanical limited-slip rear differential. In the front differential, a mechanical locking mechanism is located in parallel with the viscous coupling unit to enable the vehicle to be extricated from stag in dune.

On the rally course, the drivetrain is subjected to extremely severe conditions including impact load by big jumps. MMC ensured sufficient strength, durability, and reliability by selecting high-grade materials ($\sigma_b = 2,000 \text{ MPa}$), maximizing gear-meshing precision, and establishing optimal replacement intervals.



Air flows to and from the tire on the turning wheel via the following path: upright \leftrightarrow wheel bearing (provided with air passage in center) \leftrightarrow hub \leftrightarrow pressure selection valve \leftrightarrow wheel (provided with air passages in spokes) \leftrightarrow tire

Fig. 6 Air path

5. Suspension

The suspension stroke, which is important with respect to rough-road performance, is restricted to 250 mm by the Paris-Dakar regulations, so MMC optimized the bump-to-rebound ratio within the permitted stroke with regard to body inputs and traction.

The regulations do not permit alteration of the points at which suspension parts are mounted on the body, so the characteristics of the production model's suspension are critical. With the new PAJERO, MMC used the benefits of its rally experience to reflect off-road considerations in the suspension geometry of the production model. As a result, the suspension geometry is excellent for rally applications.

Two dampers per front wheel and three dampers per rear wheel are used to minimize heat-induced deterioration in damper performance on rough roads.

6. Technical point

Each leg (one-day) of the Paris-Dakar Rally encompasses a huge distance (300 – 800 km) and a concomitantly wide range of road-surface conditions, which necessitate different tire pressures: On relatively hard surfaces, high tire pressures are necessary to give the tires sufficient lateral rigidity and puncture resistance. On dunes, by contrast, low tire pressures, which maximize the tires' contact areas, are necessary to help prevent the vehicle from sinking. To allow the PAJERO rally car's occupants to adjust the tire pressures without stopping the car and getting out, MMC developed a system that can be used to make adjustments by means of a controller in the cabin while the car is moving.

7. Summary

MMC has competed in the Paris-Dakar Rally since creating the PAJERO nearly 20 years ago. Numerous

technical problems during this period have taught us a great deal, and we have reflected the benefits in successive PAJERO production models, making each one faster, safer, and more comfortable than its predecessors. As we make further technological advances through our Paris-Dakar participation, we shall continue to feed them back into production models in pursuit of the highest possible levels of durability, reliability, and cross-country performance.

In 2002, MMC revised the specifications of the PAJERO rally car to comply with revised regulations. Thanks to the benefits of our experience, we achieved overall victory once again. Details of the winning vehicle will be published at the next opportunity.



Yoshihiko OTOTAKE



Shuusuke INAGAKI

Development of Rally Car for World Rally Championship

Shuusuke INAGAKI* Yasuo TANAKA*

In 1995, new FIA World Rally Championship regulations enabled manufacturers that did not have turbocharged, four-wheel-drive (4WD) cars in their production-car lineups to compete in the World Rally Championship (WRC) for the first time. Specifically, the new regulations supplemented the existing Group A class (GrA) with the World Rally Car (WRC), in which front-engine, front-wheel-drive production cars could be modified to produce two-liter, turbocharged, 4WD rally cars. The WRC regulations allowed manufacturers to make extensive modifications for incorporation of turbochargers and 4WD powertrains, making WRC potentially more competitive than GrA cars.

Some manufacturers soon switched to the WRC, but Mitsubishi continued competing with GrA rally car variants owing to the technical and sales-related benefits of linkage with production cars. To maintain its competitive advantage, however, Mitsubishi later built a WRC and raced it for the first time in the 2001 Rallye Sanremo.

1. WRC regulations

The main differences between the regulations applying to WRC cars and GrA cars are shown in Table 1.

2. Development procedure for Mitsubishi WRC

For the best possible balance of performance and reliability, the development plan was devised with two stages. In the first stage, which was targeted for completion in autumn 2001, the powertrain position was revised to optimize the front-rear distribution of weight and the wheel housings were enlarged to permit longer suspension strokes and to permit MacPherson-strut rear suspension to be employed as permitted by the regulations. Existing components were used as much as possible. In addition, the position of the intercooler was revised to improve cooling efficiency for higher engine output. In the second stage, which was targeted for completion in time for competition in spring 2002, the powertrain was extensively revised. The outcome of the second stage was a combination of ample ground clearance, higher 4WD-component strength, and

Table 1 Outline of WRC and GrA regulations

WRC	GrA
The car must have an overall length of at least 4 m, and at least 25,000 units of a car with the same form (excluding bumpers) must have been manufactured in 12 months. The car may have a relatively small cabin volume.	At least 25,000 identical examples of the car must have been manufactured in 12 months. (Two-liter, turbocharged models are dominant. Cabin-volume requirements apply according to class.)
Modifications to the floor (tunnel and rear area) and front and rear wheel housings (including the fenders) necessary for adoption of a 4WD powertrain are permitted. The car's overall width may be increased (relative to that of the production model) up to 1,770 mm. (Its overall length may not be increased.) A rear spoiler and a front airdam may be added.	No body modifications are permitted. If the production model's powertrain can be replaced, it may be replaced with a stronger one.
The engine's bore, stroke, and other specifications may be changed freely, but the cylinder block and cylinder head may not be replaced with those of another engine. Cooling-system parts including the intercooler may be changed freely. Holes may be made in the front bumper and hood (within limits).	The engine's pistons, camshafts, and valves may be replaced. Other changes (except to the radiator and fan) are not permitted.
The rear suspension may be changed to another type (example technologies: MacPherson struts, trailing arms, rigid suspension).	If suspension parts can be replaced, they may be replaced with stronger ones.

4G6 turbocharged engine with new intake and exhaust systems

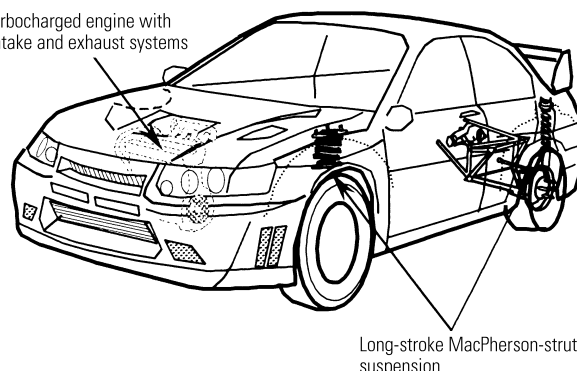


Fig. 1 Technical features of LANCER EVOLUTION WRC

improved engine performance.

3. Technical overview of rally car

3.1 Concept of WRC car

Major technical features of the LANCER EVOLUTION WRC are shown in Fig. 1.

3.2 Engine

The engine of a WRC must have a restrictor that limits its air intake rate, so significant improvements in output are difficult to achieve. Mitsubishi's engine-tuning efforts were thus focused on reducing friction, increasing the compression ratio, and reducing turbo lag. Reducing the engine's weight was another effective means of improving the car's overall performance.

Reductions in friction require improvements in com-

* Vehicle Testing Dept., Car Research & Dev. Office

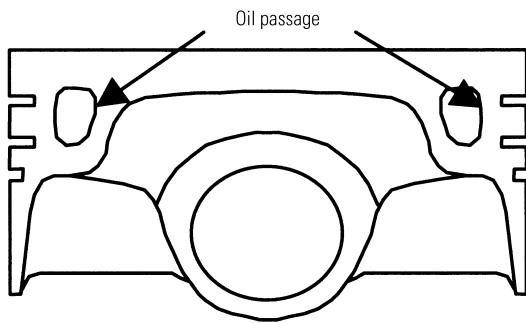


Fig. 2 Oil-cooled piston

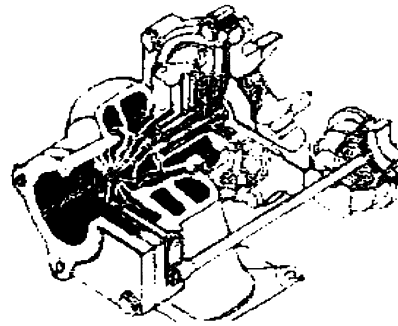


Fig. 3 Twin-scroll turbocharger

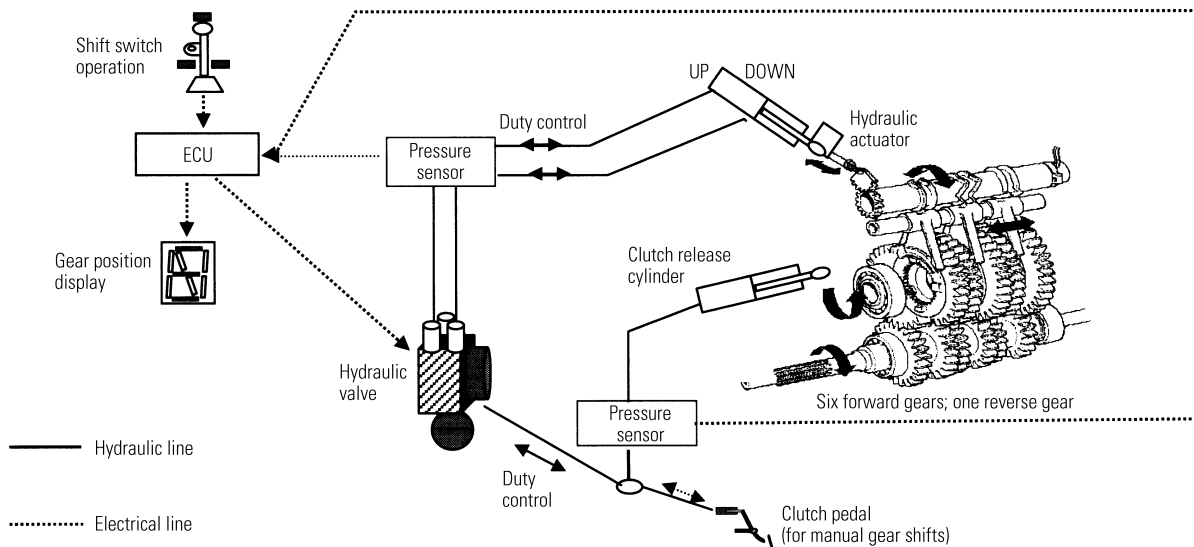


Fig. 4 Gear-change control system

ponent precision. Also, the fuel type is specified by the regulations so increases in the compression ratio require careful adjustment of the intake air temperature and ignition timing. The WRC allows a significant degree of freedom in positioning of the intercooler, so the WRC's intercooler was mounted further back than that of the production model and an air-intake guide was mounted in front of it for higher cooling efficiency. For minimal turbo lag with the WRC's engine, some of the compressed air emerging from the turbocharger's compressor is introduced into the exhaust manifold and the unburned gases' recombustion energy is used to prevent the turbine speed from dropping. This arrangement enhances turbocharger response when the throttle is opened and closed. The turbine-nozzle and intake-manifold shapes also have a significant influence on turbocharger response, so they were optimized in accordance with information gained from vehicle tests and competitive events (Fig. 2 and 3).

3.3 Powertrain

(1) 4WD system

The GrA LANCER rally car has a unique and highly effective 4WD system with which the rear wheels are driven directly without the inclusion of a center differential; torque supplied to the front wheels is adjusted as necessary by means of a clutch. The same type of

4WD system was adopted with the WRC. Its operation was described in Mitsubishi Motors Technical Review NO. 11.

(2) Gear-change system

A gear-change system that was refined in the GrA LANCER rally car was adopted again with the WRC. It combines a sequential shift pattern with technology that controls the engine speed during gear shifts such that gears are synchronized without the need for clutch-pedal depression. For greater ease of use, an electro-hydraulic system for shift operations and clutch operation was added (Fig. 4). The electrohydraulic system reduces work for the driver by making a mechanical shift lever unnecessary; the driver can perform gear shifts using a switch that is located wherever desired. Owing to reliability concerns, the existing mechanical shift lever was also retained for a redundant arrangement.

(3) Rear differential

To enable optimization of the rear-left and rear-right wheels' differential-limiting torque for maximal traction and cornering stability, an existing cam-type self-servo rear differential was supplemented with an active control system employing a mechanism that adjusts the initial differential-limiting torque by means of electromagnetic force. The aforementioned cam-type self-servo rear differential is widely used in motorsports because

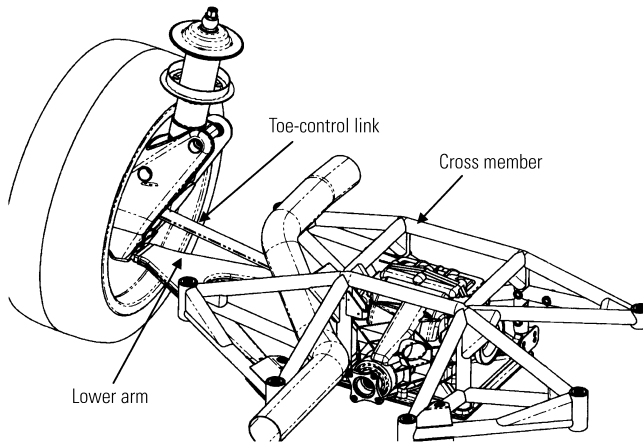


Fig. 5 Construction of rear suspension

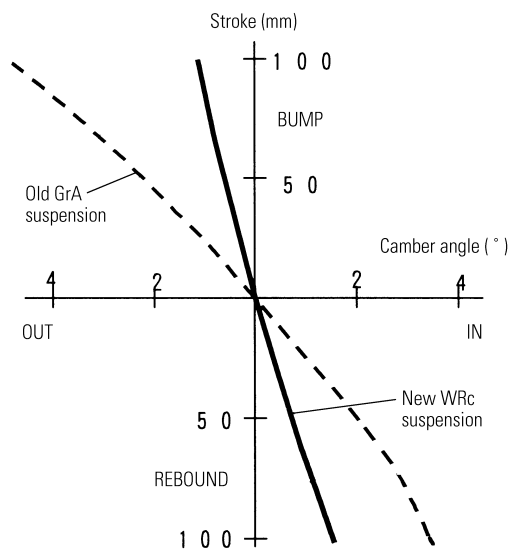


Fig. 6 Camber characteristics

it provides high differential-limiting torque within compact dimensions. Unfortunately, this type of differential is characterized by significant hysteresis (its only short-coming) so the cam angle was reduced by Mitsubishi for better response.

3.4 Suspension

The production car had trailing-arm rear suspension, but MacPherson-strut rear suspension was adopted for the WRC as permitted by the regulations (Fig. 5).

In accordance with the change in rear-suspension type, the lower arms were made as long as possible to minimize camber changes (Fig. 6). The lower arms' mounting points on the body were positioned longitudinally in parallel with the car's center line, and the toe-control links also were positioned in parallel, resulting in minimal dive, squat, and toe changes and in significantly improved stability on uneven surfaces.

3.5 Evaluation

Thanks partly to the long wheelbase of the new LANCER production model on which it is based and



Fig. 7 Test drive in France

partly to the increased suspension stroke permitted by the WRC regulations, the WRC is superior to the GrA LANCER EVOLUTION rally car in terms of high-speed stability and initial steering response. At the time of writing, Mitsubishi is fine-tuning every part of the car and rapidly implementing the second stage of component development with a view to improving performance even further (Fig. 7).

4. Summary

Mitsubishi's rally-car development program is based at the Car Research and Development Center in Okazaki, Japan. Staff here cooperate closely with the Mitsubishi rally team, which is based in the United Kingdom. By feeding rally-car technology back into production models, the company increases efficiency in production-model development. At the same time, Mitsubishi's active incorporation in rally cars of new technologies achieved through advanced research underpins Mitsubishi's continued rally dominance. In motorsports, effective new technologies make their benefits known quickly and clearly, giving engineers a sense of fulfilment. At the same time, work that is poorly focused or has been performed with less than total dedication is quickly exposed and harshly punished in competition. The Mitsubishi rally fraternity takes genuine pleasure in training new generations of engineers who can handle the challenges and in providing customers with affordable new performance-enhancing technologies that we have developed in our drive toward the highest possible performance levels. In the years ahead, we shall continue working hard on new technologies with a view to maintaining our dominant position in the rally world.



Shuusuke INAGAKI



Yasuo TANAKA

Mitsubishi's ASV-2 Passenger Car Obtained Japan's Land, Infrastructure and Transport Ministerial Approval

– Testing on Public Roads Prior to Commercialization –

Yoshiki MIICHI* Susumu MASUDA*

In 2000, Mitsubishi Motors Corporation (MMC) developed a group of Advanced Safety Vehicle-2 (ASV-2)⁽¹⁾ passenger cars employing its vast safety-technology resources. In November of the same year, these vehicles played a part in Smart Cruise 21 Demo 2000, an open demonstration that was jointly organized by Japan's former Ministry of Transport and former Ministry of Construction at that time. One of the ASV-2 vehicles is the ITS-ASV, whose design focuses on intelligent transport systems (ITS). MMC slightly modified the ITS-ASV, and in August 2001 Japan's Minister of Land, Infrastructure and Transport (subsequent ministry) granted the approval that MMC needed to use the ITS-ASV in a wide range of tests (all aimed at commercialization of new technologies) on public roads without violating safety regulations. Subsequently, MMC pursued a program of proving and evaluation tests and was able, as a corollary, to help the Ministry of Land, Infrastructure and Transport establish standards for ITS technologies⁽²⁾. The ministerial approval effectively relaxed the safety regulations applied to three technologies: light distribution control headlight; advanced high-mount stop lamp; and a lane trace assist. In all, MMC used the ITS-ASV to test eight driver support technologies (including the three aforementioned ones) on public roads.

1. Introduction

Japan's ASV project began in 1991 under the leadership of the former Ministry of Transport. MMC was actively involved in the project's first phase (1991 – 1995) and second phase (1996 – 2000) and thus made possible the commercial adoption of numerous world-first driver support technologies including the Mitsubishi Driver Support System⁽²⁾, which combines three technologies (adaptive cruise control; lane departure warning system; and side-rear monitor) and was commercially adopted by MMC in February 2000. Efforts to commercialize new ITS technologies (including those developed by MMC) are likely to expand significantly in the years ahead. Evaluation on public roads of ITS technologies that are still in development will be hugely important.

In Japan, the Minister of Land, Infrastructure and Transport has the power to relax the safety regulations applied to new ITS technologies, thereby enabling man-



Fig. 1 ITS-ASV

ufacturers to conduct tests on public roads. Manufacturers can thus boost the efficiency of their development efforts. Ministerial approval for relaxation of safety regulations is typically limited to technologies that potentially offer great benefits in terms of safety and/or environmental protection. The results of any test conducted on public roads with such ministerial approval are, of course, used commercially by the manufacturer that conducts the tests. In addition, the manufacturer is required to report the results to the ministry. Thus, the ministry gains valuable information that it can use whenever it revises safety regulations to meet changing environmental and social circumstances.

Many new ITS technologies (for example, any system that helps drivers lane keeping operation by generating slight torque in the steering wheel) were not anticipated when the current safety regulations were established, so they cannot legally be tested on public roads without special ministerial approval. MMC received such approval for technologies employed in its ITS-ASV passenger car. Consequently, MMC was able to conduct proving and evaluation tests (all aimed at commercialization of the new technologies) on public roads and was additionally able to help the Ministry of Land, Infrastructure and Transport establish standards for ITS technologies.

2. The ITS-ASV approved by the Minister of Land, Infrastructure, and Transport

With the ITS-ASV (Fig. 1), MMC conducted tests on public roads of eight technologies (Table 1) including three technologies for which the Minister of Land, Infrastructure, and Transport granted specific approval.

* Advanced Electrical/Electronics Dept., Car Research & Dev. Office

Table 1 Main technologies of ITS-ASV**Active safety technologies**

Specifically approved by Minister of Land, Infrastructure and Transport for testing on public roads

Light distribution control headlight (Variable light distribution headlight) (Fig. 2)	The distribution of light from the headlights is optimized in accordance with driving conditions (vehicle speed), driver inputs (steering wheel angle), and the road shape (from navigation data) for maximal nighttime visibility.
Advanced high-mount stop lamp (Deceleration-rate-dependent braking warning system) (Fig. 3)	The illuminated width of the high-mount stop lamp is altered in accordance with the vehicle's deceleration rate. Indication of the deceleration rate to the drivers of following vehicles helps prevent a rear collision.
Lane trace assist (Lane trace assisting system) (Fig. 4)	White lane marking on the road surface are detected using a CCD camera mounted on the rearview mirror, and slight torque is constantly generated in the steering wheel to help the drivers lane keeping operation. Thus, effort for the driver is reduced and safety is enhanced.
Driver alertness monitor (Anti-dozz warning system)	The frequency with which the driver blinks and the durations of periods when the driver's eyes are closed are monitored using a compact camera mounted on the instrument panel. The driver's level of alertness is inferred from these variables. When the driver is deemed to be asleep at the wheel or otherwise insufficiently alert, audible and visual warnings are issued.
Night pedestrian monitor (System for providing information on presence of pedestrians in front of vehicle at night)	Road conditions in front of the vehicle are monitored using an infrared camera mounted in the center of the front grille, and information on the presence of pedestrians is provided to the driver audibly and visually.
Head-up display (Advanced information display system)	Low-alertness warnings and other warnings and information are projected onto the windshield and thus conveyed to the driver with great efficiency.

Passive safety technologies

Pedestrian injury mitigating body (Shock-absorbing body structure for reduced collision on pedestrian)	In case a vehicle-to-pedestrian collision cannot be avoided using active safety technologies, the front of the body is given a shock-absorbing structure to minimize the extent of pedestrian injuries.
---	---

Fundamental automotive technologies

Voice-control system (Human interface technology for reduced driver's effort)	The driver is able to control major navigation, audio, and climate-control functions by means of spoken commands and without taking his/her eyes off the road. Thus, effort for the driver is reduced and safety is enhanced.
--	---

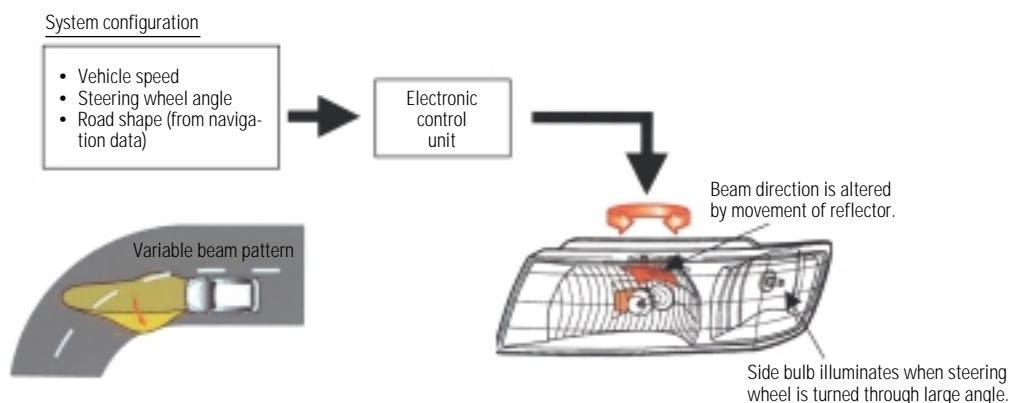
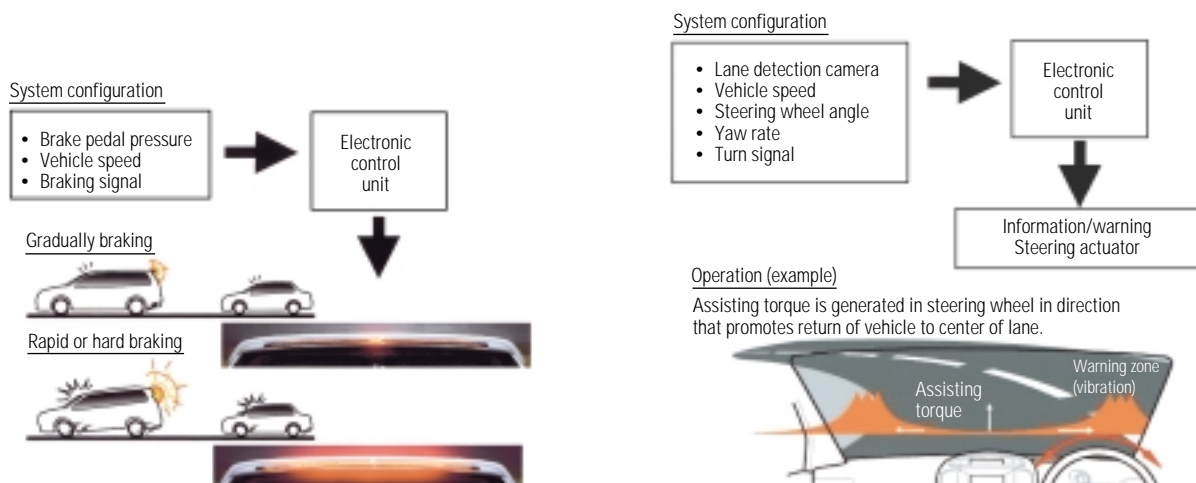
**Fig. 2 Light distribution control headlight****Fig. 3 Advanced high-mount stop lamp****Fig. 4 Lane trace assist**

Table 2 Relaxed items of safety regulations

Approved technology	Relaxed items of safety regulations
Light distribution control headlight (Variable light-distribution headlight)	Article 32 (headlights), items 1, 3, 4, 8
Advanced high-mount stop lamp (Deceleration-rate-dependent braking warning system)	Article 39, item 2 (auxiliary stop lamps) Article 42 (restrictions on lamp colors, etc.), items 5, 7
Lane trace assist (Lane trace assisting system)	Article 11, item 1 (steering systems) Article 20, item 5 (drive control systems)

In the tests, MMC evaluated the functionality and practicality of the technologies on urban roads, mountain roads, and in various other public road environments that cannot be replicated on a test track. A wide range of drivers of both sexes took part in the tests.

3. Relaxed items of safety regulations (Table 2)

Japan's current safety regulations do not make sufficient provision for new ITS technologies, so MMC was initially unable to conduct tests on public roads without violating or potentially violating nine items pertaining to headlights, steering systems, and other systems. These nine items were relaxed by the ministerial approval obtained by MMC.

4. Overview of tests conducted on public roads

The test vehicle carries control devices (including numerous general-purpose microcomputers) and measuring instruments, so its weight, current consumption, and other specifications differ from those of the base vehicle. In contrast to operation on a closed test track, operation on public roads is accompanied by the risk of unexpected obstacles. Consequently, MMC was required to submit general plans and detailed plans of its public-road tests to the Ministry of Land, Infrastructure and Transport and to effect strict control over the tests.

MMC conducted some of the tests at night. In the nighttime tests (Fig. 5), which dealt mainly with the light distribution control headlight, MMC was able to verify the practical benefits of new technologies to a much greater extent than would have been possible on a test track.

**Fig. 5 Nighttime test scene**

5. Summary

Numerous driver support systems potentially offer increased automotive safety and convenience, but their commercialization will require successful solutions to numerous technological and social issues (applicability to different environments; suitable human interfaces; compatibility with existing transport systems; the ease with which drivers can familiarize themselves with new systems and accept them as part of their usual driving experience; and so on). As driver support systems become more advanced, evaluation and proving by means of tests conducted on public roads will become increasingly important if solutions are to be found.

MMC will continue working hard on new ITS technologies with a view to enabling commercial adoption of driver support systems that deliver increased safety and convenience to automobile users everywhere.

References

- (1) Y. Miichi, K. Yamamoto et al.: Development of Mitsubishi Advanced Safety Vehicle (ASV-2), Mitsubishi Motors Technical Review, NO. 13, 2001
- (2) Y. Miichi et al.: Development of Mitsubishi Driver Support System, 6th World Congress on ITS, November 1999



Yoshiaki MIICHI



Susumu MASUDA

Development of Concept Cars for the 2001 Tokyo Motor Show – Embodying the Message of the Reborn Mitsubishi Motors –

Masashi IWATA*

Introduction

Taking advantage of the opportunities presented by its alliance with DaimlerChrysler, Mitsubishi Motors Corporation (MMC) is implementing a turnaround plan with a view to transforming itself into a dynamic new business. In this context, MMC sees product design as a vital expression of its commitment to bringing attractive, appealing products to market.

As part of its effort to establish a new carmaking philosophy and an exciting new design identity that's in tune with customers' emotions, MMC appointed Olivier Boulay, formerly of DaimlerChrysler, as head of design operations in its Car Design Division. Mr. Boulay's appointment was accompanied by a wide-sweeping review of MMC's design activities and marked the start of an MMC design renaissance.

The 2001 Tokyo Motor Show saw the unveiling of four concept cars that express the message of the reborn MMC. This paper gives an overview of MMC's four concept cars.

1. Development targets

The four concept cars indicate MMC's future car-making approach in three main areas: passenger cars, minivans, and sport utility vehicles (SUVs) (Fig. 1). Their designs reflect a shift away from predominantly engineering-oriented development toward a stronger emphasis on emotional stimulation (Fig. 2).

A new MMC exterior-design identity that's shared by all of the concept cars is created partly by an expressive front mask (this is centered on a prominent Mitsubishi logo) and partly by a striking one-motion body silhouette (Fig. 3). A shared interior design motif is based on elegant, people-friendly curves that are reminiscent of waves.

Although the four concept cars share the same basic exterior and interior forms and design motifs, each one has a unique personality that distinguishes it from the others. Further, each concept car's design incorporates, to the greatest possible extent, reflections of Japanese culture and tradition as seen in Japanese architecture and advanced technology.

The concept-car display was divided into two time-zone-themed stands – Tomorrow and Future – with two cars on each stand. The Tomorrow stand featured the CZ2, a new-generation compact car with a casual-chic personality, and the CZ3 TARMAC, a new-generation



Fig. 1



Fig. 2

compact car with a sporty personality. The Future stand featured the SPACE LINER, a new-concept minivan reflecting bold proposals for interior space and equipment, and the S.U.P. (Sports Utility Pack), a fun-oriented new-concept SUV for people who love both nature and advanced technology.

* Advanced Styling Design Dept., Car Product Design Office



Fig. 3



Fig. 5



Fig. 4

2. SPACE LINER

This comfort-oriented concept car reflects a fresh and innovative look at the significance of interior space (Fig. 4).

A futuristic monoform shape and a long wheelbase

together delineate a sporty, elegant exterior. The interior design creates a unique relaxation space that reflects Japanese tastes in lighting, colours, and materials. Features including a drive-by-wire steering system and swiveling seats minimize occupant stress.

Power for propulsion is provided by a fuel-cell system.

3. S.U.P.

The S.U.P. is designed for nature lovers who are equally happy using the latest in technology (Fig. 5).

The interior and exterior design of the S.U.P. gives graphic expression to active, fun-loving lifestyles. Imaginative and original features include a pop-art-inspired tube line that encircles the body and incorporates the front and rear lamp units; a full-length lamella roof panel; semi-transparent door panels that can be detached and used as bags; and seatback bags that can be detached and used as backpacks.

The S.U.P. is propelled by a hybrid powertrain.

4. CZ2

The CZ2 is a proposal for a casual and stylish next-generation compact car (Fig. 6).

For enjoyable daily use, the CZ2's design includes a striking one-motion silhouette, a wave-shape instrument panel, and numerous other features that excite the senses and exude refinement.

New ideas for convenience are reflected in appointments such as detachable door-trim pouches and a four-partition glass roof with independent sunlight control.

5. CZ3 TARMAC

This sporty compact car exudes the spirit of MMC's World Rally Championship machines in its performance and styling (Fig. 7).

The four-door compact body combines emotional appeal with practicality for urban lifestyles. Its dynamic



Fig. 6



Fig. 7



body lines envelop a cabin that takes a rally-car cockpit as its styling theme.

The CZ3 TARMAC has the same powertrain (four-wheel drive with Active Center Differential and Active Yaw Control) as the LANCER EVOLUTION.

6. Summary

In earlier years, MMC did not pay sufficient attention to giving its cars a clear family identity. As a result, insufficient consistency in MMC car designs tended to weaken the impression created by the MMC car range.

Customers around the world increasingly desire products whose message can be perceived at a glance, so building a distinctive brand and establishing a clear design identity are vitally important tasks.



Masashi IWATA

Mitsubishi announced and launched the new eK-WAGON on October 11, 2001. This standard for the next generation of mini-class vehicles is a semi-tall packaging, featuring wide field of view, easy getting in and out, and suitability for most multi-story parking garages. The name "eK" comes from the project code name of this vehicle, which doubles "ii-kei", meaning "good mini" in Japanese.



1. Target

The car was developed as a standard model for a broad cross section of people, regardless of generation or gender, with the following three philosophies in mind:

- (1) To make the car recognized as the standard next-generation mini-class vehicle.
- (2) To develop the car with the eyes of the customer, and never with the self-righteous attitude.
- (3) To develop the car not as a trendy vehicle, but as one with real value that will be loved for a long time.

2. Features

The product concept of eK-WAGON is "just value wagon", which means that everything related to the car is just right – just the right body size with 1,550 mm overall height, just the right level of original equipment, and just the right price for the customer, starting from ¥910,000. Further, the car has top-level collision safety in its class as well as crisp, stable and enjoyable steering performance.

- (1) Exterior styling with semi-tall, long roof

Even with the hip-point height of 630 mm, as well as 900 mm head room of the front seat, which combine to deliver a wide field of view and easy getting in and out, the car remains within the semi-tall size of 1,550 mm overall height that's accepted by most multi-story park-

ing garages. The car also has simple, clean and basic exterior styling, featuring a long roof to give an interior length of 1,830 mm, and wide leg room for the rear seat. These features are clear even from outside of the vehicle.

- (2) Speedometer located at the center and accessories with innovative new ideas

The design of the instrument panel has an open feeling, and the speedometer is located at the center, for easy focusing by not being too close to the driver's eyes and also easy recognition with minimum turning of the eyes. And there is a wealth of innovative accessories such as a petit trash box, "Mr. Defrost", inspection certificate holder, multi-cup holder and ticket holder.

- (3) Top safety performance in the class

With its high energy-absorbing front structure and high-rigidity cabin in case of the worst, the car has the top level collision safety of its class according to in-house tests, which are equivalent with New Car Assessment Japan. In addition, by improving maneuverability, the car has risk avoidance performance equivalent to a small car level for emergency situations, and ABS with a brake-assist is available as an option for every vehicle.

- (4) Power train with clean exhaust emissions and good fuel consumption in actual traffic





The car is equipped with a 660 cc, 3-cylinder, 12-valve ECI multi-point injection engine, which is certified as "good-low exhaust emission", meaning that the emission figures are 50 % or more lower than those specified in the year-2000 exhaust emission regulations.

The engine is coupled with an automatic transmission, which has good fuel consumption and efficient power transmission performance at the range typically used in practice, to realize easy daily use in urban areas.

(5) Enjoyable steering and quiet compartment

With the fine-tuned suspension and improved body rigidity, which are designed based on the results of CAE

analyses of mechanisms and structures, the vehicle offers delicate/high dimensional balance between flat ride and stable maneuverability, and with minimal rolling. Further, various countermeasures such as direct installation of the air cleaner and air duct to the engine reduce vibration transfer from the engine to the body, and the adoption of PET felt, which offers excellent noise absorption, as the material of the pad on the instrument panel, combine to deliver the best level of quietness in the class.

(6) One grade with multi-colors

The car has only one grade, "M", with an air conditioner, power steering, power windows, keyless entry system, central door locking, dual air bags, privacy window glass, etc., as standard equipment.

Customers can choose from nine body colors, based on the theme color "Aqua silver", which delicately changes color according to the direction of viewing or lighting.

3. Major Specifications

The major specifications of the eK-WAGON are shown below.

Specifications			Model		eK-WAGON	
					M	
					2WD	4WD
					3 A/T	
Dimensions	Overall length	(mm)			3,395	
	Overall width	(mm)			1,475	
	Overall height	(mm)			1,550	
	Wheelbase	(mm)			2,340	
	Tread	Front	(mm)		1,295	
		Rear	(mm)		1,295	
	Cabin length	(mm)			1,830	
	Cabin width	(mm)			1,220	
	Cabin height	(mm)			1,280	
	Weight	(kg)			790	840
					Minimum turning radius (m)	
					4.4	
Engine	Model				3G83	
	Total displacement	(cc)			657	
	Valve mechanism/No. of cylinders				SOHC, 12 valves/3	
	Maximum output	{kW (PS)/min ⁻¹ Net}			37 (50)/6,500	
	Maximum torque	{Nm (kgf·m)/min ⁻¹ Net}			62 (6.3)/4,000	
	Fuel supply system				ECI-MULTI (electronically controlled fuel injection)	
Running equipment	Steering				Rack and pinion type (power assisted)	
	Suspension	Front			McPherson struts type	
		Rear			Torque-arm, 3-link type	
	Brakes	Front			Disc	
		Rear			Leading and trailing drum	
	Tires				155/65R13	

(Car Research & Dev. Office: [Product Dev. Project] Aikawa, Morii)



AIRTREK is the first new product launched since Mitsubishi unveiled and embarked on its "Mitsubishi Turnaround Plan". It was released in June 2001.

1. Target

This car has been developed to be a "smart all-rounder", a unique product with new value, or more particularly, a next-generation all-round crossover RV that surpasses all existing RVs and is ideal for every situation.

Although the major target customers are unmarried young males to married males in their 40's, the car is designed to appeal to a wide range of customers.

2. Features

(1) Roomy comfort, whether for daily transport or leisure driving

- Packaging

Even though the car has a long 2,625 mm wheelbase to give a comfortable, roomy interior, the overall length is only 4,410 mm to ensure ease of handling. Furthermore, even though there is plenty of interior height, the overall height is just 1,550 mm, which is relatively low for an RV, making it possible to park in multi-story parking garages.

The seating height of the front seats, at 600 mm,

makes it easy to get in and out with minimum vertical waist movement of the driver and passenger, yet the high-up driving position ensures good visibility.

- Utility

To ease switching over between the driver's seat and passenger seat, the shift lever is located on the instrument panel, and the console box is set at the same height as the upper surface of the front seat cushions.

The rear seat with center armrest has a 6 : 4 split-tilting mechanism, so a wide, flat luggage space can be created by tilting the seat forward. Further, by fully reclining the front passenger seat, there is space for long luggage of up to 2,440 mm. The seat design thus offers maximum flexibility.

(2) Enjoyable, free running feel from on-road to off-road

- Engine and transmission

High performance is achieved while maintaining good fuel consumption. A 2.4-liter GDI engine and more practical 2.0-liter SOHC 16-valve ECI-MULTI engine, both of which are equipped with balance shafts, are combined with INVECS-II sport mode 4 A/T for stress-free driving. Also, the 4WD system is a full-scale, full-time 4WD, utilizing the center differential gears with VCU which have been proven on the LANCER EVOLUTION, to deliver optimum driving performance regardless of the road surface. Further, the 16-inch mud and snow tires, 195-mm minimum ground clearance, and large approach and departure angles make this car a true all-rounder and effortless off-road driving.

(3) New sensual styling to convey flexible space and free running feeling

- Exterior

Independent, uniquely-shaped four headlamps, large diameter tires, large wheel flare, rear short notch and taut surface treatment produce a strongly individual exterior styling for the next-generation RV, offering both high quality and sportiness.

- Interior

The characteristic T-shape instrument panel, combined with circular air outlets and analog clock, exudes a sporty, fresh but a nostalgic atmosphere.

Further, the interior trim can be selected from three



variations – CASUAL, GENTLE and LUXURY (with leather interior) – according to the customer's taste (except the 20E model, and the LUXURY interior is a maker option).

(4) Repletion of basic performance

- Safety performance

The car satisfies the 55-km/h frontal collision requirement as well as the 64-km/h offset collision requirements with the Mitsubishi's "RISE" collision-safe body structure. In addition, the car has various passive safety features such as pillar trims structured to reduce impact on the head, front seats structured to reduce impact on the neck, and a child seat fixing bar (maker option) to meet ISO-FIX.

The car is also designed with various active safety features such as ABS with EBD (electronic controlled brake force distribution system), excellent field of view with a high eye-point, and simple control systems that require only minimum turning of the eyes to maneuver.

- Environmental performance

The car with 2.4-liter GDI engine has obtained the Japan's "transitional low emission vehicle" certification in the first year, followed by "low emission vehicle" from 2003 model year, and that with 2.0-liter ECI-MULTI engine has achieved the "low emission vehicle" certification from the start.

Other environmental protection measures include extensive use of materials that are easy to recycle and reduced emissions of harmful materials even at the



manufacturing stage.

- Quality of the vehicles

As the AIRTREK is the first car developed based on the "Mitsubishi Turnaround Plan", as well as reflecting the concept of "Quality Gate" of DaimlerChrysler, all divisions of Mitsubishi have collaborated to develop this car that delivers "110 % Quality".

3. Major Specifications

The major specifications of the AIRTREK models are shown below.

Specifications			AIRTREK	
			CU2W	CU4W
			20E, 20V	24V, 24V-S
			2.0 L ECI-MULTI	2.4 L GDI
			2WD, 4WD, 4 A/T	
Dimensions	Overall length	(mm)	4,410	
	Overall width	(mm)	1,750	
	Overall height	(mm)	1,550	
	Wheelbase	(mm)	2,625	
	Tread	Front	(mm)	1,495
		Rear	(mm)	1,495
	Minimum ground clearance	(mm)	195	
Engine	Model		4G63	4G64
	Displacement	(cc)	1,997	2,350
	Valve mechanism/No. of cylinders		SOHC, 16 valves/4	DOHC, 16 valves/4
	Maximum output	{kW (PS)/min ⁻¹ Net}	93 (126)/5,500	102 (139)/5,500
	Maximum torque	{Nm (kgf-m)/min ⁻¹ Net}	173 (17.6)/4,500	207 (21.1)/3,500
	Fuel supply system		ECI-MULTI (electronically controlled fuel injection)	GDI (Gasoline Direct Injection)
Running equipment	Steering		Rack and pinion type (with power assist)	
	Suspension	Front	McPherson strut and coil spring type	
		Rear	Multi-link type	
	Brakes	Front	Ventilated disc (15-inch)	
		Rear	Leading and trailing drum (9-inch)	
	Tires		215/60R16 (mud and snow)	

(Car Research & Development Office [Product Development Project]: Iwamoto, Murasaki, Hagimoto)

Small-Sized Non-Step Bus "AERO-MIDI ME"

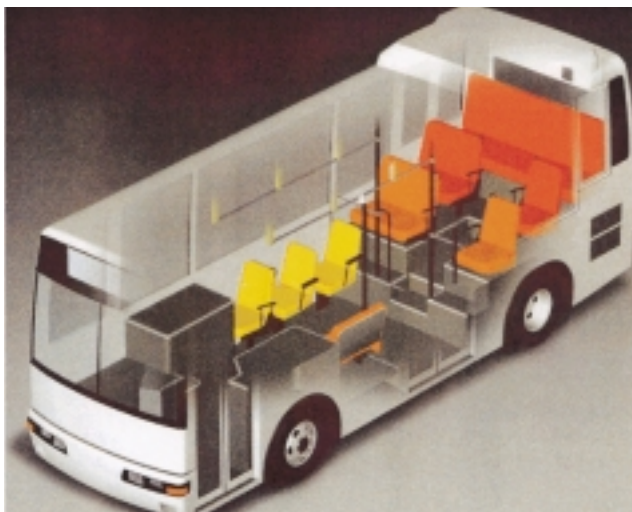
Recently, bus routes which circulate busy shopping areas and residential areas, designed to stem the decline of route bus line passengers, are helping to secure the number of passengers and restore profitability. Also, in areas suffering from aging and depopulation, local governments are operating community buses. To enable these services to be used by the physically disadvantaged, small-sized buses are being produced at a relatively healthy rate. Although Mitsubishi is marketing a small-sized bus "ROSA" for route buses, there is strong market demand for buses having a door at the front overhang portion to enable passengers to get on and off smoothly, as well as to make it easier to check the fare of each passenger. Furthermore, in November, 2000, the "Movement Smoothing Law"^{*1} (so-called "Barrier Free Law") was announced officially. At the time, there was no bus in the domestic market that met the Law and had an overall width of 2.1 m or less, to operate on routes with narrow roads of 4.5 m width or less. Mitsubishi has therefore developed the first small-sized non-step bus in the domestic market, which is equipped with doors at the front overhang portion and between the wheels, which complies with the Barrier Free law, and which has an overall width of 2 m.

^{*1}: To enable handicapped persons to move, the Law limits the ground height of the floor, and requires the mounting of facilities for ascending and descending of wheel chairs, etc.

1. Target

To develop a non-step vehicle of 2.0 m overall width class, which is relatively inexpensive and complies with the Barrier Free Law.

- (1) In spite of the vehicle being in the 2.0 m overall width class for operation on narrow routes (4.5 m road width), the floor area must be 4.5 m² ensuring the non-step portion.
- (2) To suppress the sales price, common parts proven on trucks and buses already in the market must be used.
- (3) Necessary parts to comply with the Barrier Free Law



must be equipped.

2. Features

(1) Lower floor

With the newly designed center-drop type front axle and 5-link type air suspension system, which is common with MJ, according to the narrower body width (overall width 2,060 mm, 240 mm less than the MJ model), the floor from the front door to behind the middle door has no step. To reduce costs, the rear axle was modified based on that for a small truck, and the rear suspension system, a combination of trailing type leaf springs and air springs, is a refined version of that used for the small-sized bus "ROSA". In addition, the ground height of the floor is set at 340 mm for the front door and 300 mm for the end of the entry/exit gate, thus making it "easy to get on and out and ensuring a comfortable ride for passengers". Further, by using the air suspension, vehicle height adjusting systems (4-wheel kneeling^{*2} and vehicle height raising^{*3}) are offered as an option to meet the operational needs of each user, as well as road surfaces and topographical conditions.

^{*2}: A system which makes it easier for passengers and wheelchairs to get on and out, by lowering the vehicle height (50 mm) by discharging air from the air springs of the front and rear wheels.

^{*3}: A system that prevents interference between the body and road surface, by raising the height of the air springs (50 mm) of the front and rear wheels.

(2) Basic layout

Assuming use on narrow routes, the T-drive layout with laterally mounted engine is adopted like MJ, a medium-sized non-step route bus, and with the shorter overall length of 6,990 mm (less than 7 m), wheelbase of 3,560 mm, and overall width of 2,060 mm, to make operation on 4.5 m wide roads possible. In addition, to ensure an interior passage width of 550 mm at the front axle portion to facilitate passenger movement in the bus, new steering linkages with revised steering angle are adopted.

The length of the front overhang (1,850 mm), the length of the rear overhang (1,580 mm) and the wheelbase are the same as the 7 m model of MJ, and although smaller, the middle entry/exit has the same width of 815 mm as the medium-sized bus for the smooth getting on/out of passengers. Furthermore, cost has been reduced by using

the same body side parts as the model of MJ.

The air conditioning equipment, applying the refrigerating evaporator originally for passenger cars, is newly designed to ensure sufficient cooling capacity for the body size, and is installed on the ceiling of the rear portion of the body.

(3) Interior layout

The interior room height is set at 2,285 mm, the same as MJ, to ease the closed feeling caused by the narrower vehicle width. As the fuel tank (100 liters) is installed under the left side of the floor between the wheels, the floor height of the portion is inevitably a little higher. By locating a side-facing bench seat for two persons on that floor portion, however, passengers are able to sit down from the non-step floor.

The right side of the vehicle has the same floor height continuously from the entrance, and is equipped with three front-facing one-person seats. Of the three seats, the two rearward ones are foldable to accommodate a wheel chair when necessary, and the floor has fixtures for belts to secure the wheel chair.

Although the rear portion of the floor has a stair shape because of the rear axle, the driveline and the engine, there are front-facing seats for 10 persons, thus ensuring seating for 15 persons per vehicle.

(4) Major functions

The frame has a new structure to adapt to the non-step floor, narrower overall width and the smaller engine. At the same time, it ensures lighter weight and appropriate rigidity, while keeping sufficient durability for a small-sized bus.

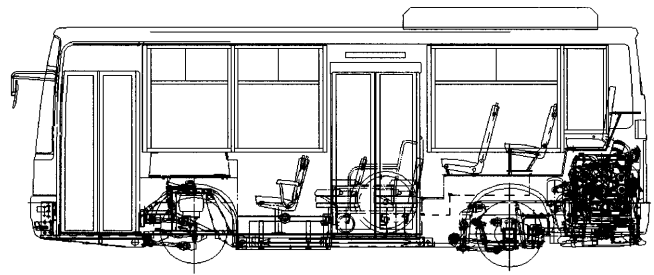
The engine is the 4M50T, which is using for small-sized trucks and buses, with a new starting motor, a large-capacity air compressor and combination of 50 A and 80 A alternators for the idling stop and starting system (ISS), which has recently become mandatory for route buses. This makes the engine able to satisfy customer requirements for similar performance to large-sized buses.

The standard 5-speed finger-control transmission (M050S5), which is the same as that of the MJ non-step bus, combined with final reduction gears of 4.875 ratio, ensures adequate driving performance for urban routes. Further, for routes in hilly residential areas, a final reduction gear with better hill climbing ability (reduction ratio 5.285) is available as an option.

The brake system is an air-over-hydraulic type, which, combined with the brakes for small-sized trucks (320 diameter x 110), has adequate functionality and is lightweight. Further, a hydraulic control type ABS, which is the same as that of other small-sized buses, is available as an option.

(5) Major equipment

- Equipment for compliance with



Barrier Free Law

As a "passenger-friendly bus", the following equipment is installed as standard:

- ① A detachable slope board for wheel chairs (at the middle door)
- ② Folding seats (two seats) to make space for a wheel chair and indicating stickers
- ③ Fixtures and belts to fix the wheel chair (for one wheel chair)
- ④ A public announcement system to provide information to the passengers, such as the next bus stop, and a LED type indicator for the name of the next bus stop (also indicating the fare at the same time)
- ⑤ Stanchions (vertical poles for holding) every 3 rows of seats to ensure safety when moving in the bus, with button switches to signal the driver to stop at the next bus stop, etc.
- ⑥ Floor covering to prevent slippage

• Seats

Seats for 15 passengers are all covered with moquette fabric, with different colors for "priority seats" on the left side between the wheels

• Trims around the passenger seats

According to the standard specification for large route buses, trims are unified to a cream color.

3. Major Specifications

The major specifications of the AERO-MIDI ME are shown below.

Specifications		Model	ME17DF
Rated passenger capacity [Seated passengers + standing passengers + driver]		(persons)	35 [15 + 19 + 1]
Dimensions	Overall length	(mm)	6,990
	Overall width	(mm)	2,060
	Overall height	(mm)	2,990
	Wheelbase	(mm)	3,560
	Tread	Front (mm)	1,695
		Rear (mm)	1,560
	Minimum turning radius	(m)	5.7
	Width of area occupied on road during a 90 degree turn	(m)	4.5
Engine	Minimum ground clearance	(mm)	150
	Model		4M50T
	Total displacement	(L)	4.899
	Maximum output	{kW (PS)/min ⁻¹ Net}	132 (180)/3,200
	Maximum torque	{Nm (kgf·m)/min ⁻¹ Net}	412 (42)/1,800
Running equipment	Steering		Ball and nut type integral power steering
	Suspension	Front	Axle type air suspension
		Rear	Axle type air suspension
	Brakes	Both front and rear	Air-over hydraulic
	Tires	Both front and rear	225/80R17.5

(Vehicle Dev. & Design Dept., Truck & Bus Rsrch & Dev. Office: Sueyoshi, Yamaguchi)

INTERNATIONAL NETWORK

Mitsubishi Motor Manufacturing of America, Inc.

100 North Mitsubishi Motorway, Normal
Illinois 61761, U.S.A.
Phone: 309-888-8000
Telefax: 309-888-8154

Mitsubishi Motor Sales of America, Inc.

6400 West Katella Avenue, Cypress
California 90630-0064, U.S.A.
Phone: 714-898-0485
Telefax: 714-373-1020

Mitsubishi Fuso Truck of America, Inc.

100 Center Sq. Road, Bridgeport
New Jersey 08014, U.S.A.
Phone: 856-467-4500
Telefax: 856-467-4695

Mitsubishi Motors America, Inc.

6400 West Katella Avenue, Cypress
California 90630-0064, U.S.A.
Phone: 714-372-6000
Telefax: 714-373-1020

Mitsubishi Motors R & D of America, Inc.

3735 Varsity Drive Ann Arbor
MI 48108, U.S.A.
Phone: 734-971-0900
Telefax: 734-971-0901

Mitsubishi Motor Sales of Caribbean, Inc.

Carretera No. 2, Km 20.1 Barrio
Candelaria Toa Baja, PUERTO RICO
Phone: 787-251-8715
Telefax: 787-251-3720

Netherlands Car B.V.

Dr. Hub van Doorneweg 1,
6121 RD Born, THE NETHERLANDS
Phone: 31-46-489-4444
Telefax: 31-46-489-5488

Mitsubishi Motors Europe B.V.

Douglassingel 1
1119 MB Schiphol-Rijk
THE NETHERLANDS
Phone: 31-20-6531862
Telefax: 31-20-6531883

Mitsubishi Trucks Europe – Sociedade

Add. Apartado 7
Tramagal 2200
Abrantes Codex, PORTUGAL
Phone: 351-41-899800
Telefax: 351-41-899875

Mitsubishi Motor Sales Europe B.V.

Douglassingel 1
1119 MB Schiphol-Rijk
THE NETHERLANDS
Phone: 31-20-4468111
Telefax: 31-20-4468135

Mitsubishi Motors Sales Nederland B.V.

Diamantlaan 29
2132 WV Hoofddorp, THE NETHERLANDS
Phone: 31-23-5555222
Telefax: 31-23-5540620

Mitsubishi Motor Sales Sweden AB

Box 8144 s-163 08 Spanga, SWEDEN
Phone: 46-8-474-5400
Telefax: 46-8-621-1794

MMC Automotive Espana S.A.

Trvesia de Costa Brava no. 6-5a planta
28034 Madrid, SPAIN
Phone: 34-91-3877400
Telefax: 34-91-3877458

Mitsubishi Motor Marketing Research Europe GmbH

Schieferstein 11A
65439 Floersheim/Main
GERMANY
Phone: 49-6145-808-107
Telefax: 49-6145-808-164

Mitsubishi Motor R & D Europe GmbH

Diamant-strass 1 65468
Trebur 2
GERMANY
Phone: 49-6147-9141-0
Telefax: 49-6147-3312

Mitsubishi Motor Sales Danmark A.S.

Provestensvej 50 DK 3000
Helsingor, DENMARK
Phone: 45-4926-6700
Telefax: 45-4926-6767

Mitsubishi Motors de Portugal, S.A.

Povos 2601 Vila Franca de Xira codex,
PORTUGAL
Phone: 351-63-2006100
Telefax: 351-63-2006232

Mitsubishi Motors Australia, Ltd.

1284 South Road, Clovelly Park
South Australia, 5042, AUSTRALIA
Phone: 8-8275-7111
Telefax: 8-8275-6841

Mitsubishi Motors New Zealand, Ltd.

Todd Park, Heriot Drive
Porirua, NEW ZEALAND
Phone: 4-237-0109
Telefax: 4-237-4495

MMC Sittipol Company, Ltd.

69-69/1-3 MUll Phaholyothin Road,
Tambol Klongneung, Ampur Klongluang,
Phatumthanee, 12120, THAILAND
Phone: 2-908-8000
Telefax: 2-908-8280

Mitsubishi Motors Philippines Corporation

Ortigas Avenue Extention,
Cainta, Rizal, Manila, PHILIPPINES
Phone: 2-658-0109
Telefax: 2-658-0006

P.T. Mitsubishi Krama Yudha Motors and Manufacturing

Petukangan 3, J1 Raya Bekasi
Km-21 Pulo Gadung, Jakarta Timur
Jakarta, INDONESIA
Phone: 021-460-2908
Telefax: 021-460-2915

MITSUBISHI MOTORS CORPORATION

- **Head Office**

33-8, Shiba 5-chome, Minato-ku, Tokyo 108-8410, Japan
Phone: +81-3-3456-1111
Telefax: +81-3-5232-7731
Telex: J26639, J26839

- **Design Center**

Tama Design Center

1-16-1, Karakida, Tama-shi, Tokyo 206-0035, Japan
Phone: +81-423-89-7307

- **Engineering Offices**

Car Research & Development Office

1, Nakashinkiri, Hashime-cho, Okazaki-shi, Aichi Pref. 444-8501, Japan
Phone: +81-564-31-3100
[Tokachi Proving Ground]
22-1, Osarushi, Otofuke-cho, Kato-gun, Hokkaido 080-0271, Japan
Phone: +81-155-32-7111

Truck & Bus Development Office

10, Ohkura-cho, Nakahara-ku, Kawasaki-shi 211-8522, Japan
Phone: +81-44-587-2000
[Kitsuregawa Proving Ground]
4300, Washijuku, Kitsuregawa-machi, Shioya-gun, Tochigi Pref. 329-1411, Japan
Phone: +81-28-686-4711

- **Plants**

Nagoya Plant

[Nagoya Plant – Oye]
2, Oye-cho, Minato-ku, Nagoya-shi, Aichi Pref. 455-8501, Japan
Phone: +81-52-611-9100
[Nagoya Plant – Okazaki]
1, Nakashinkiri, Hashime-cho, Okazaki-shi, Aichi Pref. 444-8501, Japan
Phone: +81-564-31-3100

Kyoto Plant

[Kyoto Plant – Kyoto]
1, Uzumasa Tatsumi-cho, Ukyo-ku, Kyoto-shi 616-8501, Japan
Phone: +81-75-864-8000
[Kyoto Plant – Shiga]
2-1, Kosunacho, Kosei-cho, Koga-gun, Shiga Pref. 520-3212, Japan
Phone: +81-748-75-3131

Mizushima Plant

1-1, Mizushima Kaigandori, Kurashiki-shi, Okayama Pref. 712-8501, Japan
Phone: +81-86-444-4114

Tokyo Plant

[Tokyo Plant – Kawasaki]
10, Ohkura-cho, Nakahara-ku, Kawasaki-shi 211-8522, Japan
Phone: +81-44-587-2000
[Tokyo Plant – Nakatsu]
4001, Nakatsu Aza Sakuradai, Aikawa-cho, Aikou-gun, Kanagawa Pref. 243-0303, Japan
Phone: +81-462-86-8111

